

HEAT TRANSFER AND FLUID FLOW CHARACTERISTICS OF DOUBLE PIPE HEAT EXCHANGER WITH PASSIVE TECHNIQUES

Ph.D. Thesis

By
SAURABH YADAV



**DISCIPLINE OF MECHANICAL ENGINEERING
INDIAN INSTITUTE OF TECHNOLOGY INDORE**

MAY 2020

HEAT TRANSFER AND FLUID FLOW CHARACTERISTICS OF DOUBLE PIPE HEAT EXCHANGER WITH PASSIVE TECHNIQUES

A THESIS

*Submitted in partial fulfillment of the
requirements for the award of the degree
of*
DOCTOR OF PHILOSOPHY

by
SAURABH YADAV



**DISCIPLINE OF MECHANICAL ENGINEERING
INDIAN INSTITUTE OF TECHNOLOGY INDORE**

MAY 2020



INDIAN INSTITUTE OF TECHNOLOGY INDORE

CANDIDATE'S DECLARATION

I hereby certify that the work which is being presented in the thesis entitled **HEAT TRANSFER AND FLUID FLOW CHARACTERISTICS OF DOUBLE PIPE HEAT EXCHANGER WITH PASSIVE TECHNIQUES** in the partial fulfillment of the requirements for the award of the degree of **DOCTOR OF PHILOSOPHY** and submitted in the **DISCIPLINE OF MECHANICAL ENGINEERING, Indian Institute of Technology Indore**, is an authentic record of my own work carried out during the time period from December 2014 to May 2020 under the supervision of Dr. Santosh Kumar Sahu, Associate Professor, Indian Institute of Technology Indore.

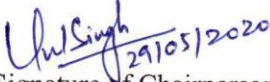
The matter presented in this thesis has not been submitted by me for the award of any other degree of this or any other institute.


July 17, 2019
Signature of the student with date
(Saurabh Yadav)

This is to certify that the above statement made by the candidate is correct to the best of my/our knowledge.


July 17, 2019
Signature of Thesis Supervisor with date
(Dr. Santosh Kumar Sahu)

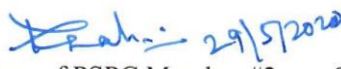
SAURABH YADAV has successfully given his/her Ph.D. Oral Examination held on **May 29, 2020**.


Signature of Chairperson (OEB)
Date: **May 29, 2020**


Signature of External Examiner
Date: **May 29, 2020**


Signature(s) of Thesis Supervisor(s)
Date: **May 29, 2020**


Signature of PSPC Member #1
Date: **May 29, 2020**


Signature of PSPC Member #2
Date: **May 29, 2020**


Signature of Convener, DPGC
Date: **May 29, 2020**


Signature of Head of Discipline
Date: **May 29, 2020**

ACKNOWLEDGEMENTS

I would like to express my sincere gratitude to my supervisor, **Dr. Santosh Kumar Sahu**, Discipline of Mechanical Engineering, Indian Institute of Technology Indore, for his valuable guidance, consistent effort and encouragement throughout my research work. I am very grateful to him for his support, patience, motivation and enthusiasm provided to me during the course of this research.

I wish to express my gratitude to **Dr. Iyamperumal Anand Palani**, Discipline of Mechanical Engineering, Indian Institute of Technology Indore and **Dr. Swadesh Kumar Sahoo**, Discipline of Mathematics, Indian Institute of Technology Indore for providing various technical inputs and valuable suggestions, which has greatly helped in shaping this thesis.

My sincere acknowledgement and respect to **Professor Neelesh Kumar Jain**, Director, Indian Institute of Technology Indore for providing me the opportunity to explore my research capabilities at **Indian Institute of Technology Indore**. I am grateful to him for providing me financial support to present my research work in International conferences within and outside India.

Also, my sincere acknowledgement to **Dr. Lakshmi Iyengar**, visiting faculty, IIT Indore for her diligent proofreading during the production of thesis.

I am thankful to the all the staff members of Workshop for their support during development of test facility at IIT Indore. Many thanks to **Mr. Arun Kumar Bhagwaniya**, Fluid Mechanics and Machinery Lab for his assistance for fabrication of test facility. I am thankful to **Mr. Rajesh Kumar and Mr. Satish Bisen**, Central Library, Indian Institute of Technology Indore for extended help during my Ph.D. work. I present my sincere thanks towards workshop team and Glass blowing section team IIT Indore for helping me in the fabrication of my experimental set up and test specimen.

I would like to appreciate the fine company of my dearest colleagues and friends especially, **Dr. Sunil Pathak, Dr. Robin Singh Bhadoriya, Dr. Hari Mohan Kushwaha, Dr. Syed Sadaf Ali, Dr. Harish Kumar Kotapally, Dr. Mini Sharma, Dr. Kadam Sambhaji, Dr. Balmukund Dhakar, Dr. Vinod Singh, Dr. Mayank Modak, Dr. Rajendra Chowdhary, Dr. Mayank Swarnkar, Mr. Gurjeet Singh, Mr. Dharmendra Panchariya, Mr. Rajendra Singh, Mr. Dhananjay Mishra.** Hearty thanks to all my lab mates, **Dr. Avadhesh K. Sharma, Dr. M. P. Paulraj, Mr. Vishal Nirgude, Mr. Rohit Kothari, Mr. Pushpanjay Singh and Mr. Anuj** for their cooperation during the course of my research.

I would like to express my heartfelt respect to my parents for their love, care and support they have provided to me throughout my life. Special thanks to my brother and sisters-in-law for their support and encouragements. I also express my deep love to my nephew whose innocence refreshed me during my difficult time.

Finally, I am thankful to all who directly or indirectly contributed, helped and supported me. To Sign off, I write a quote by Marcel Proust:

“The real voyage of discovery consists not in seeking new landscapes, but in having new eyes”

Saurabh Yadav

Dedicated to my family and friends

ABSTRACT

The present dissertation reports the experimental study pertaining to thermohydraulic characteristics of double pipe heat exchanger with passive enhancement techniques. The objective of the present study is to analyze the thermal performance of double pipe heat exchanger integrated with passive enhancement techniques for various practical applications such as solar air heating, air conditioning, space heating, chemical and petrochemical industries, food processing and power industries.

A test facility has been developed to analyze the thermohydraulic characteristics in the annulus of double pipe heat exchanger with passive techniques. Test facility includes the test specimen, water flow and air flow system and instrumentation scheme. Water flows in the inner tube of the test specimen while air is allowed to flow in the annulus in the opposite direction that of water flow. Initially, tests have been performed to study the heat transfer and pressure drop characteristics of annuli formed by smooth inner tube and corrugated outer tube in counter flow conditions for the different diameter ratios (0.53, 0.44 and 0.40), different pitches (10 mm, 20 mm, and 30 mm) for varied range of Reynolds number (3500-10500). Nusselt number, friction factor and thermal performance factor are estimated from the present test data. Correlations have been proposed for friction factor, Nusselt number and thermal performance factor as a function of various modeling parameters. Next, the double pipe heat exchanger involving plain surface disc turbulators are considered for the Investigation. Tests are performed to examine the effect of various parameters namely, diameter ratio ($DR = 0.42, 0.475$ and 0.53), pitch ratio (8.42, 9.79 and 11.79) and Reynolds number (3200 - 10500) on the thermal performance. Nusselt number, friction factor and thermal performance factor are estimated from the test data. Also, correlations are proposed to evaluate various parameters such as Nusselt number, friction factor and thermal performance factor. Based on

encouraging results, efforts have been made to estimate the thermohydraulic behavior using helical surface disc turbulators in the annulus of double pipe heat exchanger. Tests are performed for various diameter ratio ($DR = 0.42, 0.475$ and 0.53), different pitch ratio ($8.42, 9.79$ and 11.79), various helix angle ($\phi = 20^\circ, 30^\circ$ and 40°) and varied range of Reynolds number ($3500 - 10500$). Correlations are proposed for friction factor, Nusselt number and thermal performance factor as a function of various modeling parameters.

Keywords: Double pipe heat exchanger, corrugated tube, plain surface disc turbulator, helical surface disc turbulator, heat transfer, Nusselt number, Reynolds number, friction factor, thermal performance factor.

TABLE OF CONTENTS

ABSTRACT	i
LIST OF FIGURES	ix
LIST OF TABLES	xv
NOMENCLATURE	xvii
Chapter 1	
Introduction and literature review	1
1.1. General background	1
1.2. Classification of heat transfer enhancement techniques	2
1.2.1. Active techniques	2
1.2.2. Passive techniques	3
1.3. Mechanism of heat transfer enhancement	7
1.4. Literature review	9
1.4.1. Augmentation using geometrical modifications	9
1.4.2. Augmentation using swirl flow devices	13
1.5. Scope of present experimental investigation	29
Chapter 2	
Augmentation of experimental heat transfer and pressure drop characteristics in annuli formed by smooth inner tube and corrugated outer tube	33

2.1. Introduction	33
2.2. Test facility, procedure and data reduction	34
2.2.1. Test facility	34
2.2.2. Experimental procedure	40
2.2.3. Data Reduction	40
2.3. Results and discussion	43
2.3.1. Friction factor characteristics	45
2.3.2. Heat transfer enhancement	47
2.3.3. Comparison of corrugated annuli with smooth annuli	48
2.3.4. Thermal performance of annuli of DPHE	51
2.3.5. Comparison of present thermal performance with previous studies	52
2.3.6. Correlations for various parameters	53
2.4. Concluding remarks	58
 Chapter 3	
 Augmentation of heat transfer and pressure drop characteristics in annuli using plain surface disc turbulators	 61
3.1. Introduction	61
3.2. Test facility, procedure and data reduction	62
3.3. Results and discussion	65

3.3.1. Friction factor characteristics	67
3.3.2. Heat transfer enhancement	68
3.3.3. Comparison of annuli equipped with PSDTs and annuli without PSDTs	69
3.3.4. Thermal performance of annuli of DPHE using PSDTs	71
3.3.5. Comparison of present experimental results with the results of other researchers	72
3.3.6. Correlations for various parameters	74
3.4. Concluding remarks	79
 Chapter 4	
Augmentation of experimental heat transfer and pressure drop characteristics in annuli using helical surface disc turbulators	81
4.1. Introduction	81
4.2. Effect of pitch ratio and helix angle on thermo hydraulic performance of DPHE with helical surface disc turbulators	82
4.2.1. Test facility, procedure and data reduction	82
4.2.2. Results and discussion	87
4.2.2.1. Friction factor characteristics	87
4.2.2.2. Heat transfer enhancement	88
4.2.2.3. Comparison of annuli with HSDTs and without HSDTs	89

4.2.2.4. Thermal performance of annuli of DPHE	91
4.2.2.5. Comparison of present thermal performance with previous studies	92
4.2.2.6. Correlations for various parameters	93
4.3. Effect of diameter ratio and pitch ratio on thermo hydraulic performance of DPHE with helical surface disc turbulators	97
4.3.1. Test facility, procedure and data reduction	97
4.3.2. Results and discussion	97
4.3.2.1. Friction factor characteristics	97
4.3.2.2. Heat transfer enhancement	100
4.3.2.3. Comparison of annuli with HSDTs and without HSDTs	101
4.3.2.4. Thermal performance of annuli of DPHE with HSDTs	102
4.3.2.5. Correlations for various parameter	103
4.3.2.6. Comparison of present thermal performance with previous studies	109
4.4. Effect of diameter ratio and helix angle on thermo hydraulic performance of DPHE with helical surface disc turbulators	110
4.4.1. Test facility, procedure and data reduction	110
4.4.2. Results and discussion	110

4.4.2.1. Friction factor characteristics	110
4.4.2.2. Heat transfer enhancement	113
4.4.2.3. Comparison of annuli with HSDTs and without HSDTs	114
4.4.2.4. Comparison of present Nusselt number with previous studies	116
4.4.2.5. Comparison of present friction factor with previous studies	117
4.4.2.6. Thermal performance of annuli of DPHE with HSDTs	118
4.4.2.7. Correlations for various parameters	119
4.5. Concluding remarks	125
Chapter 5	
Conclusions and scope of future work	127
5.1. Introduction	127
5.2. Experimental study with corrugated outer tube in the DPHE	127
5.3. Experimental investigation involving various configuration of surface disc turbulators in DPHE	128
5.4. Scope of future work	132
References	135
Appendix	149

List of Publications	157
Curriculum Vitae	159

LIST OF FIGURES

Fig. 1.1	Corrugated tubes [8-9].	4
Fig. 1.2	Twisted tubes [26 -27].	5
Fig. 1.3	Different protruded tubes [33, 35].	6
Fig. 1.4	Various swirl flow devices (a) tape inserts (b) turbulators (c) wire coil and winglet tape inserts [7, 62 and 79].	6-7
Fig. 1.5	Flow mechanism using (a) twisted tape insert in tube (b) corrugated outer and smooth inner tube (c) circular turbulators in tube.	8
Fig. 1.6	Comparison of thermal performance factor of various passive techniques.	30
Fig. 2.1 (a)	Schematic of experimental test facility.	35
Fig. 2.1 (b)	Schematic of test specimen.	35
Fig. 2.2 (a)	Photographic view of test facility.	36
Fig. 2.2 (b)	Photographic view of test specimen.	38
Fig. 2.3 (a)	Photographic view of mixing chamber.	39
Fig. 2.3 (b)	Schematic view of mixing chamber.	39
Fig. 2.4	Cross-section and boundary conditions of double pipe heat exchanger.	45
Fig. 2.5	Variation in average friction factor of annulus with respect to Reynolds number.	46

Fig. 2.6	Variation in average Nusselt number of annulus with respect to Reynolds number.	47
Fig. 2.7	Variation in average Nusselt number ratio with Reynolds number.	49
Fig. 2.8	Variation in average friction factor ratio with Reynolds number.	50
Fig. 2.9 (a)	Schematic of corrugated tube DPHE.	50
Fig. 2.9 (b)	Idealized flow patterns through the annulus tube.	50
Fig. 2.10	Variation of thermal performance factor with Reynolds number.	51
Fig. 2.11	Comparison of TPF of corrugated DPHE with previous study.	52
Fig. 2.12	Comparison of experimental and predicted values of average Nusselt number.	55
Fig. 2.13	Comparison of experimental and predicted values of average friction factor.	55
Fig. 2.14	Comparison of experimental and predicted values of thermal performance factor.	58
Fig. 3.1 (a)	Schematic of experimental test facility.	62
Fig. 3.1 (b)	Schematic of test specimen using PSDTs.	63
Fig. 3.1 (c)	Photographic view of plain surface disc turbulator.	63
Fig. 3.2	Variation of average f with Re in the annulus using PSDTs.	67

Fig. 3.3	Variation of average Nu with Re in the annulus using PSDTs.	68
Fig. 3.4	Variation in Nu ratio with Re in the annulus using PSDTs.	69
Fig. 3.5	Variation in f ratio with Re in the annulus using PSDTs.	70
Fig. 3.6	Variation in TPF with Re in the annulus using PSDTs.	71
Fig. 3.7	Comparison of present experimental Nusselt number with previous the results of previous researchers.	72
Fig. 3.8	Comparison of present experimental friction factor with the results of previous researchers.	73
Fig. 3.9	Comparison of experimental and predicted average Nu values using PSDTs.	75
Fig. 3.10	Comparison of experimental and predicted f values using PSDTs.	76
Fig. 3.11	Comparison of experimental and predicted TPF values using PSDTs.	76
Fig. 4.1 (a)	Schematic view of experimental test facility.	83
Fig. 4.1 (b)	Schematic of test specimen using HSDTs.	84
Fig. 4.1 (c)	Photograph of helical surface disc turbulator.	84
Fig. 4.1 (d)	Photographic view of test facility.	86
Fig. 4.2	Cross-section and boundary conditions of DPHE.	87
Fig. 4.3	Variation in average friction factor variation with Reynolds number.	88

Fig. 4.4	Variation in average Nusselt number variation with Reynolds number.	89
Fig. 4.5	Variation in Nusselt number ratio and friction factor ratio with Reynolds number.	90
Fig. 4.6	Variation in thermal performance factor with Reynolds number.	91
Fig. 4.7	Comparison of thermal performance factor with the previous studies.	92
Fig. 4.8	Comparison of experimental and predicted values.	94
Fig. 4.9	Variation of average friction factor with Reynolds number in the annulus using HSDTs.	99
Fig. 4.10	Variation in average Nusselt number with Reynolds number.	100
Fig. 4.11	Variation in Nusselt number ratio with Reynolds number.	101
Fig. 4.12	Variation in friction factor ratio with Reynolds number.	102
Fig. 4.13	Variation in thermal performance factor with Reynolds number in the annulus.	103
Fig. 4.14	Comparison of experimental and predicted values of average Nusselt number.	105
Fig. 4.15	Comparison of experimental and predicted values of average friction factor.	106
Fig. 4.16:	Comparison of experimental and predicted values of thermal performance factor.	106

Fig. 4.17	Comparison of present prediction for thermal performance factor with previous work.	109
Fig. 4.18	Variation of average friction factor with Reynolds number in the annulus using HSDTs.	112
Fig. 4.19	Variation of average Nusselt number with Reynolds number in the annulus using HSDTs.	113
Fig. 4.20	Variation in Nusselt number ratio with Reynolds number in the annulus.	114
Fig. 4.21	Variation in friction factor ratio with Reynolds number in the annulus.	115
Fig. 4.22	Comparison of experimental Nusselt number.	117
Fig. 4.23	Comparison of experimental friction factor.	118
Fig. 4.24	Variation in thermal performance factor with Reynolds number in the annulus.	119
Fig. 4.25	Comparison of experimental and predicted values of average Nusselt number.	123
Fig. 4.26	Comparison of experimental and predicted values of average friction factor.	123
Fig. 4.27	Comparison of experimental and predicted values of thermal performance factor.	124

LIST OF TABLES

Table 1.1	Summary of experimental investigations for corrugated tube geometries.	24-25
Table 1.2	Summary of experimental investigation using various turbulators.	26-28
Table 2.1	Detail of experimental test specimens.	37
Table 2.2	Experimental validation of Nusselt number with smooth tubes.	44
Table 2.3	Experimental validation of friction factor with smooth tubes.	45
Table 2.4	Correlations proposed by various researchers.	56-57
Table 3.1	Detail of experimental test sections.	64
Table 3.2	Experimental validation of Nusselt number for smooth tubes.	65
Table 3.3	Experimental validation with smooth tubes.	66
Table 3.4	Correlations proposed by various researchers.	77-78
Table 4.1	Design of HSDTs involving different pitch ratios and various helix angles.	85
Table 4.2	Correlations proposed by various researchers.	95-96
Table 4.3	Design of HSDTs involving different diameter ratios and various pitch ratios.	98

Table 4.4	Correlations proposed by various researchers.	107-108
Table 4.5	Design of HSDTs involving different diameter ratio and various helix angle.	111
Table 4.6	Correlations proposed by various researchers.	121-122

NOMENCLATURE

English Symbols

A	Heat transfer area, m^2
C_p	Specific heat of fluid, J/kg-K; $(C_p)_{\text{water}} = 4.18 \times 10^3$; $(C_p)_{\text{air}} = 1.005 \times 10^3$
D	Hydraulic mean diameter of annulus, m
$DPHE$	Double pipe heat exchanger
DR	Diameter ratio (d_o/D_i)
D_i	Inner diameter of outer tube, m
d_i	Inner diameter of inner tube, m
D_o	Outer diameter of outer tube, m
d_o	Outer diameter of inner tube, m
e	Height of corrugation, m
f	Average friction factor
FR	Friction factor ratio
h	Heat transfer coefficient, $W/m^2\text{-K}$
$HSDT$	Helical surface disc turbulator
k	Thermal conductivity, $W/m\text{-K}$
L	Length of test section, m

L_t	Length of inner tube, m
L_s	Length of outer tube, m
m	Mass flow rate of fluid, kg/s
NR	Nusselt number ratio
Nu	Average Nusselt number
P	Pitch, m
$PSDT$	Plain surface disc turbulator
PR	Pitch ratio (P/d_o)
Pr	Prandtl number
Q	Heat duty, W
R	Resistance, $m^2\text{-K/W}$
Re	Reynolds number
T	Temperature, K
TPF	Thermal performance factor
U	Overall heat transfer coefficient, $W/m^2\text{-K}$
v	Mean velocity of fluid, m/s

Greek Symbols

ρ	Density kg/m^3
Φ	Helix angle, Degree ($^\circ$)

μ	Dynamic viscosity, kg/m-s
ΔP	Pressure difference across test section, Pa
η	Thermal performance factor

Subscripts

a	Augmented tube (corrugated tube)
an	Annulus
avg	Average
c	Cold
h	Hot
in	Inlet
$LMTD$	Logarithmic mean temperature difference
out	Outlet
s	Surface
sm	Smooth
T	Turbulator
w	Wall

Chapter 1

Introduction and literature review

1.1 General background

Heat transfer in pipe flow plays a crucial role in various industrial and scientific applications. The performance of heat exchanging equipment affects the system efficiency and operating cost. Enhancement in heat transfer rate can lead to various advantages such as a reduction in the size, higher efficiency, and saving in operating cost and materials. Therefore, it is essential to improve the thermal performance of heat exchanging equipment for sustainable energy development. Heat exchanging equipment is widely used in various applications such as refrigeration, air conditioning, chemical and petrochemical industries, and power industries.

The thermal performance is mostly expressed by two parameters, such as friction increase ratio and heat transfer enhancement ratio. Therefore, the heat transfer enhancement techniques should be selected in such a way that the heat transfer enhancement ratio is larger to the pressure drop increase ratio. In general, heat transfer enhancement can be achieved by two different ways, such as active and passive methods [1-7]. The active method uses external power for heat transfer enhancement. It is quite complex and difficult to design in certain applications. Passive methods do not need any external power for heat transfer enhancement. Passive methods usually employ either modified surfaces or geometries such as rough surfaces, extended surfaces, turbulators, and inserts to achieve the heat transfer enhancement.

In this chapter, various passive augmentation techniques, associated heat transfer mechanism, and a brief review of the literature on passive heat transfer augmentation methods are discussed. In addition to this, the objectives of this investigation are highlighted.

1.2 Classification of heat transfer enhancement techniques

The enhancement techniques are broadly classified into two categories, namely, active and passive techniques. These are detailed in this section.

1.2.1 Active techniques

Active techniques need external power to enhance the heat transfer coefficient of the fluid. Here, the external power helps to develop the modifications in the flow field, generates turbulence and mixing that results in improvement in the heat transfer. The details of active techniques are summarized below.

Mechanical Aids

These techniques involve stirring the fluid either by mechanical means or rotating the surface. Mechanical surface scrapers can be applied to the duct flow involving gaseous fluids. Because of stirring of the fluids, better mixing takes place and improves the heat transfer [2-7].

Surface vibration

In this active technique, the surface of the heat exchanger is allowed to vibrate at different frequencies. This technique disturbs the boundary layer, induces secondary flow, which in turn increases the turbulence intensity. Furthermore, these vibrations enhance mixing of fluid that improves heat transfer enhancement [2-7].

Fluid vibration

In this technique, pulsation or oscillating motion is provided to heat transfer fluid to disturb the thermal boundary layer. The pulsation value of the

fluid depends upon the mass of the heat exchangers. This technique is mainly used for the single-phase fluid flow application [2-7].

Electrostatic fields

The electrostatic fields are applied to the dielectric fluids. This technique improves the bulk mixing of fluids near heat transfer surface, resulting in the increase in heat transfer rate. In addition to this, both electric and magnetic fields are used simultaneously to improve fluid convection. This results enhancement in heat transfer [2-7].

Injection

In this method, same fluid or different fluid is injected to the flow of liquid through a porous heat transfer surface. The injected fluid is found to augment the heat transfer [2-7].

Jet impingement

In this technique, fluids are allowed to impinge either normally or obliquely to the hot wall. Because of the interaction of fluid and hot wall, higher heat transfer takes place on the impingement surface [2-7].

However, because of certain reasons such as the use of external power, complex design of the thermal systems, active techniques are not used in most of the applications.

1.2.2 Passive techniques

Passive techniques do not require any external power for the heat transfer augmentation. In order to enhance the heat transfer rate, passive techniques utilize various surface and geometrical modifications. Also, inserts are used inside flow regime to enhance the thermal performance of the heat exchangers [1-7]. The modified tube geometries can enhance the heat transfer of heat exchanging tubes. These include various shapes of the tube geometry such as corrugated tubes,

twisted tubes, protruded tubes, and grooved tubes. The geometrical modifications of the tubes are useful for both single-phase flow and two-phase flow heat transfer [1-7].

Corrugated tubes

Corrugated tubes are used to enhance heat transfer characteristics of the heat exchanger tubes [8-23]. The main functions of corrugation are to promote the secondary recirculation flow by inducing radial velocity components, mixing the fluid layers and increase the wetted perimeter resulting in improvement in heat transfer. This augmentation technique is extensively being used in modern heat exchanger tubes. Different corrugated tube geometries are shown in Fig 1.1.

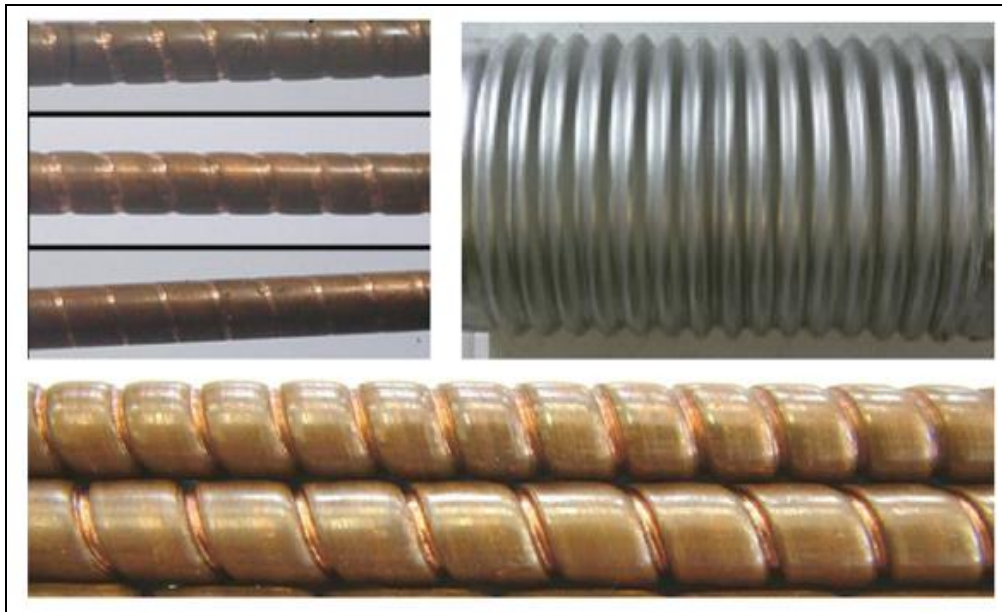


Fig. 1.1: Corrugated tubes [8-9].

Twisted tubes

Twisted tube heat exchangers are being used to enhance the heat transfer rate in various industrial applications. These tubes are used as a replacement for straight circular tube in shell and tube heat exchanger. These tubes enhance the heat transfer of fluid that flows in the tube side, and shell side as well. The size of

the heat exchanging equipment can be reduced by employing twisted tubes [24-32]. Fig. 1.2 depicts the twisted tube geometries used by earlier researchers [26-27].

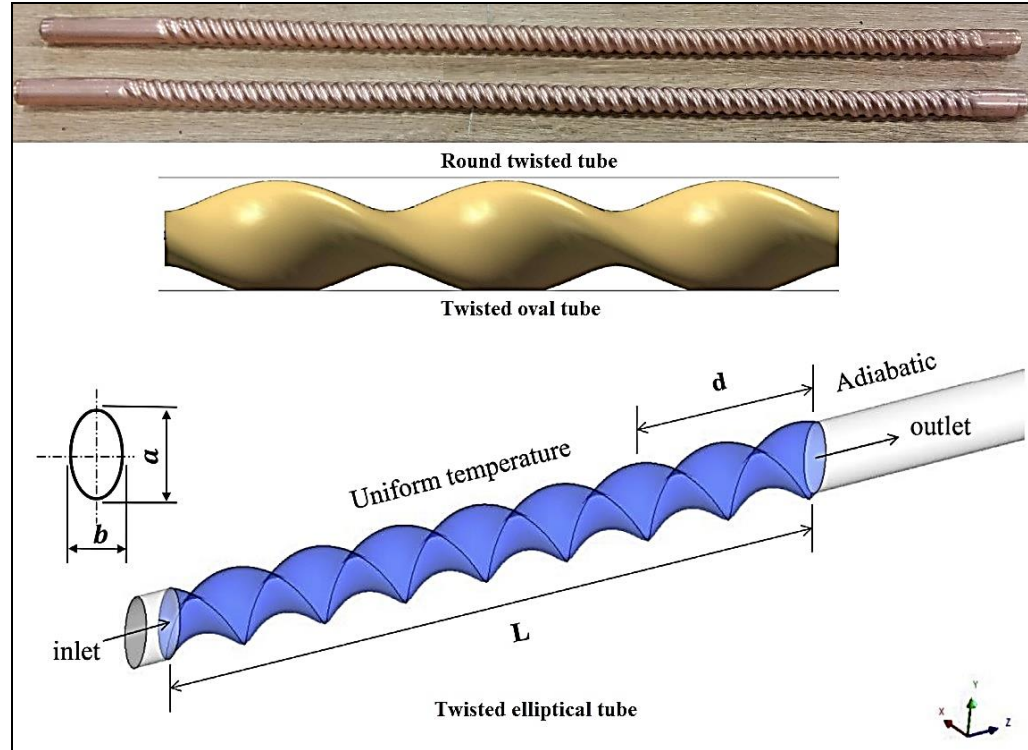


Fig. 1.2: Twisted tubes [26 -27].

Protruded tubes

Many a time, the tube surfaces are provided with ribs, arrays of pin fins, arrays of shaped roughened elements and are termed as protruded tubes [33-36]. These tubes offer a considerable increase in the surface area that leads to heat transfer enhancement with relatively small improvements in pressure drop. These tubes are significantly being used in a variety of practical applications, such as heat exchangers, electronics cooling, cooling passage for turbine blades, biomedical devices, micro-scale passages for heat transfer, and combustion chamber liners [7, 33]. Fig. 1.3 depicts different design of the protruded or dimpled tubes.

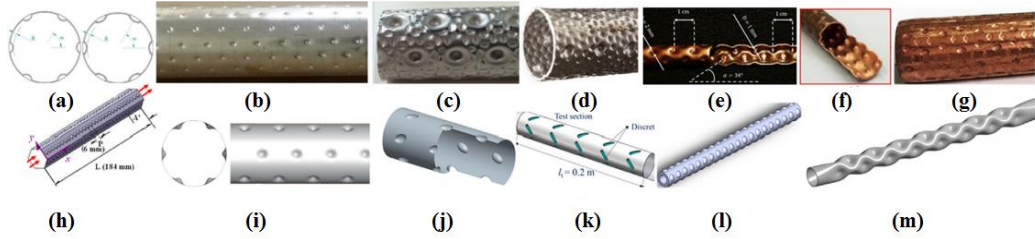
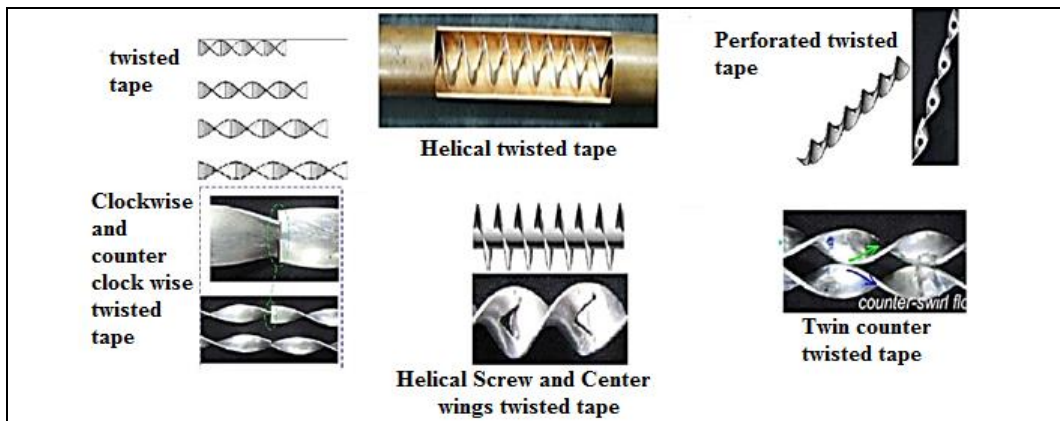


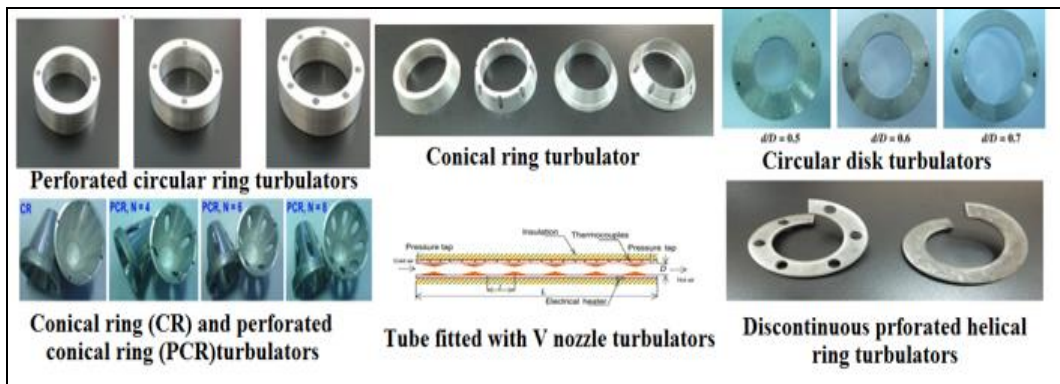
Fig. 1.3: Different protruded tubes [33, 35].

Swirl flow devices

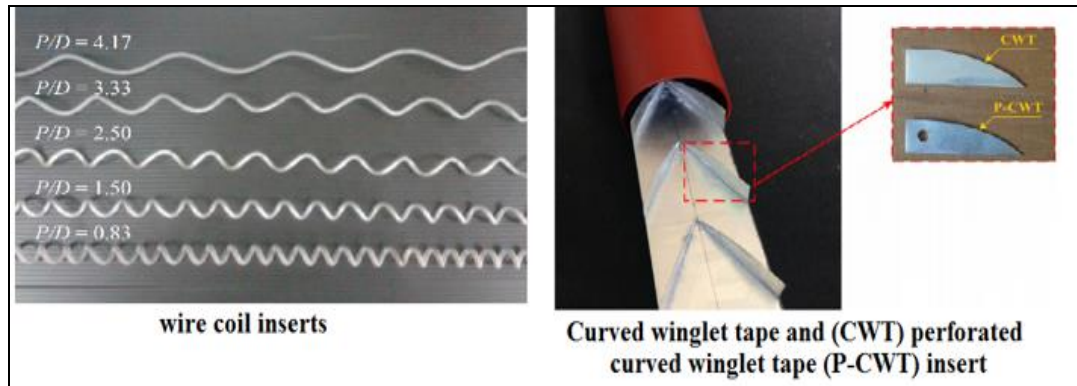
Passive augmentation of heat transfer is also achieved by inserting various swirl flow devices. These include various type of twisted tape inserts, winglets tape inserts, wire coil inserts, and different design of turbulators [5 – 7, 37 - 79]. These swirl flow devices are very useful for the single-phase heat transfer.



(a)



(b)



(c)

Fig. 1.4: Various swirl flow devices (a) tape inserts; (b) turbulators (c) wire coil and winglet tape inserts [7, 62, and 79].

Fig. 1.4 depicts various swirl flow services used by previous researchers. These devices generate the secondary flow in the flow regime resulting in increase in the turbulence, which leads to enhancement in heat transfer [5-7].

1.3 Mechanism of heat transfer enhancement

Various heat transfer augmentation techniques are used to improve thermal performance. The mechanism of heat transfer may be due to the following.

Reduction in the thermal boundary layer

Very often, geometrical modifications such as corrugation, grooves, protrusion are provided on the tube surface to improve thermal performance. In such a case, improved mixing takes place due to continuous breakdown in the thermal boundary layer and variations in streamlines and path lines. Enhanced mixing and increase in turbulence, promote heat transfer.

Shear stress enhancement near wall surface

It is argued that swirl is generated inside the flow due to helical corrugation, twisted tubes, insertion of tapes, and turbulators. This improves fluid mixing and leads to enhancement in heat transfer. In addition to this, the fluid

licks larger surface area and is able to exchange more amount of heat between surface and fluid.

Swirl flow generation

By using tape inserts and turbulators, the swirl inside flow regime increases and improves fluid mixing. This improves the heat transfer rate.

The idealized flow mechanism using some of the passive techniques are shown in Fig. 1.5.

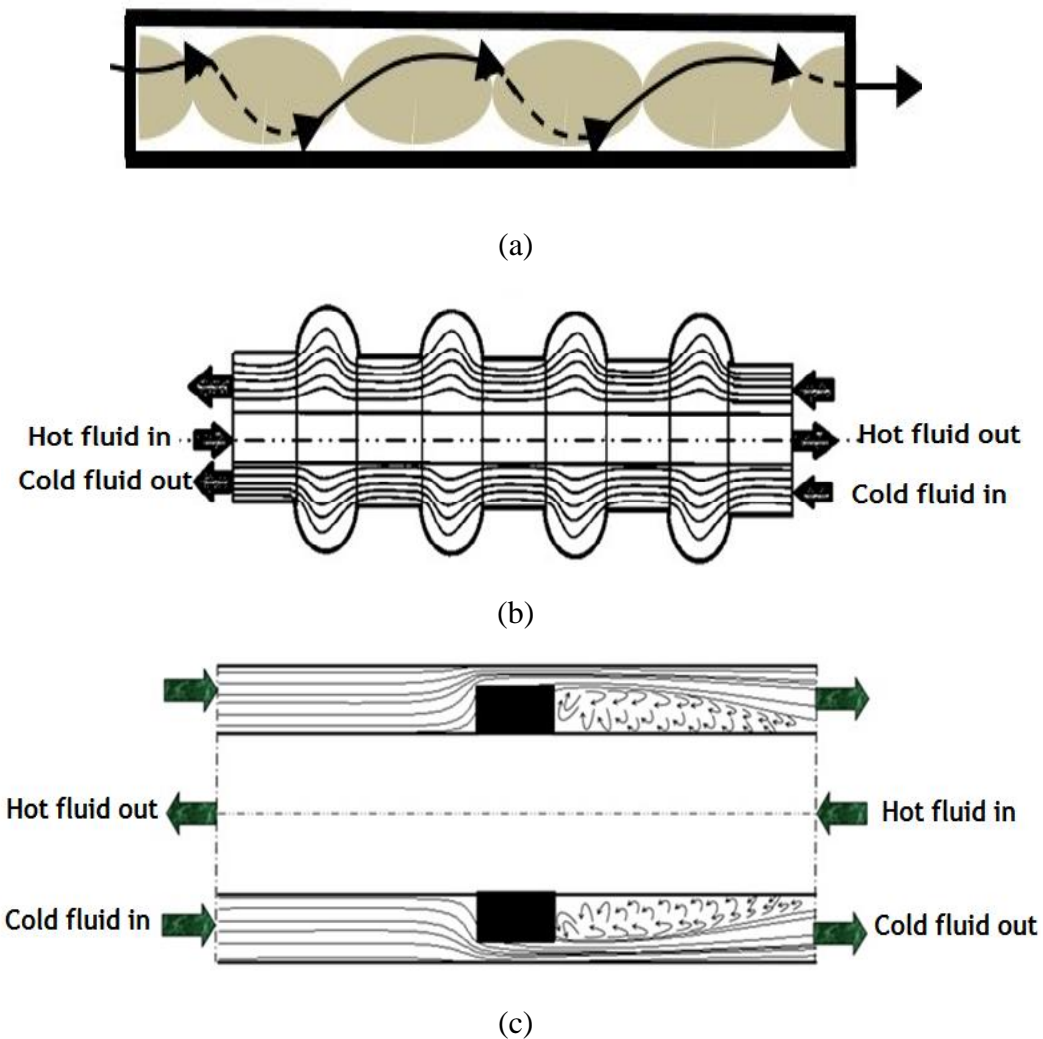


Fig. 1.5: Flow mechanism using (a) twisted tape insert in tube; (b) corrugated outer and smooth inner tube; (c) circular turbulators in tube.

1.4 Literature review

Augmentation of heat transfer plays a vital role in various heat exchanging equipment. Active techniques usually have high heat transfer enhancement potential, although they are very complex in nature. While, passive techniques are widely used in industries due to their simple design, less expensive, and increased reliability, compared to the active techniques [6-8]. Different passive techniques are employed depending upon the requirement of heat exchanging equipment. Several studies [10- 79] have been reported to estimate the heat transfer and pressure drop characteristics in various ducts that employ various passive techniques. Some of the important studies employing such techniques to improve thermal performance for single phase flow, are detailed below.

1.4.1 Augmentation using geometrical modifications

Over the years, various geometrical modifications have been made in tubes to improve thermal performance. These include twisted tubes, corrugated tubes, grooved, and protruded tubes [10-36].

Corrugated tubes

Numerous studies [10-22] have been reported that investigate the heat transfer performance of various fluids by using corrugated tubes. Corrugation on the tube geometry creates artificial roughness, improves mixing in the fluid resulting in enhancement in the heat transfer performance [10]. In these configurations, the wetted area increases and fluid licks larger surface area, resulting in the enhancement in heat transfer. Rainieri and Pagliarini [11] performed experiments to study the thermal performance of tubes with different corrugation pattern, such as helical corrugation and axial symmetrical corrugation at the entry region by using ethylene glycol. The authors reported that in the turbulent flow, the Nusselt number was independent of the corrugation shape. Ahn [12] carried out experiments in the parallel flow heat exchanger, with a smooth outer tube and a corrugated inner tube. Water was used as the working

fluid in both tube and annuli, and the Reynolds number (Re) varied between 17000-13000. The Nusselt number in the annuli was found to decrease by increasing the radius ratio. Vicente et al. [13] experimentally investigated the heat transfer and pressure drop in different corrugated tubes for laminar and transition flow regime using water and ethylene glycol as the test fluid. The maximum enhancement in heat transfer and pressure drop of corrugated tube compared to the plain tube was found to be 30% and 25%, respectively. Aroonrat et al. [14] carried out experiments with double pipe counter flow concentric heat exchanger with refrigerant flowing inside the inner tube and water flowing through the annulus. A corrugated inner tube and a smooth outer tube was used in the study. The maximum enhancements in heat transfer and friction factor by using corrugated tube were found to be 1.22 and 4.0, respectively. Pethkool et al. [15] reported the heat transfer performance of single-phase fluids in a double pipe heat exchanger with inner helically corrugated tubes and outer smooth tubes for varied range of pitch to diameter ratio. The corrugated tube with the highest pitch ratio was found to exhibit the highest Nusselt number (up to 300% more) compared to the smooth tube. Wongcharee and Eiamsa-ard [16] reported the combined effect of corrugation, twisted insert, and CuO-water nanofluids in their experimental study. The heat transfer was found to increase with the increase in CuO/water nanofluid concentration and decreases with twist ratio. The configuration with corrugation and twist insert exhibited the highest thermal performance factor of 1.57 for 0.7% (by volume) nanofluid concentration. In their experimental investigation, Han et al. [17] performed tests in DPHE with inner corrugated tube for various pitches (16, 24 and 32 mm) and reported significant enhancement in the heat transfer. Dizaji et al. [18] reported the heat transfer and pressure drop characteristics of corrugated tubes through experimental investigation. Recently, Dizaji and Jafarmadar [19] carried out experiments to study the effect of various corrugation shapes in both inner and outer tube on the thermal performance. The authors considered different combination of corrugation shapes such as concave and convex for both inner and outer tube [18-19]. The combination of corrugation

shape for both inner and outer tubes significantly affects the thermal performance. It was reported that only for one combination, i.e., the heat exchanger with concave corrugated outer tube and convex corrugated inner tube, the thermal performance was found to be greater than unity for a wide range of Re. Darzi et al. [20] carried out their experimental investigation using helically corrugated tube with Al_2O_3 / water nanofluid with three corrugated pitches (5, 7 and 8 mm) and different corrugated heights (0.75 – 1.25 mm). The authors reported that the heat transfer increased with the increase in the volume of the nano particle in the nanofluids, and the maximum heat transfer were found for the helically corrugated tube with least corrugated pitch and highest corrugation height. Srinivasan and Christensen [21] carried out tests by using spirally fluted tubes for different design parameters involving varied range of flute depth ($e/D_{vi} = 0.1-0.4$), different flute pitches ($p/D_{vi} = 0.4 - 7.3$), various helix angles ($\theta/90^\circ = 0.3 - 0.65$), different Reynolds numbers ($Re = 500 - 80000$) and various Prandtl numbers ($Pr = 2 - 7$). The authors reported that heat transfer increased with the decrease in flute pitch and increases with flute depth and helix angle. The end of laminar region was found to exhibit the highest thermal performance. Barba et al. [22] carried out their experimental investigation using corrugated tube with corrugated pitch of 11.5, corrugation angle of 45° , ridge depth of 1.5 and severity index of 0.135 for a single-phase Newtonian fluid with varying Reynolds number (100 - 800). The authors reported that the heat transfer rate enhances significantly using corrugated tube. In their experiments, Harless et al. [23] investigated thermo-hydraulic characteristic of single-start and three-start corrugated tubes, using exhaust gases as working fluid at various pitch ratios (0.27 – 1.53), corrugation height to diameter ratios (0.02 – 0.056), corrugation angles ($9.2^\circ - 37^\circ$) and Reynolds number varying between 5000 – 23000. The highest thermal performance was found with single start corrugated tube for corrugated pitch ratio of 0.517 and corrugation height ratio of 0.040.

Twisted tubes

Twisted tubes of different shapes and sizes have been used in place of straight circular tube in shell and tube heat exchangers. The twisted ducts are found to enhance the heat transfer of fluids in both tube and shell side. Various experimental and numerical studies have been reported that consider the heat transfer and pressure drop characteristics of twisted ducts in double pipe heat exchanger and tube bundles [24-32]. Tests were carried out with various configurations such as inner twisted square duct, and outer circular tube by Bhadouriya et al. [27-28]. The authors used air as working fluid in the annulus [28] for different twist ratios (10.6 and 15), and various annulus parameters (0.19 - 0.51) for the Reynolds number ranging between 400 - 60000. In addition to this, tests were conducted with air as working fluid in the inner twisted tube [27] for different twist ratios (11.5 and 16.5) and varied range of Reynolds number (600 - 70000). The heat exchanging equipment, with lowest twist ratio and annulus parameter was found to exhibit the highest enhancement. Heat exchanger with twisted oval inner tubes and outer circular tubes were investigated by Tan et al. [29] for varied range of major axes (24-28 mm), various minor axes (9-15.5 mm) and different twist pitches (100 - 200 mm). The heat exchanging equipment with major axis of 28 mm, minor axis of 9 mm and twist pitch length of 100 mm exhibited the highest thermal performance. The thermal performance of double pipe heat exchanger with spiral, tri-lobed, and oval shape twisted tube was estimated through both experimental and numerical investigation by Tang et al. [30]. The authors used water as working fluid, and tests were conducted for varied range of Reynolds number (8000 - 21000). The equipment with tri-lobed twisted tube exhibited the highest thermal performance. Yang et al. [31] carried out tests with elliptical twisted tubes inside double pipe heat exchanger. The authors used water as the working fluid and tests were conducted for varied range of twist pitches (104 – 192 mm), different aspect ratios (1.62 – 2.15) and different Reynolds numbers (600 – 50000). The tube with least twist pitch and largest aspect ratio were found to exhibit the higher heat transfer. Tests were also been

carried out with twisted divergent and twisted convergent ducts by Wang et al. [32]. The twisted divergent duct was found to exhibit better enhancement in heat transfer performance. While, the twisted convergent duct deteriorates the heat transfer performance and the heat transfer performance of twisted duct with constant cross-section duct lies in between the convergent and divergent duct [32].

Protruded, grooved and dimpled tubes

In an experimental investigation, protruded surface heat exchanger tube has been used to evaluate heat transfer characteristics for various stream wise spacing ($x/d = 10, 20, 30, 40$), numerous span wise spacing ($y/d = 10, 20, 30, 40$) and Reynolds number in the range of 6000–35,000 [34]. The maximum enhancement in thermo hydraulic performance factor was found to be 2.31 for span wise spacing (y/d) of 10. Xie et al. [35] numerically investigated the heat transfer characteristics of protruded and dimpled tubes with varying protrusion depth (D), different protrusion pitches (P) for varied range of Reynolds number (5000 - 30000). The highest thermal performance was reported for the tube with $D = 3$ mm, $P = 30$ mm, and $R = 4$ mm. Jianfeng et al. [36] used spirally grooved tubes to estimate heat transfer characteristics. Tests was performed for wide range of relative grooved height (0.0238, 0.0306, 0.0381 and 0.0475), different Reynolds numbers (5000 - 15000) and various Prandtl numbers (13.5 – 15.2). Spirally grooved tubes was found to enhance the heat transfer with the increase in Prandtl number and relative grooved height.

1.4.2 Augmentation using swirl flow devices

Studies have been made to analyze the influence of different swirl flow devices on the thermal performance of heat exchanging equipment. These include twisted tape inserts, winglet tape inserts, wire coil inserts, and turbulators [5 – 7, 37 - 79]. These are discussed below.

Twisted tape inserts

Twisted tapes usually have length equal to the length of exchanger tube. The configurations of the twisted tapes are shown in Fig. 1.4. Different configurations of tape inserts are used by various researchers. Experimental investigation has been made [37] for a solar water heater with twisted tape inserts having various twist ratios (3 - 12) and different Reynolds numbers (4000 - 21000). The authors reported that twisted tapes generate swirl inside the flow regime, increase the turbulence intensity, promotes fluid mixing leads to heat transfer enhancement. The lowest value of twist ratio was found to generate the highest swirl that results in higher heat transfer rate and the pressure drop. Esmailzadeh et al. [38] reported heat transfer and friction factor characteristics of Al_2O_3 - water nanofluids with various volume concentration (0.5 and 1%) through circular tube fitted with twisted tape inserts. Tests were performed for a constant twist ratio of 3.21, varied range of thicknesses (0.5 – 1 mm) and various Reynolds numbers (150 - 1600). The highest heat transfer enhancement was obtained for the nanofluids with the highest nanoparticle concentration of 1%. Friction factor is found to increase with the thickness of the twisted tapes. This may be due to larger contact surface and reduction of fluid flow area. The convective heat transfer enhancement outweighs the effect of friction factor increase, resulting in the enhancement in the thermal performance. Experiments were performed with dimple tube integrated with twisted tape inserts by Thianpong et al. [39]. The author conducted tests for various pitch ratios (0.7 - 1) and different twist ratios (3, 5 and 7) and varied range of Reynolds number (12000 – 44000). Heat transfer and friction factor were found to increase with the decrease in pitch ratio and twist ratio.

Helical twisted tape insert

Numerous studies have been made that use helically twisted tape inserts for the thermal augmentation [39, 40, and 60]. Eiamsa-ard et al. [40] studied the heat transfer enhancement by using helically twisted tapes. Tests were performed

for various twist ratios (2, 2.5 and 3), different pitch ratios (1, 1.5 and 2) and varied range of Reynolds number (6000 – 20000). The heat transfer and friction factor were found to increase with the decrease in twist ratio and helical pitch ratio. While the thermal performance of the tube was found to have opposite trend. In their experimental investigation, Jaisankar et al. [41] used helical twisted tapes to evaluate the heat transfer and friction factor characteristics in tubes for solar water heater system. The tube fitted with helical twist tape was found to have highest thermal performance compared to the smooth tube. Chougule and Sahu [42] evaluated the heat transfer characteristics of Al₂O₃/water and CNT/water nanofluids using helical screw tape inserts in the tube for varied range of particle volume concentration (0.15%, 0.45%, 0.60%, and 1%) and three different twist ratios (1.5, 2.5 and 3). The CNT/water nanofluid ($\phi = 1\%$) with helical tape inserts of twist ratio 1.5 was found to yield maximum heat transfer enhancement.

Twisted tape with varying length and axes

Twisted tape inserts with different length, various alternate-axes, and numerous pitches have also been used by various researchers. Experimental investigation was carried out to estimate the thermohydraulic performance in the tube fitted with twisted tape insert. Tests were performed for varying width (10 – 22 mm), various twist ratios (3, 4 and 5) and different Reynolds numbers (6000 - 13000) by Sarada et al. [43]. The enhancement of heat transfer with twisted tape inserts was found to vary between 36% to 48% and 33% to 39% for full width and reduced width inserts, respectively. This enhancement was mainly due to the centrifugal forces resulting from the spiral motion of the fluid. The thermohydraulic characteristics of the circular tubes equipped with alternate clockwise and counterclockwise twisted- tapes were investigated by Wongcharee and Eiamsa-ard [44]. Tests were conducted for the different twist ratios (3, 4 and 5) and varied range of Reynolds number (830 -1990). The thermal performance was found to increase with the increase in Reynolds number and decrease with

twist ratio. Highest thermal performance was found for the circular tube fitted with alternate clockwise and counterclockwise twisted tapes for the smallest twist ratio. Heat transfer characteristics of short-length twisted tape inserts in tubes were investigated by Eiamsa-ard et al. [45]. Tests were performed for different tape length ratios (0.29, 0.43 0.57 and 1.0) and various Reynolds numbers (4000 - 2000). The heat transfer performance was found to reduce by 14%, 9.5% and 6.7% for the short length tapes having tape length ratio 0.29, 0.43 and 0.57, respectively compared to tape length ratio 1.0. While, the friction factor values were found to reduce by 21%, 15.3%, and 10.5% for the tape length ratio 0.29, 0.43 and 0.57, respectively, compared to the tape length ratio of 1.0. Wongcharee and Eiamsa-ard [46] carried out tests in tubes involving twisted tapes with alternate-axes and wings. Experiments were conducted for different wing-chord ratios ($d/W = 0.1, 0.2$ and 0.3), a constant twist ratio (y/W) of 4.0 and different Reynolds numbers (5500 – 20200). For $Re = 5500$, $d/W = 0.3$, the tube fitted with twisted tape involving trapezoidal wings exhibited maximum thermal performance. The maximum enhancement factor in the heat transfer and friction factor were found to be 2.84 and 8.02, respectively compared to the plain tube. Eiamsa-ard and Promvonge [47] investigated the heat transfer, and pressure drop characteristics in a tube with alternate clockwise and counterclockwise twisted tapes with the different twist angles. The heat transfer is found to decrease with the reduction in the twist angle. Experiments were performed through tube fitted with peripherally cut twisted tape involving alternate axis (PTA), peripherally cut twisted tape (PT) and twisted tape (TT) by Seemawute and Eiamsa-ard [48] for varied range of Reynolds number (5000 - 20000). For $Re = 5000$, the tube fitted with peripherally cut twisted tape with alternate axis exhibited the maximum thermal performance of 1.25. While, the highest thermal performance factor for the peripherally cut twisted tape and twisted tape were found to be 1.11 and 1.02, respectively.

Multiple twisted tape inserts

Numerous studies have been made that consider multiple twisted tapes in heat exchanging equipment [49 - 54]. Bhuiya et al. [49] used double counter twisted tapes to evaluate heat transfer and fluid friction characteristics in a heat exchanger tube. Tests were performed using air as working fluid for different twist ratios (1.95, 3.85, 5.92 and 7.75) and varying range of Reynolds number (6950 – 50050). Significant enhancement in the thermal performance was reported using double counter twisted tapes. Maximum thermal enhancement factor of 1.34 was reported for the lowest twist ratio. Promvonge et al. [50] performed the experiments using helical-ribbed tube with double twisted tape inserts to investigate heat transfer characteristics. Tests were conducted for a given value of rib-height to tube diameter ratio ($e/D_H = 0.06$) and rib-pitch to diameter ratio ($P/D_H = 0.27$), wide range of twist ratio ($Y = 2.17 - 9.39$) and varying range of Reynolds number (6000 – 60000). The highest thermal performance was obtained for the twist ratio of 8.09. Bhuiya et al. [51] investigated the heat transfer characteristics in a tube fitted with triple twisted tape inserts for different twist ratios ($y = 1.92, 2.88, 4.81$ and 6.79) and varied range of Reynolds number (7200 – 50200). The Nusselt number and friction factor were found to increase by 3.85 and 4.2 times, respectively, compared to the plain tube. Vashistha et al. [52] carried out their experimental investigation using single, twin and four twisted tape inserts in a tube with three twist ratios (2.5, 3 and 3.5) and Reynolds number varied between 4000 - 14000. The highest thermal performance was found to be 1.26 for a set of four counter-swirl twisted tapes with a twist ratio of 2.5. While, the maximum heat transfer and friction factor enhancement were found to be 2.42 and 6.96 times, respectively, compared to the smooth tube. Tests were carried out by using perforated double counter twisted tape inserts in a circular tube by Bhuiya et al. [53]. Tests were performed with twisted tapes of four different porosities ($R_p = 1.2, 4.6, 10.4$ and 18.6%) for the varied range of Reynolds number (7200 – 50000) with air as the working fluid under uniform wall heat flux boundary condition. The highest thermal performance was obtained

for $R_p = 1.2\%$. The increase in heat transfer and friction factor were found to vary between 80 to 290% and 111 to 335%, respectively by using perforated double counter twisted tape inserts. In their experimental investigation, Chang et al. [54] used twist-fin inserts with five different twist ratios (2, 2.5, 3, 3.5 and infinite) for the varied range of Reynolds number (750 – 70000). The authors reported that Nusselt number ratio was increased by 1.87–4.98 and 1.3–1.95 for laminar and turbulent flow conditions, respectively.

Twisted tape inserts with slots, holes, and cuts

Twisted tapes involving slots, holes, and cuts have also been used for the heat transfer augmentation. Thianpong et al. [55] studied the effect of perforated twisted tapes with parallel wings on heat transfer enhancement in a heat exchanger tube. Study was made for different hole diameter ratios (0.11, 0.33 and 0.55), various wing depth ratios (0.11, 0.22 and 0.33) and Reynolds number varying between 5500 - 20500. The heat transfer and friction factor were found to increase with the increase in the wing depth ratio and decrease in hole diameter ratio. The perforated twisted tapes with parallel wings were found to exhibit the heat transfer enhancement of 208% compared to the smooth tube for the hole diameter ratio of 0.11 and wings depth ratio of 0.33. The circular tubes fitted with and without V-cut twisted tape insert were used by Murugesan et al. [56] to estimate the heat transfer and friction factor characteristics. Experiments were conducted for various twist ratios ($\gamma = 2.0, 4.4$ and 6.0), different combinations of depth and width ratios (DR= 0.34 and WR= 0.43, DR= 0.34 and WR= 0.34, DR= 0.43 and WR= 0.34), and varied range of Reynolds number (2000 – 12000). The tube fitted with V-cut twisted tape was found to offer higher heat transfer rate, friction factor, and thermal performance factor compared to the plain twisted tape. In addition to this, the thermal performance for the tube fitted with V-cut twisted tape was found to increase with the decrease in twist ratio and width ratio. While the thermal performance increases with the increase in depth ratio. The peripherally cut twisted tape insert were used in the tube to estimate heat transfer

and friction factor characteristics for a constant twist ratio (y/W) of 3.0, different tape depth ratios ($DR = d/W = 0.11, 0.22$ and 0.33), numerous tape width ratios ($WR = w/W = 0.11, 0.22$ and 0.33) and various Reynolds numbers (1000 – 20000) [57]. The peripherally cut twisted tape was found to offer higher thermal performance. The enhancement in Nusselt number was found to be 2.6 and 12.8 times compared to the plain tube for turbulent and laminar flow conditions, respectively. While, the maximum thermal performance factor was found to be 1.29 and 4.88 for turbulent flow and laminar flow regime, respectively. Eiamsa-ard and Promvonge [58] carried out their experiments in the tube fitted with twisted tape insert of serrated-edge (STT) to evaluate the heat transfer and pressure drop behavior. Tests were conducted for different serration width ratios ($w/W = 0.1, 0.2$ and 0.3), various serration depth ratios ($d/W = 0.1, 0.2$ and 0.3) and different Reynolds numbers (4000 - 20000). The mean heat transfer rate of the tube fitted with the STT was found to increase up to 72.2% compared to the plain tube. The thermal performance of the tube increases with the increase in depth ratio and decrease in serration-width ratio.

Winglet inserts

Oblique delta-winglet twisted tapes (O-DWT) and straight delta-winglet twisted tapes (S-DWT) were used in heat exchanging tubes by Eiamsa-ard et al. [59]. Tests were conducted with tapes for different twist ratios (3, 4 and 5), numerous depth wing cut ratios (0.11, 0.21 and 0.32) with varied range of Reynolds number (3000–27000). The tube fitted with O-DWT was found to exhibit the highest thermal performance compared to the S-DWT. For the tube with O-DWT, enhancement in Nusselt number, friction factor, and thermal performance factor were found to be 1.04 – 1.64, 1.09 – 1.95 and 1.05 – 1.13 times, respectively, compared to the plain tube. Different tape inserts, including butterfly, classic, and jagged twisted tapes were used to evaluate thermohydraulic performance in the heat exchanging tubes through both experimental and

numerical investigation [60]. The highest thermal performance factor of 1.62 was found by employing butterfly inserts in the heat exchanging tube.

Wire coil inserts

Roy and Saha [61] carried out their investigation using helical screw tape with oblique teeth inserts and wire coil inserts for the heat transfer enhancement in a circular tube. The authors reported that increase in the helix angle enhances the heat transfer in the tube. Promvonge [62] investigated the heat transfer characteristics using twisted tape and wire coil turbulators in a tube for varied range of Reynolds number (3000 - 18,000). The heat exchanger involving wire coils with twisted tape exhibited better enhancement in heat transfer compared to the system that used either wire coils or twisted tape. Hamid et al. [63] used wire coil inserts to evaluate the heat transfer performance of nanofluids in a tube for various volume concentrations of nanofluids (0.5 - 3.0%), numerous ratios of pitch to diameter ($P/D = 0.83 - 4.17$) and different Reynolds numbers (2300 - 12000). For 2.5% volume concentration and $P/D = 1.5$, the tube integrated with the wire coil insert and SiO_2 - water nanofluids exhibited optimum performance. Coiled wire inserts [64] were used to estimate the heat transfer characteristics of tube for varied range of pitch-to-diameter ratios ($P/D = 1, 2, 3$) and different Reynolds numbers (3429 - 26663). The maximum thermal performance was found to be 1.82 for $P/D = 1$ and $Re = 3429$.

Turbulators

Turbulators of various designs and shapes have been used by different researchers [65-77]. Turbulators are found to generate the swirl inside the flow regime, increase the fluid mixing, enhance the turbulence intensity, and provide heat transfer enhancement. In addition to this, turbulators are found to increase the heat transfer surface area. The heat transfer augmentation using various design of turbulators are discussed below.

Turbulators in the form of vortex ring were used for the heat transfer augmentation. The influence of inclined vortex rings (VR) on heat transfer augmentation were studied by Promvonge et al. [65]. Experiments were performed for different relative ring-width ratios ($BR = b/D = 0.1, 0.15$ and 0.2), four relative ring pitch ratios ($PR = P/D = 0.5, 1.0, 1.5$ and 2.0) and various Reynolds numbers ($5000 - 26000$), using air as working fluid. Heat transfer and pressure drop values were found to increase with BR. The tube fitted with $BR = 0.1$ and $PR = 0.5$ was found to exhibit the highest thermal performance. Kongkaitpaiboon et al. [66] carried out experiments for a round tube fitted with circular-ring turbulators at various diameter ratios ($0.5- 0.7$), different pitch ratios ($6-12$) and varied range of Reynolds number ($4,000-20,000$) with air as working fluid. The turbulators with smallest pitch ratio and diameter ratio exhibited the highest heat transfer rate. In their experimental investigation, Thianpong et al. [67] employed twisted ring turbulators in the tubes with different width ratios ($W/D = 0.05, 0.1$ and 0.15), numerous pitch ratios ($p/D = 1, 1.5$ and 2) and various Reynolds numbers ($6000 - 20000$). Twisted rings were found to yield lower value of Nusselt number and friction factor compared to the circular rings. The maximum thermal performance factor associated with twisted ring turbulators was obtained at smallest width ratio and pitch ratio. Tubes involving circular-ring turbulator (CRT) and twisted tape (TT) were investigated by Eiamsa-ard et al. [68]. Tests were performed for different pitch ratios ($l/D = 1.0, 1.5,$ and 2.0) of the CRT, various twist ratios ($y/W = 3, 4,$ and 5) of the TT and different Reynolds numbers ($6000 - 20000$). The tube integrated with CRT and TT was found to exhibit 25.8%, 82.8%, and 6.3% higher value in Nusselt number, friction factor, and thermal performance, respectively compared to the tube with CRT alone. Akansu [69] studied heat transfer and pressure drop for porous ring turbulators in a circular pipe. The authors reported that the recirculation regions were larger at higher blockage ratio.

Karakaya and Durmus [70] reported the heat transfer behavior of converging, diverging, and converging-diverging conical spring turbulators in the

inner tube of DPHE tube for the varied range of Reynolds number (10,000-34,000). Saturated steam was used to maintain the constant wall temperature for the inner tube. The authors reported that the highest rate of heat transfer was obtained with diverging array of conical spring turbulators at $Re = 34000$. Eiamsa-ard and Promvonge [71] carried out experiments in a tube using V-nozzle turbulators for pitch ratio varying between 2- 7 and varied range of Reynolds number (8,000-18,000) for constant heat flux condition with air as working fluid. The authors reported that the lowest pitch ratio provided the highest thermal performance. Sheikholeslami et al. [72] investigated the heat transfer and pressure drop characteristics using discontinuous helical turbulators in the annulus of double pipe heat exchanger (DPHE) for varied range of pitch ratio (1.83–5.83), various open area ratios (0– 0.0625) and different Reynolds numbers (6000–12,000). They used water in the inner tube and air in the annulus as the working fluid. The authors reported that friction factor and Nusselt number were decreased with the increase in open area ratio and pitch ratio. Sheikholeslami and Ganji [73] investigated the heat transfer characteristics of a DPHE with air as a working fluid in the annulus and water in the inner tube by using perforated turbulators in the annulus for wide range of pitch ratio (1.06-5.83), various open area ratios (2.26-2.92) and varied range of Reynolds number (6,000-12,000). The maximum thermal performance was found to be 1.59 at $Re = 6000$ and $PR = 1.06$. In their numerical and experimental study, Sheikholeslami et al. [74] investigated the heat transfer and pressure drop characteristics using two arrays of perforated conical ring turbulators such as direct conical ring array and reverse conical ring in the annulus. Tests were conducted for different conical angles (0° – 30°), numerous open area ratios (0–0.0833), various pitch ratios (1.83–5.83) and different Reynolds numbers (6000–12,000). The authors used water in the inner tube and air in the annulus. The thermal performance was found to increase with decrease in pitch ratio and with increase in open area ratio and conical angle. Ruengpayungsak et al. [75] used gear as turbulator in tubes with different free-space length ratios ($SR = 1.0, 2.0$ and 3.0), various tooth numbers ($N = 8, 16$ and

24) and varied range of Reynolds number (6000 - 20000) with air as working fluid. For $SR = 2.0$ and $N = 24$, the tube fitted with turbulator exhibited maximum thermal performance. Sheikholeslami et al. [76] investigated the heat transfer characteristics in an annulus of DPHE by using circular-ring and perforated circular-ring turbulators at various pitch ratios (1.83, 2.92 and 5.83), different perforated holes (0, 2, 4 and 8) for Reynolds number varying between 6,000-12,000. Here, air and water were allowed to flow in the annulus and the inner tube, respectively. The thermal performance was found to increase with the increase in the number of holes in the turbulators. The thermal performance was found to decrease with increase in Reynolds number and pitch ratio. Sheikholeslami and Ganji [77] carried out their experiments using discontinuous helical turbulators in the annulus of DPHE for different open area ratios (0 and 0.0625), various pitch ratios (1.83, 2.92 and 5.83) and varied range of Reynolds number (6000-12000) with air as the working fluid. Discontinuous helical turbulators with perforation was found to exhibit higher thermal performance. In their experimental investigation, Kumar et al. [78] used solid and perforated circular disk with twisted tape insert in the tube for different pitch ratios (1, 2, and 3), various perforation indexes (0%, 8%, 16%, and 24%) and various Reynolds numbers (6500 to 26500). The thermal performance factor of tube with turbulators was found to be 1.18 – 1.64 times compared to smooth tube. The maximum heat transfer enhancement was obtained at the lowest pitch ratio and the lowest perforation index. A brief summary of the literature pertaining to the corrugated tube geometries and turbulators in the heat exchanging equipment are discussed in Table 1.1 and 1.2, respectively.

Table 1.1: Summary of experimental investigations for corrugated tube geometries.

Source	Corrugation Type	Pitch (P)/Height of corrugation (e)/ helix angle θ	Working fluid	Reynolds Number	Remarks
Rainieri and Pagliarini [11]	Transverse corrugated tube	$P=16-64\text{mm} / e = 1.5 / \theta = 0$	Water	90-800	Heat transfer depends upon the ration of Re and pitch in the entry region.
Ahn [12]	Helically corrugated inner tube in DPHE	$P= 2-10\text{mm}/ e = 0.75-1.25 \text{ mm}/ \theta = 61.2 - 86.4$	Water in annuli	1700-13000	Significant enhancement in the heat transfer is observed by using corrugated tube for DPHE.
Vicente et al. [13]	Corrugated tube	$P = 15.95- 20.84/ e= 0.48-1.03$	Water and ethylene glycol / Pr = 4-7	200-90000.	Heat transfer is found to increase by 30% in laminar region
Pethkool et al. [15]	Helically corrugated inner tube in DPHE	Pitch= 4.5, 5.5 and 6.5/ e = 0.5, 1.0 and 1.5/ $\theta = 15$	Water in annulus	5500-60000	Thermal performance was found to be 2.3for the corrugated tube with $P/D_H=0.27$ and $e/D_H=0.06$ at lower Re.

Table 1.1 (Continued).

Wongcharee and Eiamsa-ard [16]	Inner corrugated tube equipped with twisted tape inserts in DPHE	CuO concentrations 0.3, 0.5 and 0.7% by volume. twist ratios =2.7, 3.6 and 5.3	CuO/water nanofluid in annuli	6200 – 24000	At $Re = 24000$, CuO volume concentration 0.7% at twist ratio 2.7, the performance was found to be highest. Performance increased with the combined effect of corrugation and inserts.
Dizaji et al. [18]	Both corrugated tube inner and outer	$P = 16.52 \text{ mm} / e = 4 \text{ mm} / \theta = 0$	Water in annuli	3500-18,000	Concave and convex combination of corrugated tube was investigated and reported highest performance for corrugated concave outer tube and convex corrugated inner tube.
Harless et al. [23]	Single and three start corrugated tubes	$P=6.21-35.08 \text{ mm} / e = 0.46-1.28 / \theta = 9.2 - 36.9$	Air	5000-23000	Heat transfer was found to be highest for the case of single start tube with lowest pitch and $e = 0.74$.
Jianfeng et al. [36]	Spirally grooved tube	$P=10.2 / e=0.38-0.76 / \theta = 78$	Molten salt/ $Pr=13.5-15.2$	5000-15000	Enhancement in heat transfer and pressure drop is observed with spirally grooved tube.

Table 1.2: Summary of experimental investigation using various turbulators.

Source	Types of turbulator	Pitch/Height/angle/Ratios	Working fluid	Reynolds Number	Remark
Kongkaitpaiboon et al. [66]	circular ring turbulators in tube	diameter ratios (DR=d/D=0.5, 0.6 and 0.7) and pitch ratios (PR=p/D=6, 8 and 12)	Air	4000 - 20000	Heat transfer enhanced 57% to 195% compared to smooth tube.
Thianpong et al. [67]	twisted ring turbulators	Width ratios (W/D=0.05, 0.1 and 0.15), pitch ratios of (p/D=1, 1.5 and 2)	Air	6000 - 20000	Higher twisted rings yield lower Nu and f values; except at the largest width ratio (W/D=0.15) and the smallest pitch ratio (p/D=1.0).
Karakaya and Durmus [70]	conical spring turbulators	300, 450 and 600 (cone angle)	Air	10,000–34,000	Reduction in exergy losses was observed with rise in conical angle while using converging and diverging turbulators in the annulus of DPHE.
Eiamsa-ard and Promvonge [71]	V-nozzle turbulators	PR=2.0, 4.0, and 7.0	Air	10,000 – 18,000	A maximum enhancement in efficiency was 1.19 at smallest pitch ratio (PR=2.0).

Table 1.2 (Continued).

Sheikholeslami et al. [72]	Discontinuous helical turbulators	open area ratio (0–0.0625), pitch ratio (1.83–5.83)	Air	6000 - 12000	f and Nu values reduce with rise of open area ratio and pitch ratio. While TPF is an increasing function of open area ratio and decreasing function of pitch ratio.
Sheikholeslami and Ganji [73]	perforated turbulators	open area ratio (0–0.0833), pitch ratio (0.72–5.83)	Air	6000 - 12000	Maximum value of thermal performance is 1.59 at optimized PR = 1.06 for Re = 6000 and $\lambda = 0.07$.
Sheikholeslami et al. [74]	Direct conical ring (DCR) array and Reverse conical ring (RCR) array	open area ratio (0–0.0833), pitch ratio (1.83–5.83) and conical angle (0° – 30°).	Air	6000 - 12000	thermal performance rises with augment of conical angle for direct conical ring array
Ruengpayungsak et al. [75]	gear-ring elements as turbulator	tooth numbers (N = 8, 16 and 24) and free-space length ratios (SR = s/D = 1.0, 2.0 and 3.0)	Air	6000 - 20000	A maximum number of teeth and the largest free space length ratio poses the highest thermal performance factor of 1.3 using the gear ring elements in the tube.

Table 1.2 (Continued).

Sheikholeslami et al. [76]	perforated circular ring	pitch ratio (1.83, 2.92 and 5.83) and perforated hole (0, 2, 4 and 8).	Air	6000 - 12000	Thermal performance increases with increase of number of holes, but it decreases with increase of Reynolds number and pitch ratio.
Kumar et al. [80]	hollow circular disk	Thickness ratio = 0.0075, diameter ratios (0.6, 0.7 and 0.8) and pitch ratios (1, 2, 3 and 4).	Air	6500 - 23,000	4.45 times enhancement in heat transfer in case of PR = 1 and DR = 0.6, and around 1.4 times enhancement in thermal performance factor for PR = 1 and DR = 0.8
Promvongse and Eiamsa-ard [81]	Converging and diverging conical nozzle turbulators	PR=2.0, 4.0, and 7.0	Air	8,000 - 18,000	236 to 344% enhancement is obtained in heat transfer using conical nozzle turbulators.

1.5 Scope of the present experimental investigation

The literature review reports the thermohydraulic performance of heat exchanging equipment involving various passive techniques through both experimental and numerical investigations. It may be noted that passive techniques are advantageous due to its various advantages such as simple manufacturing process with low cost, easy installation and removal, preservation of mechanical strength original plain tube, possibility of installation in an existing smooth tube heat exchanger, fouling mitigation in refineries, chemical industries and marine application [4]. Passive technique includes corrugated tubes, twisted tubes, tape inserts, wire coil inserts, and turbulators for varied range of coolant flow rate and experimental parameters. These techniques are used based on its possibility of installation in a heat exchanging equipment and their improved thermal performance. The comparison of thermal performance factor obtained utilizing various passive techniques in tube and DPHE are provided in the fig. 1.6. Nevertheless, various issues pertaining to the thermal hydraulic performance of heat exchanging equipment need further investigation. These are detailed below.

1. The heat transfer in corrugation geometries is found to depend on Reynolds number, corrugation pitch, and corrugation height. Further investigation is needed to identify the different configurations of geometrical modifications for the corrugated tube to achieve better thermal performance.
2. Studies with air as working fluid involving corrugated geometry for varied range of diameter ratios and pitches are limited in the literature.
3. Studies using turbulators at various pitch ratios, and diameter ratios with air as working fluid, have not been reported comprehensively in the literature. In case of helical surface turbulators, different helix angle is not studied extensively.
4. The influence of the helical surface turbulators on thermal performance of the double pipe heat exchanger has not been studied extensively.

5. Report the thermal performance data for DPHE with various passive enhancement techniques involving varied range of coolant flow rate and design parameters.

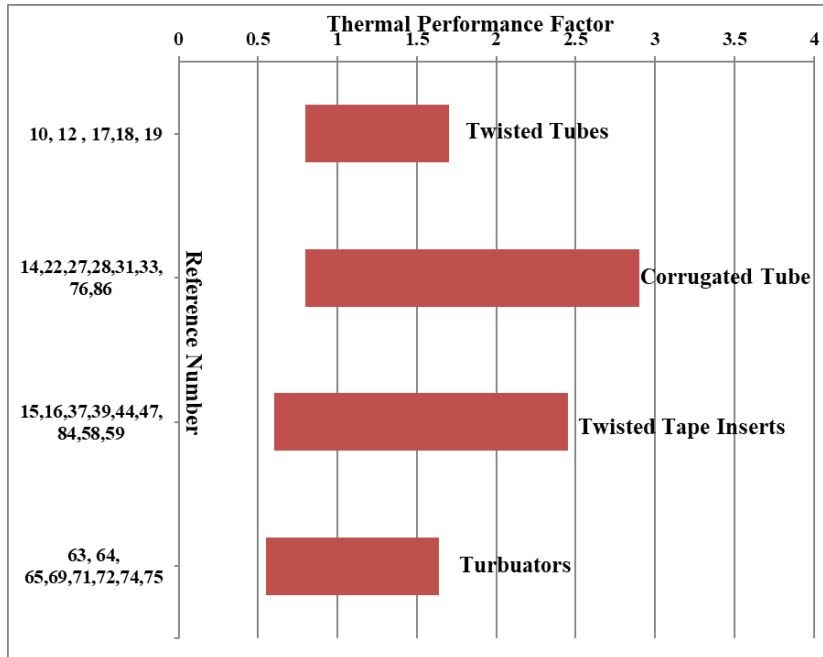


Fig. 1.6: Comparison of thermal performance factor of various passive techniques.

The present study is aimed to obviate some of the aforementioned limitations through experimental investigation. Here, efforts have been made to analyze the heat transfer, pressure drop characteristics, and thermal performance parameters of DPHE involving various passive techniques.

The organization of the thesis is as follows:

The thesis contains five chapters. The organization of the chapter is as follows:

Chapter 1: It introduces various augmentation techniques. A brief review of various passive techniques is discussed in this chapter. Finally, objectives of the present investigation are highlighted.

Chapter 2: This chapter deals with the experimental study on the heat transfer and pressure drop characteristics in the annulus of DPHE formed by inner smooth tube and outer corrugated tube with varying diameter ratio and corrugated pitch.

Chapter 3: This chapter reports the effect of plain surface disc turbulators on the thermohydraulic performance of DPHE.

Chapter 4: The chapter presents the experimental investigation to analyze the effect of helical surface disc turbulators on the thermal performance of DPHE.

Chapter 5: Conclusions obtained from the present experimental investigation are presented in this chapter. In addition, the scope for further investigation is discussed.

Chapter 2

Augmentation of experimental heat transfer and pressure drop characteristics in annuli formed by smooth inner tube and corrugated outer tube

2.1 Introduction

Heat transfer enhancement plays an important role during the design of heat exchanging equipments. The enhancement in heat transfer not only improves the system efficiency but also reduces size and operating cost. In view of this, efforts have been made to employ various techniques to improve the heat transfer performance. The enhancement techniques can be broadly classified into two categories. Active techniques that need external power source, passive techniques that do not need external power. The effectiveness of these techniques is found to depend on the mode of heat transfer that includes single phase free convection, single phase forced convection, pool boiling, convective boiling, and convective condensation. Numerous studies have been made that report enhancement up to 200% by using various passive techniques [13-24]. These include rough tubes, corrugated tubes, inner fin tubes, and twisted tape inserts. Experimental studies involving corrugated tubes for various corrugation geometry and fluid types are limited in the literature. In view of this, a systematic experimental study has been made to evaluate the thermal performance of various corrugated geometry for varied range of operating and design parameters.

In the present chapter, an experimental investigation has been carried out to study the heat transfer and pressure drop characteristics of annuli formed by smooth inner tube and corrugated outer tube in counter flow conditions for the different diameter ratios (0.53, 0.44 and 0.40) and various pitches (10 mm, 20 mm, and 30 mm), and Reynolds number varying between 3500-10500 with air as working fluid. In addition to this, correlations have been proposed for friction

factor, Nusselt number, and thermal performance factor as a function of various modeling parameters.

Different terminologies are used in the present experimental investigation and are discussed below.

Pitch (P)

Pitch of the corrugated tube is defined as the distance between two consecutive points, where the orientation of the tube cross-section exactly coincides with each other along the length of tube.

Diameter ratio (DR)

Diameter ratio is defined as the ratio of outer diameter of inner tube to the inner diameter of outer tube.

$$DR = \frac{d_o}{D_i} \quad (2.1)$$

2.2 Test facility, procedure and data reduction

2.2.1 Test facility

Figs.2.1 (a-b) show the schematic view of the test facility and test specimen, respectively, used to estimate the heat transfer and friction factor characteristics of flow through annuli formed by smooth inner tube and corrugated outer tube in counter flow conditions and schematic of test specimen, respectively. While, Figs. 2.2 (a-b) show the photographic view of the test facility and test specimen, respectively. The test facility includes the test specimen, water flow system, and air flow system and instrumentation scheme. The test specimen is a DPHE formed by smooth inner tube and corrugated outer tube. The corrugation height (e) is kept 2.5 mm for all the test specimens. Detail of the test specimen is provided in Table 2.1. Twelve test specimens are used (TS1-TS12) in

the investigation. Here, TS1, TS2, and TS3 denote the DPHE made of smooth inner and smooth outer tubes. While, TS4 to TS12 denote the DPHE with smooth inner and corrugated outer tube of three different corrugated pitches and three different diameter ratios. Inner tube is made of copper material while outer tube is made of borosilicate glass material for each test specimen. Purpose of using borosilicate glass (as corrugated outer tube), is easy manufacturing of corrugation on glass tube. The specimens are prepared using the glass blowing lathe machine.

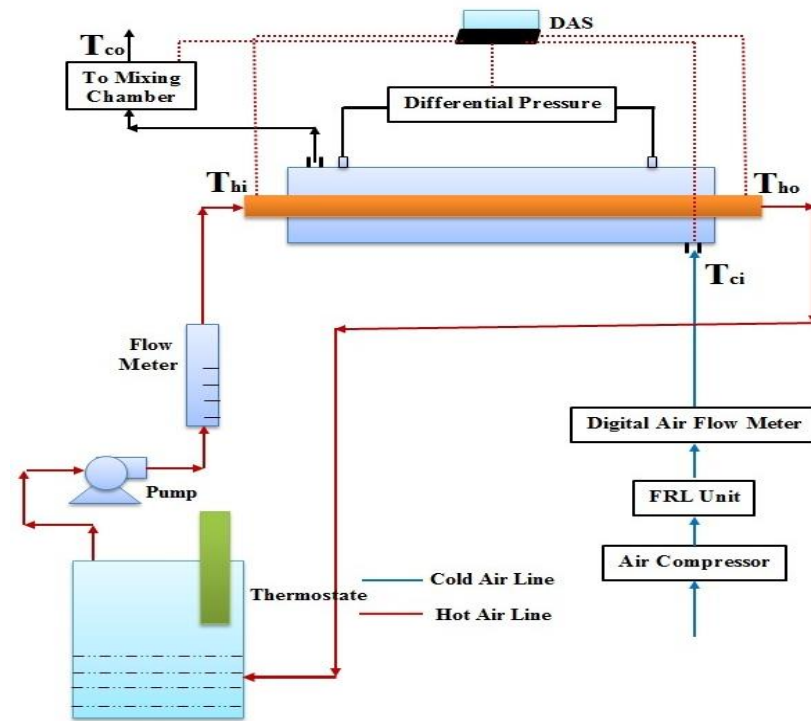


Fig. 2.1 (a): Schematic of experimental test facility.

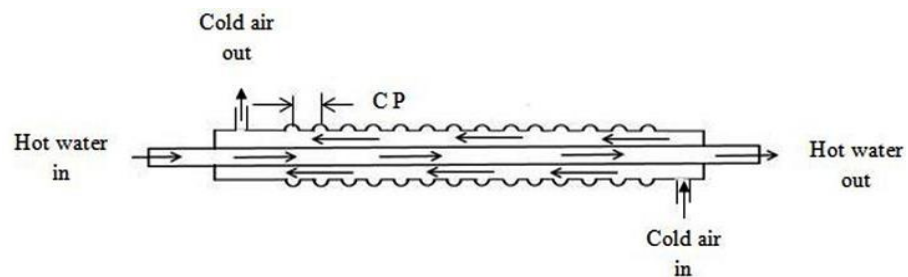
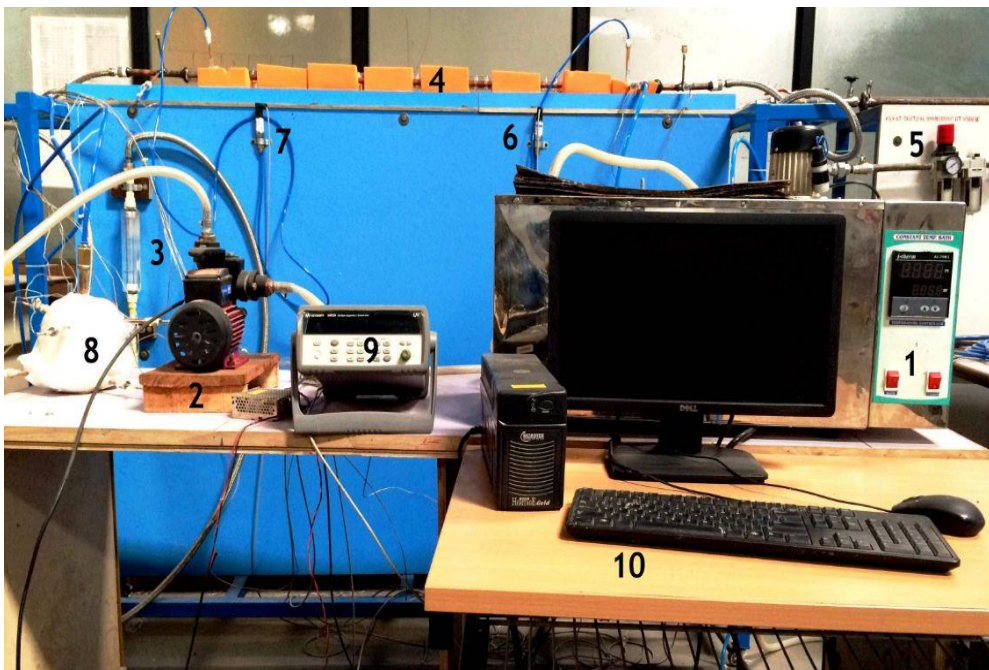


Fig. 2.1 (b): Schematic of test specimen.

In this study, water (hot fluid) flows in a closed circuit and through the smooth inner tube. While, air (cold fluid) flows through the annulus formed by smooth inner tube and corrugated outer tube. The main aim of the study is to estimate the friction factor and heat transfer characteristics of air through the annulus. A constant temperature bath (Thermostat- BTI-11) of 35 liters capacity is used for supply water through inner tube. Water in the constant temperature bath is heated by using 2 KW heaters. After attaining the required temperature, water is pumped to the flow circuit by using a centrifugal pump (1-phase, 2800rpm, 0.5 HP). The water flow rate is measured by calibrated rotameter of range 0.05 - 0.35 kg/s with least count 0.05 kg/s and the flow rate of the water is maintained nearly 0.173 kg/s for the entire duration of experiments. Here, water enters in the inner tube of DPHE and exit water from the heat exchanger is sent back to the constant temperature bath for further use.



1.	Thermostat	2.	Centrifugal pump
3.	Rota meter	4.	Test section
5.	FRL unit	6.	Pressure transducer at air inlet
7.	Pressure transducer at air outlet	8.	Mixing chamber
9.	Data Acquisition System	10.	Computer unit

Fig. 2.2 (a): Photographic view of test facility.

Table 2.1: Detail of experimental test specimens.

Test section	Diameter ratio (DR)	Inner tube			Outer tube (Shell)			Corrugated Pitch (CP) (mm)
		Length, L_t (mm)	Internal Diameter, d_i (mm)	External Diameter, d_o (mm)	Length, L_s (mm)	Internal Diameter, D_i (mm)	External Diameter, D_o (mm)	
TS1	0.40	1800	14	16	1600	40	45	Infinite
TS2	0.44	1800	14	16	1600	36	41	Infinite
TS3	0.53	1800	14	16	1600	30	35	Infinite
TS4	0.40	1800	14	16	1600	40	45	10
TS5	0.40	1800	14	16	1600	40	45	20
TS6	0.40	1800	14	16	1600	40	45	30
TS7	0.44	1800	14	16	1600	36	41	10
TS8	0.44	1800	14	16	1600	36	41	20
TS9	0.44	1800	14	16	1600	36	41	30
TS10	0.53	1800	14	16	1600	30	35	10
TS11	0.53	1800	14	16	1600	30	35	20
TS12	0.53	1800	14	16	1600	30	35	30



Fig. 2.2 (b): Photographic view of test specimen.

In this study, air flows in an open circuit. The atmospheric air is compressed by using air compressor (Make: Ingersoll Rand Make; Maximum pressure: 12.30 kg/cm²; capacity: 225 L). The compressed air is allowed to flow through the annulus of heat exchanger opposite to the direction of flow of water. The air flow rate issuing from the compressor is measured by using a digital compressed air counter (make: Testo Inc.; model: 6441; range: 0.25-75 Nm³/h), which works on the calorimetric principle of flow measurement with a reading accuracy of $\pm 0.3\%$. An FRL unit (Filter Regulator and Lubricator) is fitted at upstream of the compressed air counter to filter air and to maintain the required downstream pressure. A ball valve located in the upstream direction of the compressed air counter is used to achieve the desired flow rate. Two absolute pressure transmitters (Make: Omicron; model: P8741-6-010BG; pressure range: 0-10 bar) with an accuracy of $\pm 0.25\%$, are used to measure the pressure drop across the annulus. The air flowing through the annulus takes heat from the water and exits to the atmosphere. The inlet and outlet bulk temperature of both air and water are measured by using pre-calibrated RTD, having an accuracy of 0.1°C. Air inlet, water inlet, and water outlet temperatures were measured by using single thermocouple at each location. While a mixing chamber [27 - 28] is used to measure the mean temperature of outlet air. Mixing chamber made of glass vessel and equipped with six thermocouples located at two different planes (3 on each plane). These planes are 80 mm apart from each other. The Photographic and schematic view of mixing chamber is shown in Fig. 2.3.

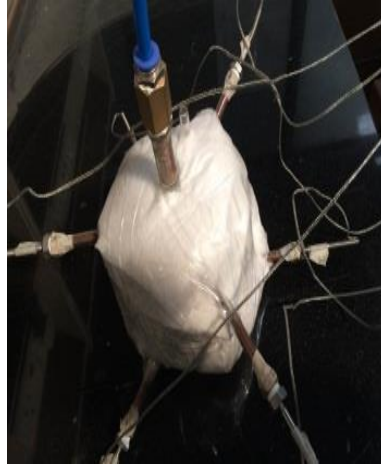


Fig. 2.3 (a): Photographic view of mixing chamber.

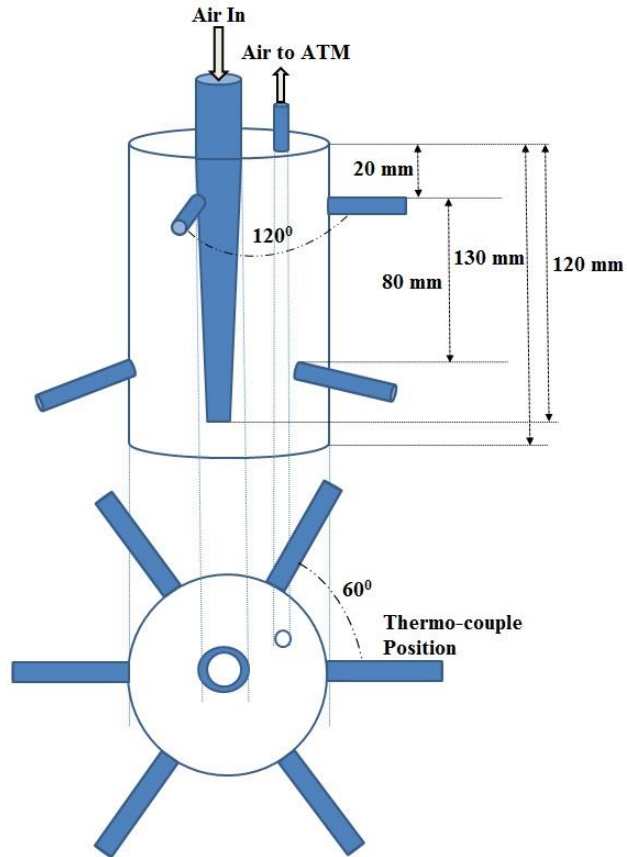


Fig. 2.3 (b): Schematic view of mixing chamber.

2.2.2 Experimental procedure

Before starting the test run, water is heated to a temperature of 70- 75°C in the constant temperature bath. Initially, the compressed air is allowed to flow through the annulus of heat exchanger. The temperature of inlet air is maintained at temperature varying between 25 – 27°C. The flow rate of air is adjusted to obtain a required Reynolds number. Subsequently, hot water is allowed to flow through the inner tube of heat exchanger. Temperatures are measured at the regular interval of 10 seconds. After attaining the thermal equilibrium, the final readings are noted. After taking one set of readings, the air flow rate is adjusted to a new Reynolds number. Tests have also been carried out to confirm the reliability of the measured data. The mass flow rate of water is kept constant for the entire duration of experiments because the annulus is of primary interest. A large range of air flow rates is covered in this study.

2.2.3 Data reduction

Here, the entry length was kept constant of 500 mm and hydraulic mean diameter of the annulus is varied (14 – 24 mm) for all the configuration of corrugated DPHE. Therefore, length to hydraulic mean diameter ratio (L/D) of the test section varies between 21- 35 and flow in the annulus is assumed to be fully developed [24]. The average Nusselt number and the friction factor for the fluid flow through the annulus can be evaluated as below.

The heat duty supplied by hot fluid can be expressed as:

$$Q_h = m_h C_{ph} (T_{h,in} - T_{h,out}) \quad (2.2)$$

Where Q_h , m_h , C_{ph} represents the heat supplied by the hot fluid, mass and specific heat of hot fluid, respectively. While, $T_{h,in}$ and $T_{h,out}$ denotes the inlet and outlet temperatures of hot fluid, respectively.

The heat duty absorbed by cold fluid can be expressed as:

$$Q_c = m_c C_{pc} (T_{c,out} - T_{c,in}) \quad (2.3)$$

Where Q_c , m_c , C_{pc} represents the heat absorbed by the cold fluid, mass, and specific heat of cold fluid, respectively. While, $T_{c,in}$ and $T_{c,out}$ denotes the inlet and outlet temperatures of cold fluid, respectively.

The experimental test specimen was well insulated to prevent heat losses. The average heat duty of the system is calculated using Eq. (2.4):

$$Q_{avg} = \frac{Q_h + Q_c}{2} \quad (2.4)$$

For the counter flow double pipe heat exchanger, the heat transfer coefficient is calculated using Eq. (5) [28]

$$Q_{avg} = UA_s \Delta T_{LMTD} \quad (2.5)$$

Where, U , A_s and ΔT_{LMTD} denotes the overall heat transfer coefficient, Heat transfer area, and logarithmic mean temperature difference respectively. Here, ΔT_{LMTD} can be calculated as below:

$$\Delta T_{LMTD} = \frac{(T_{h,in} - T_{c,out}) - (T_{h,out} - T_{c,in})}{\ln \frac{T_{h,in} - T_{c,out}}{T_{h,out} - T_{c,in}}} \quad (2.6)$$

The overall heat transfer coefficient can be written in term of individual heat transfer coefficients as given below:

$$\frac{1}{UA_s} = \frac{1}{(hA_s)_h} + \frac{1}{(hA_s)_c} + R_w \quad (2.7)$$

Where, U , A_s , h and R_w denote the overall heat transfer coefficient, surface area of heat transfer, heat transfer coefficient and wall resistance respectively. The inner tube and outer tube are thoroughly cleaned before conducting experiment, and therefore, the fouling resistance is neglected for the analysis. The thickness of the inner tube is of 1 mm, and thermal conductivity of

copper material is considered as 401W/m-k [82]. In such case, one can evaluate the wall resistance R_w as below:

$$\begin{aligned} R_w &= \frac{\text{Wall thickness}}{\text{thermal conductivity of copper}} \\ &= 0.001/401 \\ &= 2.49 \times 10^{-6} \text{ m}^2\text{K/ W} \end{aligned} \quad (2.8)$$

In this study, the thickness of inner tube is very small, and thermal conductivity is very high. Therefore, the wall resistance of the tube material can be neglected for the analysis. Neglecting the wall resistance (R_w), Eq. 2.7 can be written as:

$$\frac{1}{UA_s} = \frac{1}{(hA_s)_h} + \frac{1}{(hA_s)_c} \quad (2.9)$$

Initially, Dittus-Boelter equation [83] is used to estimate the heat transfer coefficient for both water side and air side for the lowest flow rate of the air. Subsequently, the thermal resistances were calculated for both water and air sides. The maximum water side resistance is less than 1% of the air side resistance.

$$\frac{1}{(hA_s)_h} \ll \frac{1}{(hA_s)_c} \quad (2.10)$$

Under this condition, the water side resistance can be neglected for estimating the heat transfer coefficient in the air side [27] and Eq. 2.9 can be written as:

$$\frac{1}{UA_s} = \frac{1}{(hA_s)_c} \quad (2.11)$$

In such case, the overall heat transfer coefficient can be written as:

$$U = h_c \quad (2.12)$$

Nusselt number can be calculated by using following equation

$$Nu = \frac{h_c D}{K} \quad (2.13)$$

Where, h_c , D , K denotes air side convective heat transfer coefficient of cold fluid side, hydraulic mean diameter of annulus and thermal conductivity of air, respectively.

In this study, pressure drop is measured along the length of test section in the annulus. The average friction factor is calculated as below:

$$f = \frac{\Delta P D}{2L\rho V^2} \quad (2.14)$$

Where, f , ΔP , D , L , ρ and V denotes average friction factor, pressure difference, hydraulic mean diameter of annulus, length of tube, air density and velocity of air in annulus, respectively. The results obtained from this study are elaborated in the next section.

2.3 Results and discussion

Initially, tests have been performed with smooth tube DPHE without corrugation at three different value of DR (0.40, 0.44, and 0.53) to validate the test facility. The Nusselt number results for the smooth tube DPHE are compared with the Dittus-Boelter correlation [83] while friction factor correlation [83] has been used to validate the friction factor that has been obtained from experimental results and are shown in Tables 2.2 - 2.3, respectively.

Tests are conducted with smooth and corrugated tubes, and the detail of the test sections are provided in Table 2.1. This includes three different values of DR and three different value of P. Later on, tests are conducted in corrugated tubes with three different P values (10, 20 and 30 mm) and three different values of DR (0.40, 0.44 and 0.53). In all the cases, the water (hot fluid) flows inside the inner tube, and the air (cold fluid) is issued through the annulus. During the experiments, the rise in temperature of water is found to 8 - 13°C. While, the maximum difference between inlet and outlet of water temperature is found to be

1°C. This may be due to large difference in specific heat of water and air. In such case, one can assume the outer wall of inner tube is at constant temperature [27]. Here, outer wall of outer tube is covered with the ceramic glass wool insulation and therefore the outer wall of heat exchanger is assumed to be adiabatic. The cross-section boundary conditions considered in this study is of third kind [83] and is shown in Fig.2.4.

Table 2.2: Experimental validation of Nusselt number with smooth tubes.

DR	Re	Nusselt number			Remarks
		Experiment	Correlation	% variation	
0.40	3900	13.41	14.88	-9.88	Turbulent flow, compared with Dittus-Boelter Correlation [83] $Nu = 0.023 Re^{0.8} Pr^{0.4}$
	5800	19.46	20.44	-4.78	
	9300	30.61	29.82	2.66	
0.44	4400	14.91	16.38	-9.00	
	6300	20.72	21.84	-5.09	
	9200	29.95	29.56	1.32	
0.53	4300	13.72	16.09	-14.72	
	7600	22.87	25.37	-9.87	
	9700	29.70	30.84	-3.71	

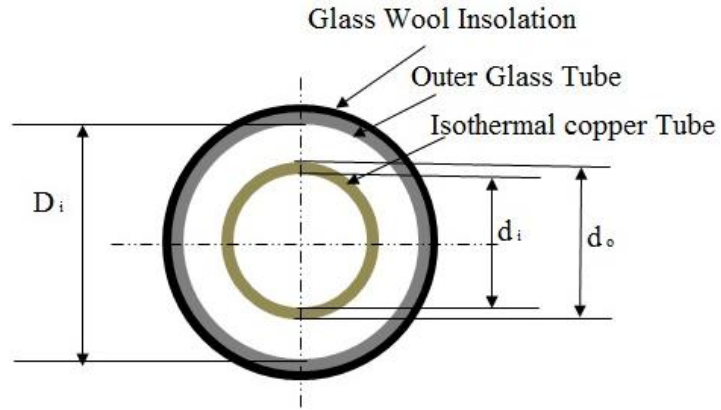


Fig.2.4: Cross-section and boundary conditions of double pipe heat exchanger.

Table 2.3: Experimental validation of friction factor with smooth tubes.

DR	Re	Friction factor			Remark
		Experiment	Correlation	% variation	
0.40	4000	0.00903	0.00993	-9.11	Compared with $f = 0.079Re^{-0.25}$ [83]; Re >2300
	6300	0.00834	0.00886	-5.88	
	8700	0.00790	0.00818	-3.36	
0.44	4800	0.00812	0.00949	-14.42	
	6800	0.00751	0.00869	-13.57	
	8600	0.00739	0.00820	-9.83	
0.53	5800	0.00777	0.00905	-14.14	
	9000	0.00706	0.00811	-12.87	
	9700	0.00691	0.00796	-13.09	

2.3.1 Friction factor characteristics

Fig. 2.5 depicts the variation of f values of corrugated tubes with Re, P and DR. The value of f is found to decrease with increase in Re value. Higher f value is obtained for the lower value of DR. Lower value of DR indicates higher

annulus diameter resulting in higher friction in the fluid layers. Similar results for the f values have been reported by earlier researchers Dirker et al. [84] and Darzi et al. [20]. It is observed that lower value of P exhibits higher f values. Smaller P value over a given length of the tube results in higher corrugation effect.

It may be noted that the corrugation on the tubes cause the variation in streamlines and the path lines [18 - 19] and hence generates more turbulence in the flow, which causes more drop in the pressure inside flow passage, resulting in increase in f values. The maximum value of f is obtained at lower P value 10 mm at lower Re for each DR . For a given P value 10 mm, the f values for different configurations ($DR=0.4$, $Re = 3500$), ($DR = 0.44$, $Re = 3500$) and ($DR = 0.53$, $Re = 3500$) are found to be 0.0476, 0.0412 and 0.0376, respectively. The maximum percentage increment in f value is found to be 81% for $DR=0.40$ and $P = 10$ mm compared to the smooth tube DPHE.

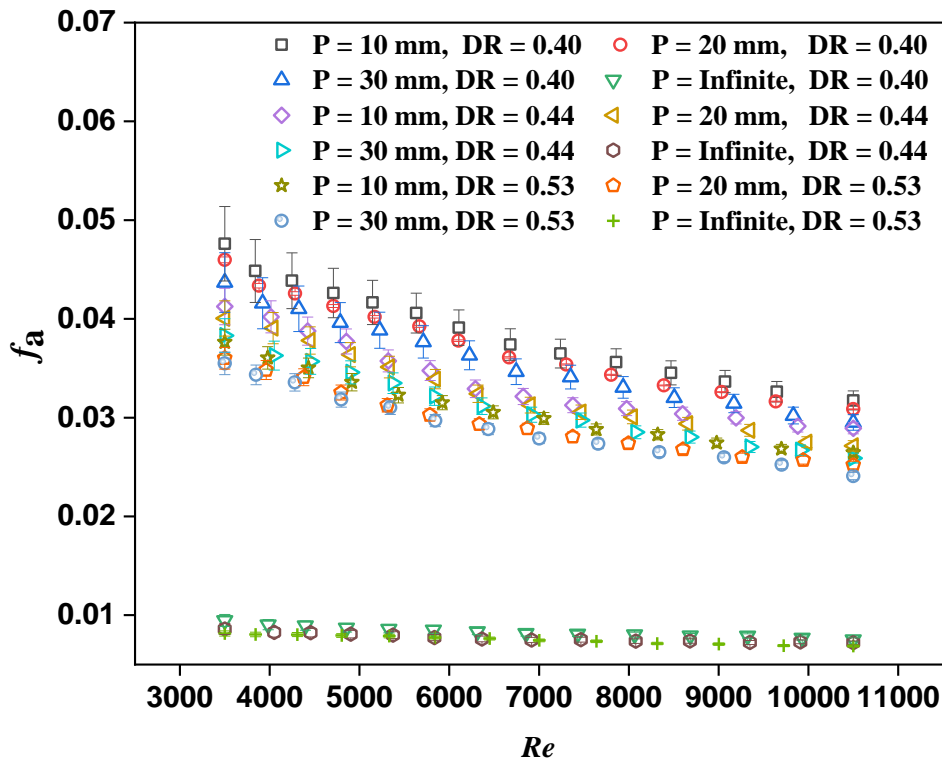


Fig. 2.5: Variation in average friction factor of annulus with respect to Reynolds number.

2.3.2 Heat transfer enhancement

The variation of the average value of Nu with Re for various values of P and DR is shown in Fig. 2.6. In both cases, the corrugation effect exhibits better heat transfer performance compared to smooth tubes. Also, the enhancement in heat transfer is found to increase with the increase in Re. The corrugated tube with P = 10 mm and DR = 0.4 exhibits better heat transfer performance and corrugated tube with P = 30 mm, DR = 0.53 exhibits lower heat transfer performance compared to the other cases. At Re = 10500, DR = 0.40 and P = 10 mm, the corrugated tube exhibits the highest Nu. This may be due to the fact that lower DR and lower P results in higher corrugation effect and more variation in streamlines [18 - 19]. This causes better turbulence and increase in the residential time of the fluid inside flow regime, results in higher fluid mixing. This may be -

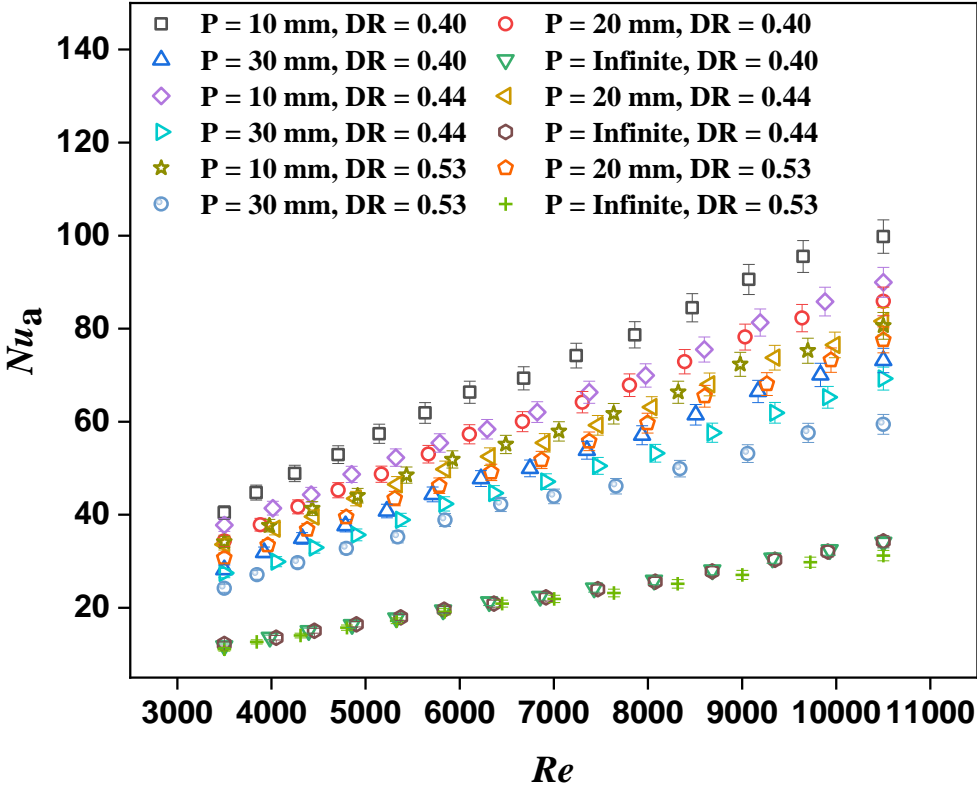


Fig. 2.6: Variation in average Nusselt number of annulus with respect to Reynolds number.

the reason for the enhancement in the heat transfer performance of the DPHE. Dirker and Meyer [84] studied the smooth tube DPHE for various diameter ratios (0.31 – 0.59) and reported that the average Nusselt number increases with the decrease in the diameter ratio. While, effect of corrugation on the tube geometry was studied by various researchers [19-20]. Dizaji et al. [19] studied heat transfer characteristics of DPHE involving corrugations in both tubes. In another study, Darzi et al. [20] reported the another study, Darzi et al. [20] reported the heat transfer characteristics of helically corrugated tube. The authors reported that corrugated tube generates the secondary flow which in turn increase the turbulence intensity inside flow regime and lead to increase in heat transfer rate. Similar observations have been made in the present study.

2.3.3 Comparison of corrugated annuli with smooth annuli

Performance of DPHE can be judged by comparing the experimental results of the corrugated outer tube DPHE with smooth tube DPHE. The variation in the values of Nu ratio (ratio of Nu for corrugated tube to Nu for smooth tube DPHE) with varied range of Re, various values of P and DR are shown in Fig. 2.7 for the cases considered here. The Nu ratio is found to be greater than unity value. The value of Nu ratio is found to decrease with increase in Re. The maximum value of Nu ratio is found to be 3.42 for P = 10 mm and DR=0.40 at Re = 3500. The DPHE with P =10 mm, DR=0.4 exhibits higher Nu ratio compared to the DPHE with P = 30 mm and DR= 0.53. It may be noted that the wetted perimeter increases with the increase in the corrugation and the fluid licks a larger surface area resulting in a better heat transfer compared to the smooth tube. Also, corrugation generates secondary flow, i.e., swirl inside flow region, leading to enhancement in heat transfer rate. It is observed that with the increase in the DR, the influence of corrugation effect decreases. This may be due to the fact that higher DR poses lower annular space and thus path line (travel path) is reduced, resulting in the reduction of mixing of the fluid [18 - 19].

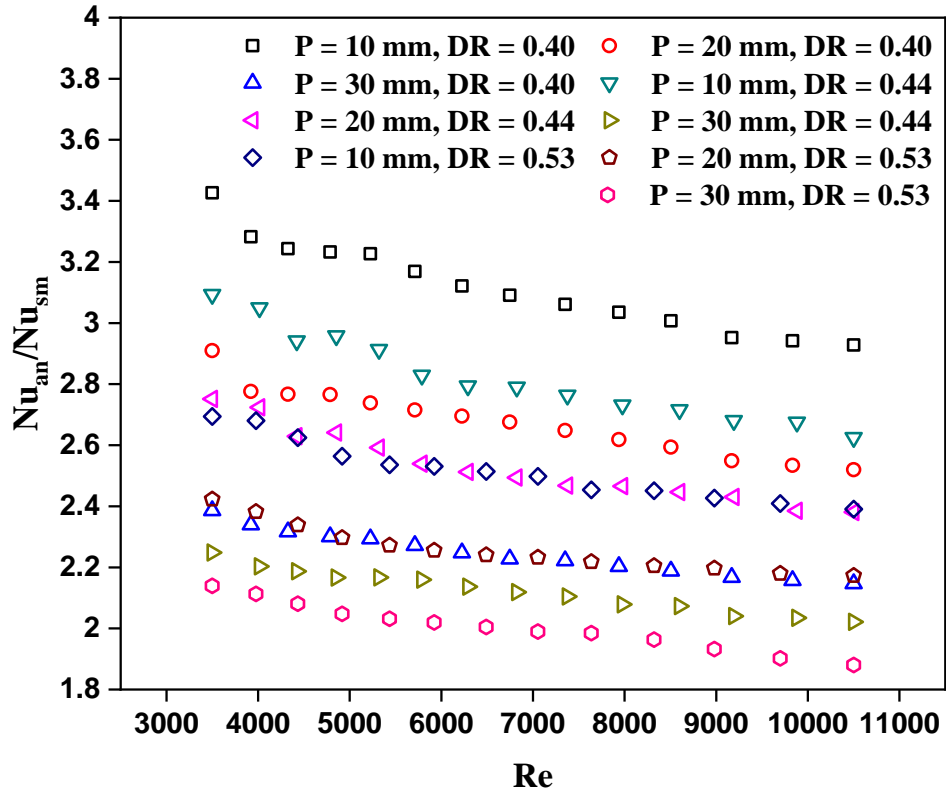


Fig. 2.7: Variation in average Nusselt number ratio with Reynolds number.

The variation in the values of f ratio (ratio of f for corrugated tube DPHE to the smooth tube DPHE) with Re for various values of P and DR are shown in Fig.2.8. The f ratio decreases with the increase in Re . The maximum value of f ratio is found to be 5.03 for $P = 10$ mm and $DR=0.4$ at $Re= 3500$. The DPHE with $P = 10$ mm, $DR=0.4$ exhibits higher f ratio values compared to the DPHE with $P = 30$ mm and $DR= 0.53$.

The idealized flow patterns through the corrugated tube are shown in Fig. 2.9. Corrugation geometry generates the variation in streamlines through the annular space between two tubes. It may be noted that corrugation promotes the secondary flow through the tube and promotes fluid mixing. In corrugation geometry, the interruption of thermal boundary layer occurs. This may be the reason for enhancement in heat transfer in corrugated tubes compared to the plain DPHE.

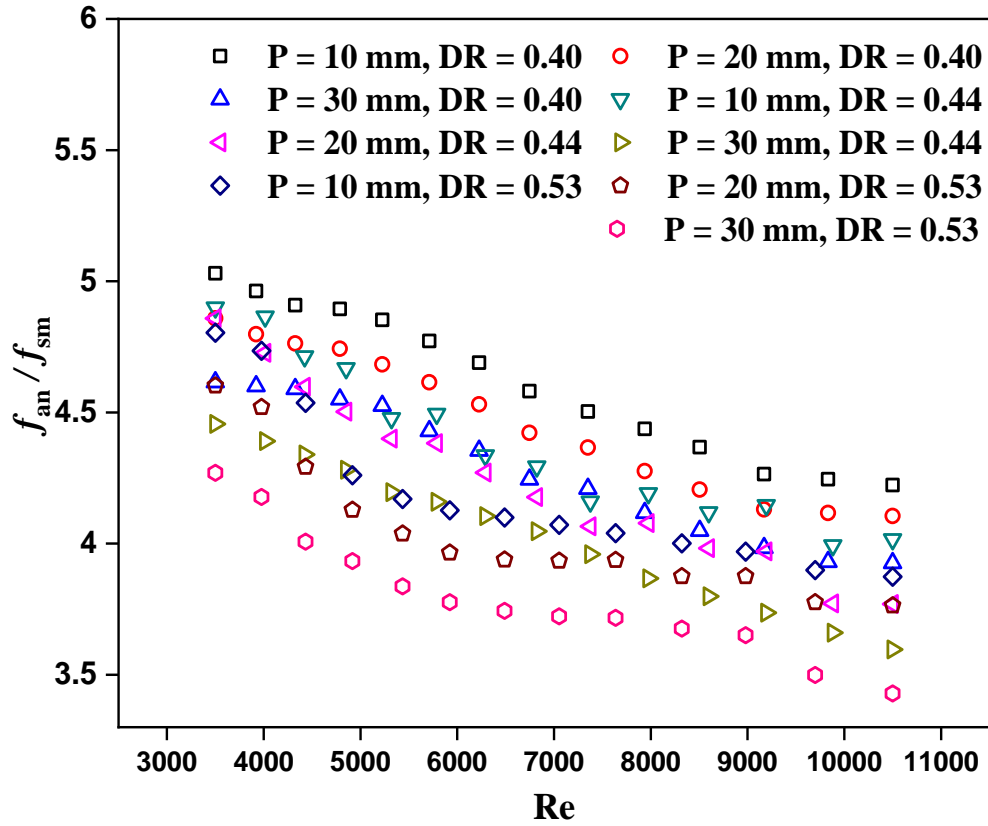


Fig. 2.8: Variation in average friction factor ratio with Reynolds number.

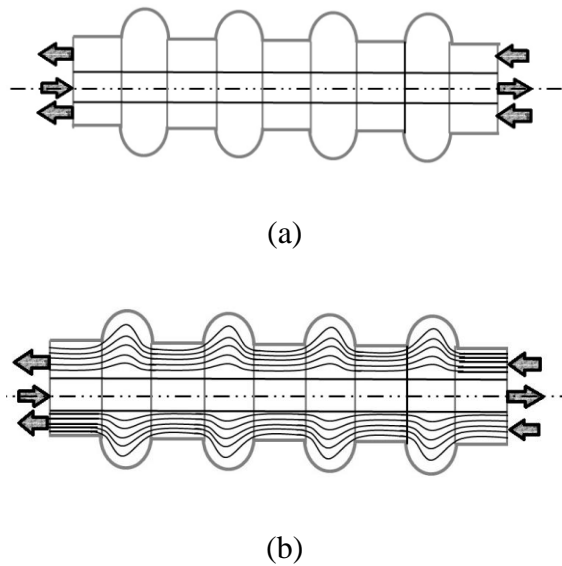


Fig. 2.9: (a) Schematic of corrugated tube DPHE and (b) idealized flow patterns through the annulus tube.

2.3.4 Thermal performance of annuli of DPHE

The effective assessment of the modified surfaces directly relates to the cost of operation in heat exchangers. Webb and Eckert [85] and Webb and Scott [86] selected the optimum geometry for the specified operating conditions for the performance evaluation criteria, keeping in view of various parameters such as pressure drop, heat transfer rate and flow rate. TPF is the parameter usually used to evaluate the effect of enhancement in heat transfer rate compared to the increase in the pressure drop. This is defined as the ratio between Nu ratio (Nu_a/Nu_{sm}) and one-third power of the f ratio (f_a/f_{sm}) for the same pumping power condition and expressed as [10 - 22]:

$$TPF(\eta) = \frac{(Nu_a/Nu_{sm})}{(f_a/f_{sm})^{1/3}} \tag{2.15}$$

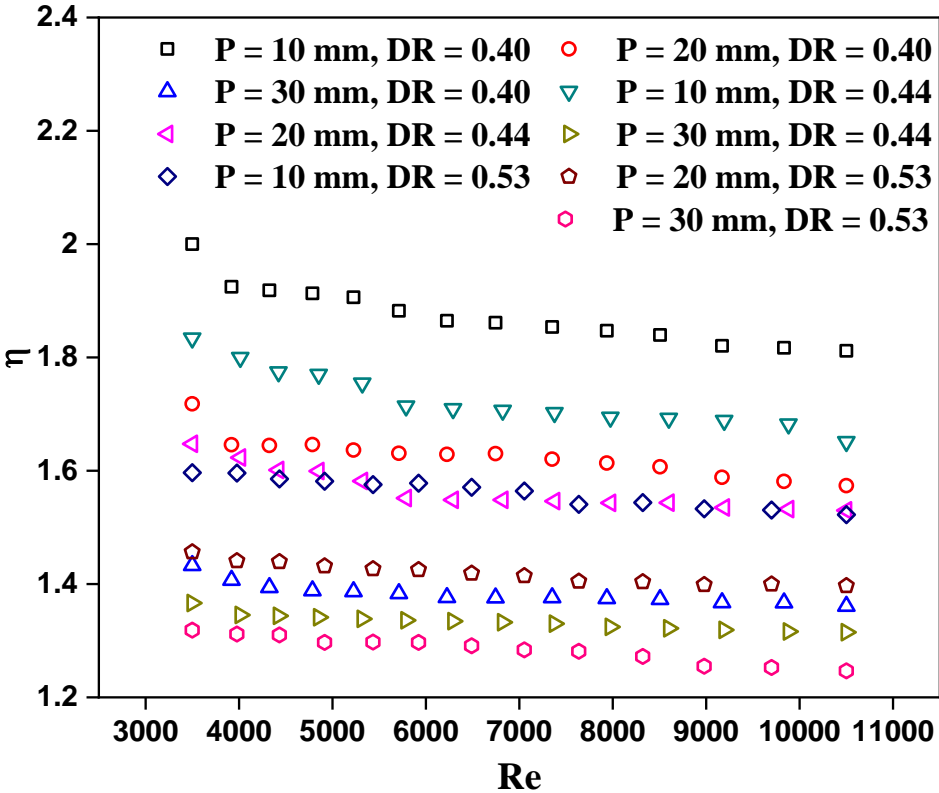


Fig. 2.10: Variation of thermal performance factor with Reynolds number.

The variation of TPF for various P values of corrugated tubes at different DR and Re are shown in Fig. 2.10. It is observed that for all the cases tested in this study, the TPF is found to be greater than unity and decreases gradually with increase in Re. The maximum value of TPF for outer corrugated tube DPHE with P = 10 mm and DR = 0.40, is found to be 1.99 at Re = 3500.

2.3.5 Comparison of present thermal performance with previous studies

Fig. 2.11 depicts the comparison of maximum TPF values obtained from the present experimental investigation involving corrugated DPHE with the maximum TPF values obtained by Wongcharee and Eiamsa-ard [16] that employ corrugated tube equipped with twisted tape with CuO- water nanofluids, test

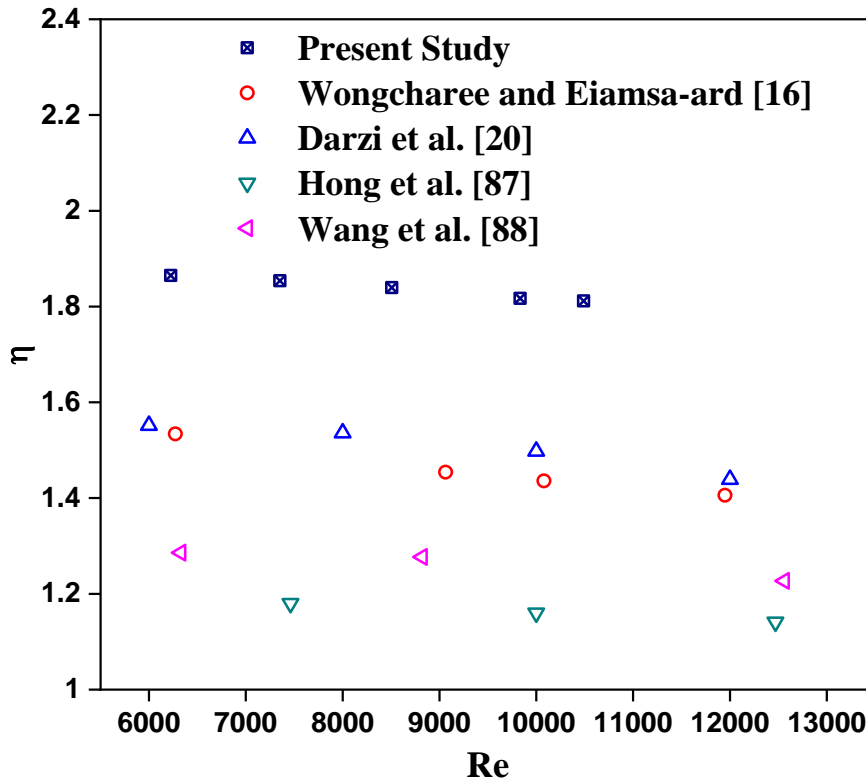


Fig. 2.11: Comparison of TPF of corrugated DPHE with previous study.

results of Darzi et al. [20] that use helically corrugated tube with Al₂O₃/water nanofluid, experimental results of Hong et al. [87] that use wavy corrugated tube with water as working fluid and experimental results of Wang et al. [88] that employ outward corrugated tube with Helium gas. Here, TPF value is found to decrease with the increase in Re value. Previous researchers [16, 20, 87-88] also obtained similar observations in their experimental investigation. The maximum TPF value is obtained at lower Re value. The TPF obtained from the present experimental investigation for P = 10 mm and DR = 0.40 is nearly 18%, 17%, 37% and 31% higher compared to the TPF values of Wongcharee and Eiamsa-ard [16], Darzi et al. [20], Hong et al. [87] and Wang et al. [88], respectively. This can be noticed from the fig. 2.11 that the TPF for the configuration used in present experimental investigation is higher compared to the previous studies [16, 20, 87 – 88].

2.3.6 Correlations for various parameters

Present test data are used to derive the correlation for Nu, f, and TPF as a function of various parameters such as Re, P/D_{an} and DR by using least square method of regression analysis and is expressed in Eqs. 2.16 -2.18.

$$Nu_a = 0.0382 Re^{0.81} (P/D_{an})^{-0.253} (DR)^{-0.148}; \left\{ \begin{array}{l} 3500 \leq Re \leq 10500 \\ 10mm \leq P \leq 30mm \\ 0.40 \leq DR \leq 0.53 \end{array} \right\} \quad (2.16)$$

$$f_a = 0.475 Re^{-0.36} (P/D_{an})^{-0.065} (DR)^{-0.612}; \left\{ \begin{array}{l} 3500 \leq Re \leq 10500 \\ 10mm \leq P \leq 30mm \\ 0.40 \leq DR \leq 0.53 \end{array} \right\} \quad (2.17)$$

$$\eta = 2.23 Re^{-0.051} (P/D_{an})^{-0.218} (DR)^{-0.064}; \left\{ \begin{array}{l} 3500 \leq Re \leq 10500 \\ 10mm \leq P \leq 30mm \\ 0.40 \leq DR \leq 0.53 \end{array} \right\} \quad (2.18)$$

Wide variety of studies have been reported that consider artificially roughened surfaces of various roughness shapes, types, different boundary

conditions, and various fluids to enhance heat transfer rates in heat exchanger tubes. Several authors proposed correlations to predict Nu and f as a function of various parameters, including roughness pitch, roughness height, and Re . Some of these correlations for Nu , f , and TPF are summarized in Table 2.4. It is interesting to note that the exponent of Re for Nu correlation varies significantly based on the experimental design conditions. The corrugation pitch was found to interrupt boundary layer, increase turbulence, and enhance better mixing. This promotes higher heat transfer rates, and therefore, the exponent of Re is higher in the present proposed correlation (Eq. 16). Earlier different authors have conducted experiments with helically corrugated tubes [15], protruded surface heat exchanger tubes [34], spirally grooved tubes [36], spirally fluted tubes [89], and elliptical axis tubes [93]. These authors have proposed correlation for Nusselt number and friction factor as a function of different operating parameters including Reynolds number. Similar value of exponent for Reynolds number have been reported by previous researchers [15, 34, 36, 89 – 93]. The functional dependence of f with Re is very complex in corrugated tubes compared to the smooth tubes. The dependence of f with Re for various corrugation geometries are summarized in Table 2.4. Srinivasan and Christensen [89] reported the heat transfer and pressure drop characteristics of flow through spirally fluted tubes through experimental investigation. The authors reported that f depends on flute depth, flute pitch, helix angle, and Re with cross effects of these parameters. Here, f is found to strongly dependent on Re for higher pitch to diameter ratios (0.983, 0.92). While, for other pitch to diameter ratios (0.367-0.587) the friction factor is found to be a weak function of the Re . In the present study, we have considered different pitch to diameter ratios (0.41- 2.142). This may be the reason that the friction factor is found to strongly dependent on Re value.

Also, an attempt has been made to compare the present test data with the proposed correlation. In the case of Nu , proposed correlations (Eq. 2.16) are able to predict 96% of experimental test data within an error band of $\pm 9\%$ depicts in Fig. 2.12. While, in case of f , proposed correlations (Eq. 2.17) are able to predict

92% of experimental test data within an error band of $\pm 5\%$ depicts in Fig. 2.13. Also, the proposed correlation (Eq. 2.18) for the TPF is able to predict 94% of experimental test data within an error band of $\pm 5\%$ and depicted in Fig. 2.14.

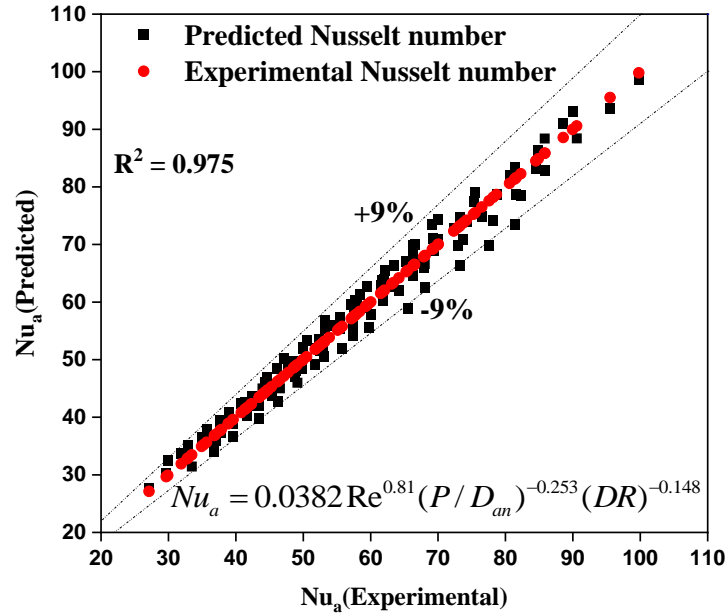


Fig. 2.12: Comparison of experimental and predicted values of average Nusselt number.

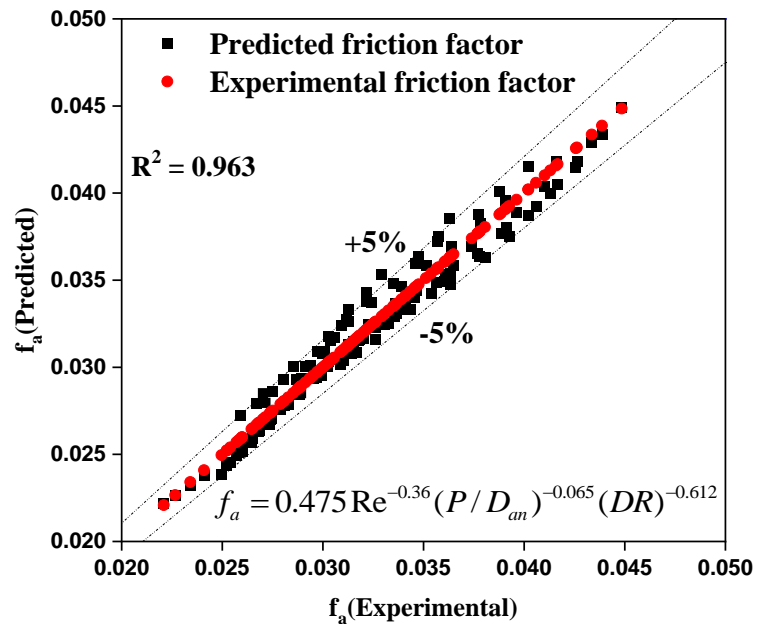


Fig. 2.13: Comparison of experimental and predicted values of average friction factor.

Table 2.4: Correlations proposed by various researchers.

Source	Type/method of passive enhancement	Reynolds number	Remark/correlations
Pethkool et al. [15]	Helically corrugated tube	5500 – 60000	$f = 1.15 \text{ Re}^{-0.239} (e/D_H)^{0.179} (P/D_H)^{0.164}$ $\eta = 39.419 \text{ Re}^{-0.161} (e/D_H)^{0.375} (P/D_H)^{0.283}$
Jianfeng et al. [36]	Spirally grooved tube	8000-15000	$\text{Nu} = 0.0984 \text{ Re}^{0.748} \text{Pr}^{1/3} \left(\frac{e}{d}\right)^{0.38} \left(\frac{\mu}{\mu_w}\right)^{0.14}$
Kumar et al. [34]	Protruded surface tube	6000-35000	$f = 3.7117 \text{ Re}^{-0.4421} \left(\frac{x}{d}\right)^{0.2526}$ $X \exp[(-0.0717)\{\ln(x/d)\}^2](y/d)^{0.6876}$ $X \exp[(-0.1565)\{\ln(y/d)\}^2]$ <p>x/d = stream wise spacing and y/d = span wise spacing</p>
Srinivasan and Christensen [89]	Spiral fluted tubes	500 – 5000	$\text{Nu} = 0.014 \text{ Re}^{0.842} (e^*)^{-0.067} (P^*)^{-0.108} (\theta^*)^{-0.599}$ $f = 12.745 \text{ Re}^{(-0.474-0.209P^*+0.685\theta^*)} e^{*(1.292+0.031P^*)}$ $Xp^{*(9.908+0.331 \times 10^{-5} \text{ Re}-12.074\theta^*)}$

Table 2.4 (Continued).

Source	Type/method of passive enhancement	Reynolds number	Remark/correlations
Sun and Zeng [90]	Corrugated tube	4000 - 800000	$Nu = 0.0331Re^{0.787}$ $f = 0.0320Re^{-0.385}$
Naphon et al. [91]	Helically ribbed tubes	5000 – 25000	$f_{he} = 7.85 \left(\frac{x}{d_i} \right)^{1.68} \left(\frac{p}{d_i} \right)^{-0.54} Re^{-0.21}$
Bharadwaj et al. [92]	Spirally grooved tube	Re > 3000	$Nu = 0.0017 Re^{1.1931} ; 3000 < Re < 7000$ $Nu = 0.1325 Re^{0.7517} ; Rr > 7000$
Meng et al. [93]	Elliptical axis tube	500-50000	$Nu = 0.0615 Re^{0.76} Pr_f^{1/3} \left(\frac{Pr_f}{Pr_w} \right)^{0.11}$

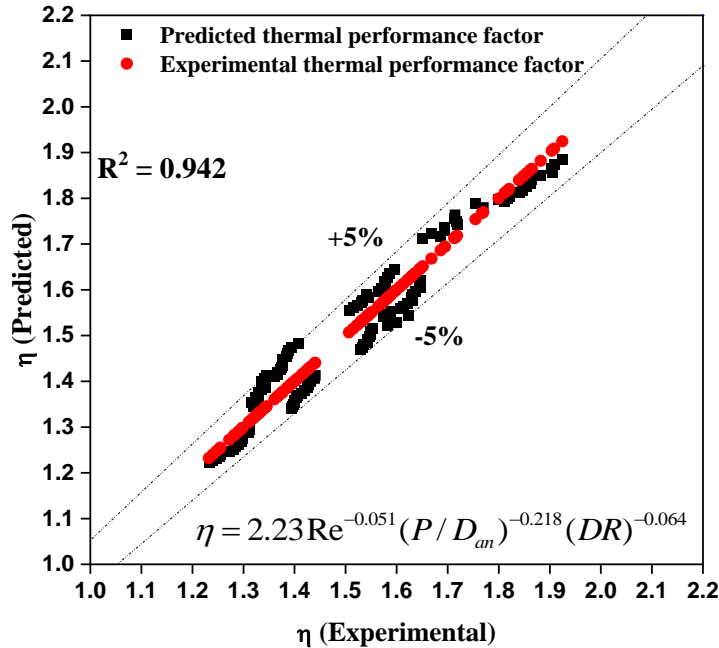


Fig. 2.14: Comparison of experimental and predicted values of thermal performance factor.

2.4 Concluding remarks

Experimental investigation has been carried out to evaluate the heat transfer and pressure drop characteristics of DPHE with the corrugated outer tube and smooth inner tube. Water (hot fluid) flows in the inner tube, and air (cold fluid) flows through the annulus. Tests are conducted for air with uniform wall temperature condition. The effect of corrugated outer tube is analyzed with three corrugation pitches ($P = 10, 20$ and 30 mm), three diameter ratios ($DR = 0.53, 0.44$ and 0.40) and varied range of Reynolds number ($Re = 3500 - 10,500$). The effect of various parameters such as flow rate, corrugated pitch, and diameter ratio on Nusselt number, friction factor, and thermal performance factor are discussed.

It is observed that both Nusselt number and friction factor increase with the decrease in corrugated pitch and diameter ratio. Lower value of the pitch improves better mixing of the fluid and promotes turbulence that leads to the improvement in the heat transfer. It is observed that the corrugation generates the

variation in streamlines through the annular space between two tubes. The enhancement in heat transfer in corrugated wall is owing to various reasons such as interruption of thermal boundary layer, flow mixing due to secondary flow. Thermal performance is evaluated based on heat transfer enhancement ratio and ratio of enhancement in friction factor. The thermal performance is found to be greater than unity for all the cases considered here. In addition to this, correlations are proposed for Nusselt number, friction factor, and thermal performance factor as a function of various modeling parameters.

Chapter 3

Augmentation of heat transfer and pressure drop characteristics in annuli using plain surface disc turbulators

3.1 Introduction

In the previous chapter, efforts have been made to study the thermo-hydraulic behavior of air through annulus of DPHE involving corrugated tubes. In addition to this, various passive heat transfer techniques such as swirl flow devices and turbulators (baffles, ribs, delta winglets, vortex generators, obstacles, perforated blocks) are used in various applications including processing of papers and drying of vegetable products [4]. Turbulators usually alter the flow and generate higher re-circulation, increase the contact surface area between the fluid and the heating wall surface, resulting in higher mixing in the flow regime and enhancement in the heat transfer [4, 65-78]. Numerous studies have been reported considering different turbulators in the heat exchanging tubes or in the annulus of DPHEs [65-78] for varied range of pitch ratio, diameter ratio, and Reynolds number. Although numerous studies have been made [65-78] involving turbulators in tubes, the study involving turbulators in DPHE with various diameter ratios, open area ratios are not extensively reported in the literature. It may be noted that the thermal performance of a tube with turbulators rely on various parameters, namely, pitch ratio, open area ratio, and Reynolds number. Diameter ratio plays a crucial role during design of heat exchangers due to space constraints. The combined effect of diameter ratio, pitch ratio, and Reynolds number on thermal performance of DPHE with turbulators need to be studied for design of heat exchanging equipments. It is very challenging to design the DPHE with turbulators that provide heat transfer enhancement and pressure loss at the acceptable limits especially in turbulent flow conditions. Here, tests are performed to examine the effect of various parameters namely, diameter ratio ($DR = 0.42, 0.475$ and 0.53), pitch ratio ($8.42, 9.79$ and 11.79) and Reynolds number ($3200 -$

10500) on the thermal performance in the annuli of DPHE with plain surface disc turbulators (PSDTs). Based on the test data, the thermal performance of DPHE involving turbulators are estimated. Also, correlations are proposed to evaluate various parameters such as Nusselt number, friction factor, and thermal performance factor.

3.2 Test facility, procedure and data reduction

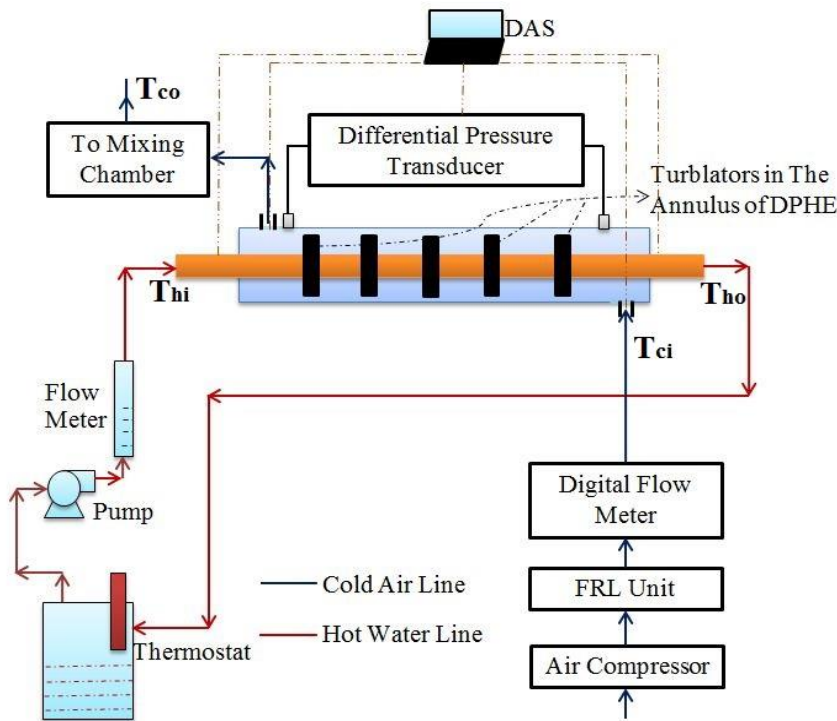


Fig. 3.1 (a): Schematic of experimental test facility.

Fig. 3.1a shows a schematic view of experimental apparatus used for experimental investigation. The schematic views of test specimen using plain surface disc turbulators (PSDTs) and photographic view of plain surface disc turbulators (PSDTs) with dimensional specification are shown in Figs. 3.1 (b-c), respectively. The experimental apparatus consists of test section, air and water flow scheme, and instrumentation module. The detail of test apparatus is described in Chapter 2 and therefore, it is not elaborated here. A DPHE involving both plain inner tube (copper tube) and outer tube (stainless steel material) is used

as test specimen. The PSDTs made of stainless steel is fitted in annuli of test section. Table 3.1 summarizes twelve test sections (TS1-TS12) used in this study. The length of test specimen and test section was kept at 1.8 m and 1.1 m, respectively.

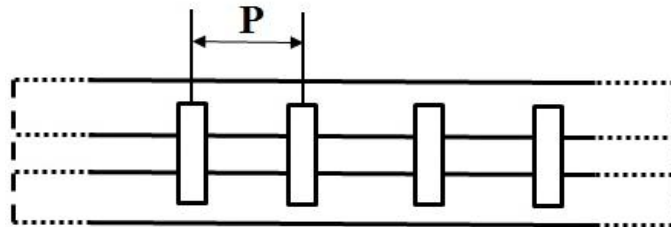


Fig. 3.1 (b): Schematic of test specimen using PSDTs.

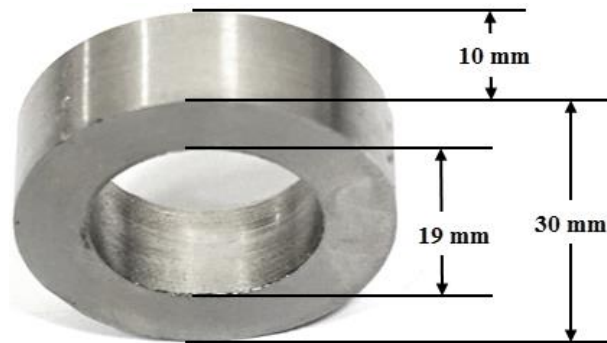


Fig. 3.1 (c): Photographic view of plain surface disc turbulator.

Before conducting experiments, water temperature is raised to 70- 75°C by using a constant temperature bath. Flow of compressed air is initiated along annuli of DPHE and adjusted to attain the desired Reynolds number. Subsequently, the flow of hot water is initiated along the inner tube. Fluid temperature of (air and water) at both inlet and outlet locations is recorded by using data acquisition system. Final readings are noted after the system attains thermal equilibrium. Efforts have been made to conduct number of tests run to ensure the reliability of test data. The annulus is of primary interest and therefore experiments are performed constant water flow rate and varied range of air flow rate. The results obtained from the present study are elaborated in the next section.

Table 3.1: Detail of experimental test sections.

Test section	DR	Tube			shell			Pitch ratio	Number of PSDT's
		Lt(mm)	di(mm)	do(mm)	Ls(mm)	Di(mm)	Do(mm)		
TS1	0.54	1800	17	19	1800	35	40	Infinite	0
TS2	0.54	1800	17	19	1800	35	40	11.79	4
TS3	0.54	1800	17	19	1800	35	40	9.79	5
TS4	0.54	1800	17	19	1800	35	40	8.42	6
TS5	0.475	1800	17	19	1800	40	45	Infinite	0
TS6	0.475	1800	17	19	1800	40	45	11.79	4
TS7	0.475	1800	17	19	1800	40	45	9.79	5
TS8	0.475	1800	17	19	1800	40	45	8.42	6
TS9	0.420	1800	17	19	1800	45	50	Infinite	0
TS10	0.420	1800	17	19	1800	45	50	11.79	4
TS11	0.420	1800	17	19	1800	45	50	9.79	5
TS12	0.420	1800	17	19	1800	45	50	8.42	6

3.3 Results and discussion

Initially, to validate the present experimental test facility, the DPHE made of smooth tube of different diameter ratio (DR=0.42, 0.475, and 0.54) is used in this study. The Re values are varied in the range of 3500- 10000 during the experiments.

Table 3.2: Experimental validation of Nusselt number for smooth tubes.

Re	Nusselt number			Remarks
	Experiment	Correlation	% variation	
For DR= 0.42				Compared with the Dittus-Boelter Correlation [83] $Nu = 0.023 Re^{0.8} Pr^{0.4}$
4700	18.63	17.27	7.86	
6800	25.24	23.21	8.75	
9400	32.96	30.08	9.59	
For DR= 0.475				
4200	14.49	15.79	-8.19	
6300	22.95	21.84	5.09	
8400	29.21	27.49	6.28	
For DR= 0.54				
4300	14.43	16.09	-10.27	
6100	20.35	21.28	-4.36	
9100	30.38	29.31	3.65	

Experimental Nu for varied range of Re and different DR are compared with the results obtained by Dittus-Boelter correlation [83] and is summarized in Table 3.2. The maximum variation in Nu value with Dittus-Boelter correlation [83] is found to be 9.59%, -12.08% and -10.27% for DR=0.42, DR = 0.475 and DR= 0.54, respectively. Here, efforts have also been made to validate the experimental f value for smooth tube with the result of friction factor correlation

[83] for varied range of Re and different DR and are summarized in Tables 3.3. The maximum variation between the experimental f value and the results for f value obtained by correlation [83] is found to be 6.87%, 3.66% and 2.99% for DR=0.42, DR = 0.475 and DR= 0.54, respectively.

Table 3.3: Experimental validation with smooth tubes.

Re	Friction factor			Remark
	Experiment	Correlation	% variation	
For DR= 0.42				Compared with $f = 0.079 \text{ Re}^{-0.25}$; Re > 2300 [83]
4300	0.01027	0.00975	5.32	
5500	0.00980	0.00917	6.83	
8300	0.00877	0.00827	5.97	
For DR= 0.475				
4500	0.00977	0.00964	1.36	
6900	0.00890	0.00867	2.69	
8400	0.00846	0.00825	2.59	
For DR= 0.54				
4300	0.00967	0.00975	-0.80	
5700	0.00923	0.00909	1.59	
7200	0.00875	0.00857	2.12	

Tests are conducted with smooth tubes DPHE with and without PSDTs. This includes three PR and three different DR. Initially, tests are conducted with smooth tube for three different DR values (0.42, 0.475, and 0.54). Later, tests are conducted in DPHE with PSDTs with varying PR (8.42, 9.79 and 11.79) and DR (0.42, 0.475 and 0.54). During the experiments, the rise in air temperature is found to 7-11.5°C. The maximum difference between inlet and outlet of water temperature is found to be 1°C. This may be due to large difference between specific heat of water and air. Therefore, outer wall of inner tube is assumed to be

at constant temperature. Here, ceramic glass wool insulation covers the outer wall of outer tube. Therefore, outer wall of the outer tube is assumed to be adiabatic.

3.3.1 Friction factor characteristics

The distribution of f values with Re, PR, and DR for DPHE with PSDTs is shown in fig.3.2.

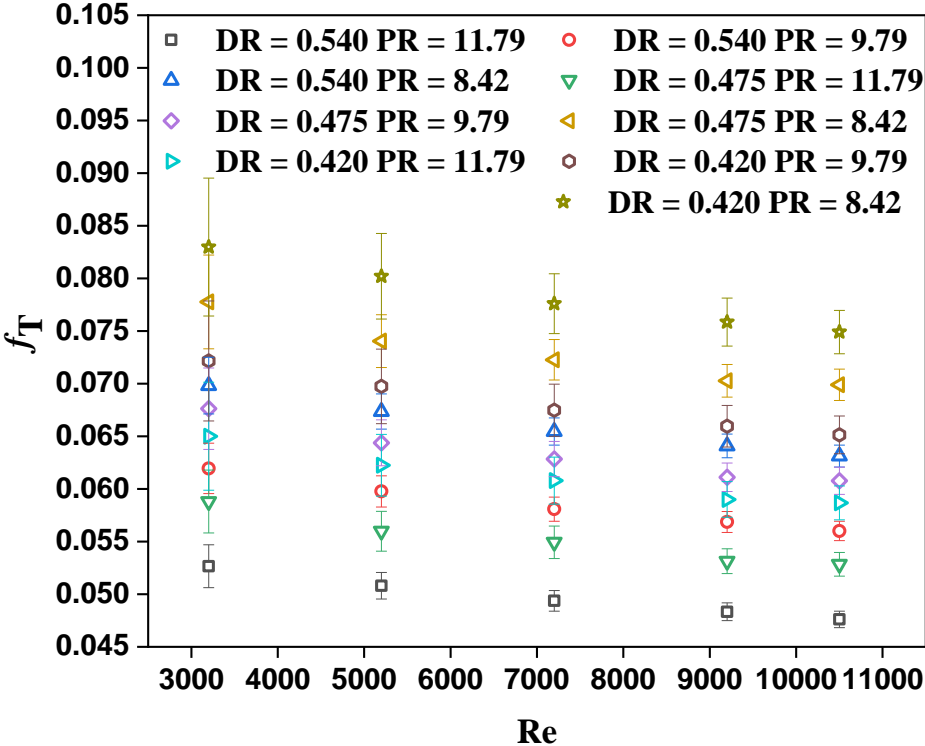


Fig. 3.2: Variation of average f with Re in the annulus using PSDTs.

With increase in Re value, a gradual decrement is found to be in f values and highest for smallest DR value. Smallest DR value shows increase in annulus space, which results in higher f value, similar to the results obtained by Dirker et al. [84] for f values. For a given DR, lower PR value yields higher f values. It may be noted that use of PSDTs in the annulus varies path lines and streamlines that improves re-circulation. This results in higher turbulence intensity [65-78]. Therefore, significant drop in pressure is noticed across annulus that lead to rise in f values. The smallest value of PR, DR, and Re are found to results in maximum f

value. For different configurations of DR = 0.420, 0.475 and 0.530, the maximum f values are observed to be 0.0829, 0.0777 and 0.0698, respectively at $Re = 3200$. While the highest factor of enhancement in f value is observed to be 9.58 at $DR = 0.420$ and $PR = 8.420$ at $Re = 10500$ compared to DPHE without turbulators.

3.3.2 Heat transfer enhancement

Fig. 3.3 shows the distribution of Nu value with Re value for different PR and DR. The DPHE with PSDTs exhibits better thermal performance compared to DPHE without PSDTs.

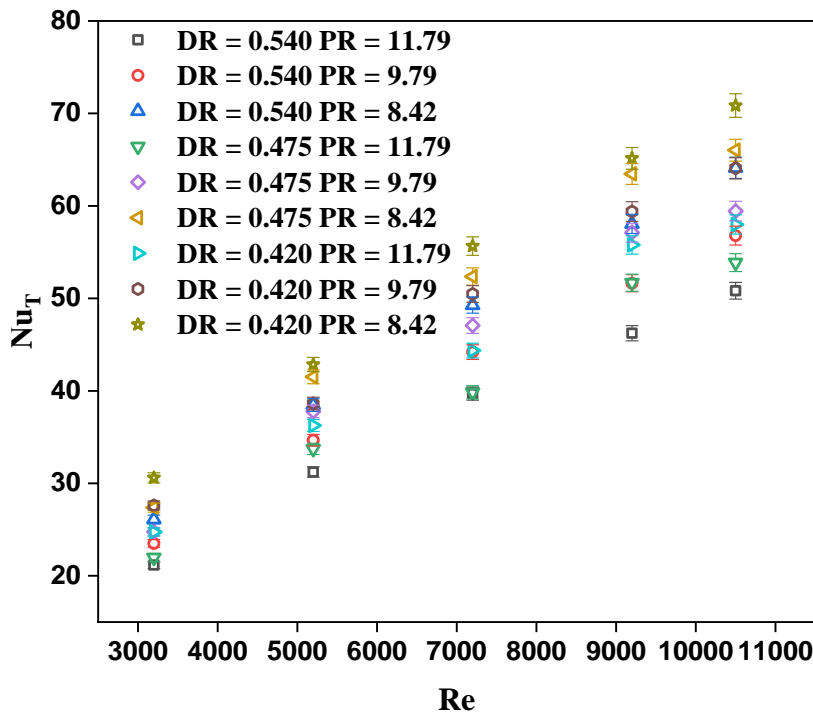


Fig. 3.3: Variation of average Nu with Re in the annulus using PSDTs.

The improvement in heat transfer is noticed with rise in Re value, and highest performance is obtained for DPHE using PSDTs at $PR = 8.420$ and $DR = 0.420$. While the lowest performance is found to be for DPHE using PSDTs at $PR = 11.790$ and $DR = 0.540$ compared to other configurations. Highest Nu values is observed with DPHE with PSDTs for $Re = 10500$, $DR = 0.420$ and $PR = 8.420$. It is argued that lower diameter ratio provides the higher annulus space. In such

case, the residential time of the fluid increases in the annulus regime [84]. Also, lower PR value provides the higher number of turbulators in the annulus of DPHE. The turbulators in the flow regime generates the re-circulation which in turn increase the turbulence intensity and promotes higher fluid mixing [65-78]. At lower values of DR and PR, recirculation in the flow increases and results higher turbulence and promotes enhanced fluid mixing [65-78].

3.3.3 Comparison of annuli equipped with PSDTs and annuli without PSDTs

Here, performance of DPHE with and without PSDTs have been compared. The variation in Nu ratio (It is ratio of Nu for the DPHE with PSDTs to the DPHE without PSDTs) with varied range of Re, PR and DR are shown in Fig. 3.4.

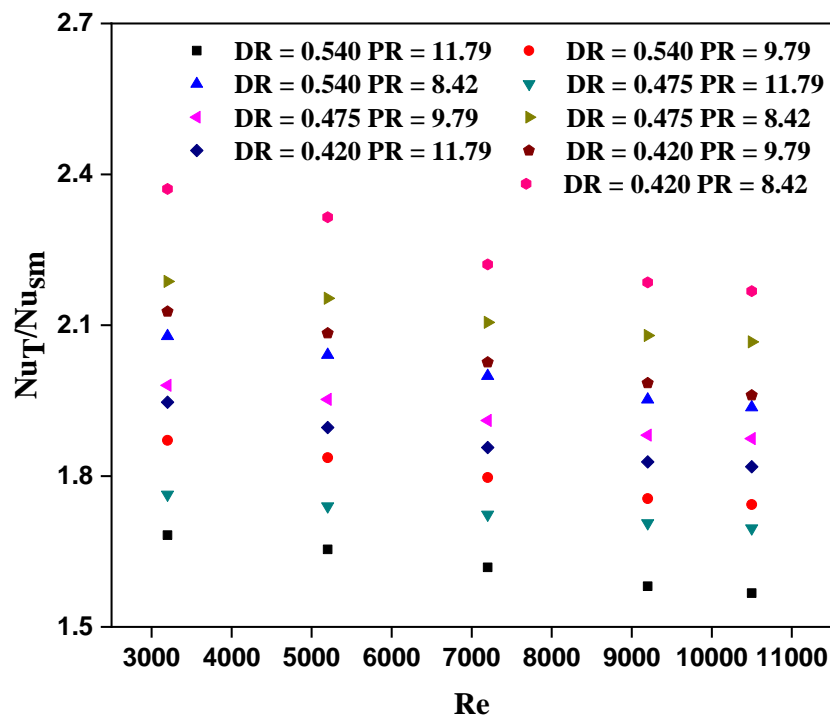


Fig. 3.4: Variation in Nu ratio with Re in the annulus using PSDTs.

It is interesting to note that for each case, Nu ratio is higher than unit value. The Nu ratio is found to reduce gradually with the rise in Re. The highest value of Nu ratio is found to be 2.37 for PR = 8.42 and DR = 0.42 and Re = 3200. Contact surface area rises with the increase in number of turbulators, and the fluid comes

in contact with more surface area that leads to have better heat transfer in comparison with DPHE without turbulators. In addition to this, turbulators increase the recirculation leading to high rate of heat transfer. The effect of turbulators reduces with the increase in DR. Owing to higher value of DR, annular space reduces and lead to reduction in path line and mixing of the fluid [82, 84 and 94].

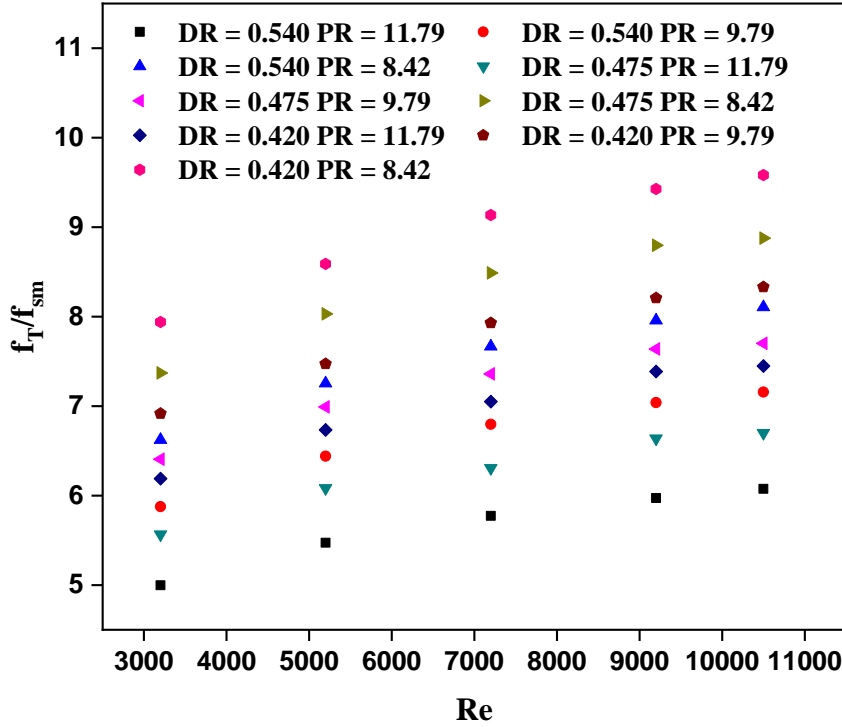


Fig. 3.5: Variation in f ratio with Re in the annulus using PSDTs.

The variation in f ratio (It is the ratio of f value for DPHE with PSDTs to DPHE without PSDTs) with varied range of Re , PR and DR and is shown in Fig. 3.5. The f ratio increases with Re value and achieves peak value of 9.58 at $Re = 10500$ for $PR = 8.420$ and $DR = 0.420$. The higher f ratio value is obtained for DPHE with $PR = 8.420$ and $DR=0.420$ compared to the DPHE with $PR = 11.790$ and $DR= 0.540$. The turbulators are found to provide high heat transfer area and, promote re-circulation inside annulus [65-78]. That lead to increase in the

intensity of turbulence, which in turn promote the higher fluid mixing and enhances pressure loss.

3.3.4 Thermal performance of annuli of DPHE using PSDTs

The heat exchanging equipments need to be designed, keeping in view of both heat transfer enhancement and pressure penalty. In general, the improvement in heat transfer rate is expressed by considering ratio of Nusselt number in DPHE involving enhancement device to that in the without enhancement device (Nu_T/Nu_{sm}). While the enhancement in friction factor is defined as the ratio of friction factor in the DPHE with enhancement device to that in the DPHE without enhancement device (f_T/f_{sm}). Thermal enhancement factor is usually evaluated under the constraint of pumping power. At constant pumping power, thermal enhancement factor is expressed as [65-78]:

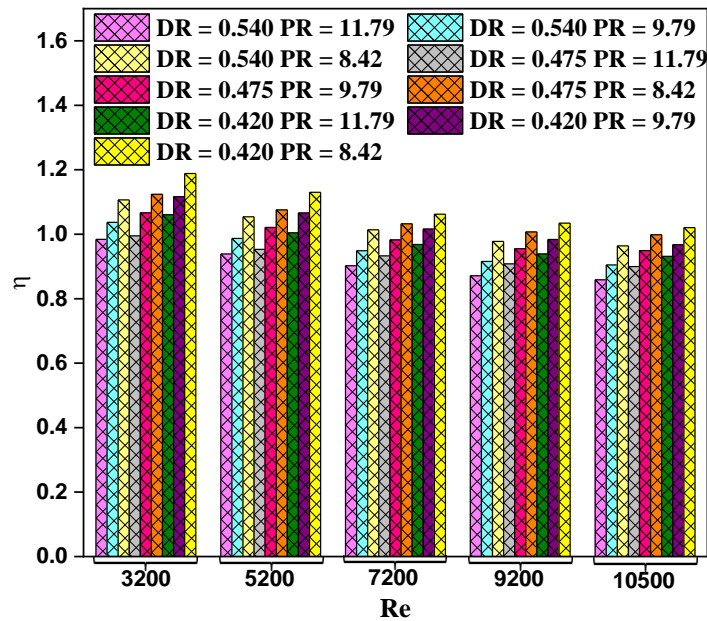


Fig. 3.6: Variation in TPF with Re in the annulus using PSDTs.

TPF for the DPHE using PSDTs in the annulus at various values of DR, PR and Re are shown in Fig. 3.6. The TPF value decreases with increment in Re value while it increases with decrease in DR and PR. The TPF value is observed

to be greater than unity for TS 12 (DR = 0.42, PR = 8.42) and is acceptable for the heat transfer enhancement. While for other configurations, the TPF is less than unity after certain Re value. The highest TPF is found to be 1.19 for DPHE using PSDTs at DR = 0.42 and PR = 8.42.

$$TEF(\eta) = \left(\frac{Nu_T}{Nu_{sm}} \right) \times \left(\frac{f_T}{f_{sm}} \right)^{-1/3} \quad (3.1)$$

3.3.5 Comparison of present experimental results with the results of other researchers

Studies have been made using different turbulators both in the tube and in DPHE by previous researchers [67, 74, 75, 76]. Sheikholeslami et al. [74]

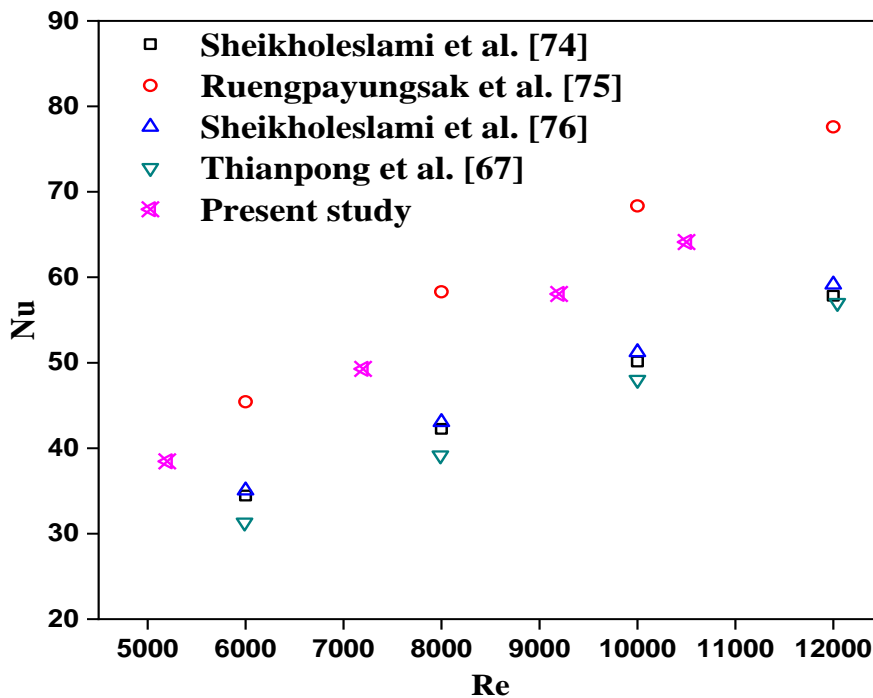


Fig. 3.7: Comparison of present experimental Nusselt number with previous the results of previous researchers [67, 74 - 76].

considered conical ring turbulator and air as working fluid in the annulus of DPHE in their experimental investigation. In their another study, the authors [76] performed the experiments using perforated circular ring turbulators and air as working fluid in the annulus of DPHE . While, Ruengpayungsak et al. [75] performed tests using gear ring as turbulator and air as working fluid in tube. Tests has also been conducted with twisted ring turbulator and air as working fluid in a tube by Thianpong et al. [67]. The present study has been made using plain surface disc turbulators and air as working fluid in the annulus. Therefore, efforts have been made to compare the present experimental results for Nu and f values with the previous studies [67, 74, 75, 76] based on use of different turbulators and a common working fluid (air). Comparisons for Nu and f values are depicted in Figs. 3.7 – 3.8, respectively.

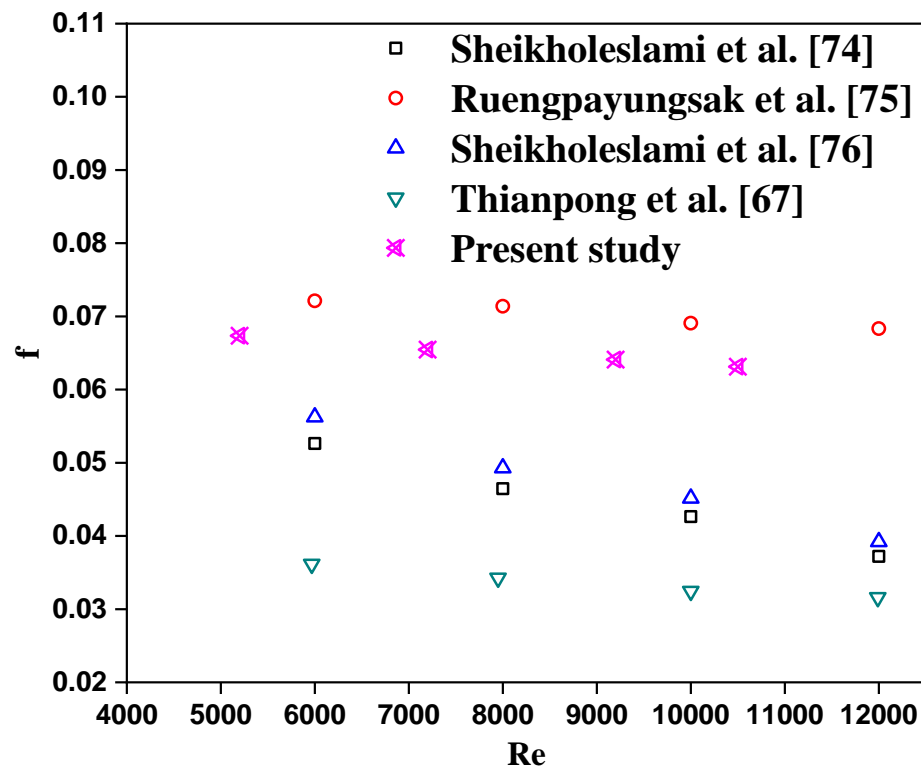


Fig. 3.8: Comparison of present experimental friction factor with the results of previous researchers [67, 74 - 76].

The Nu and f values obtained from present investigation shows higher values compared to the results of Sheikholeslami et al. [74, 76], and Thianpong et al. [67]. This may be due to the fact that perforation on the turbulator [74, 76] reduces the re-circulation effect inside the flow regime while twisted ring turbulator [67] was used in the round tube. However, present results exhibit lower value of Nu and f compare to the test results obtained by Ruengpayungsak et al. [75] because gear rings turbulators [75] offers more re-circulation and high surface area.

3.3.6 Correlations for various parameters

Utilizing the present experimental data for Nu , f , and TPF, are correlated with Eq. 3.2 – 3.4 as below:

$$Nu_T = 0.18 Re^{0.736} (PR)^{-0.59} (DR)^{-0.499}; \left\{ \begin{array}{l} 3200 \leq Re \leq 10500 \\ 8.42 \leq PR \leq 11.79 \\ 0.42 \leq DR \leq 0.54 \end{array} \right\} \quad (3.2)$$

$$f_T = 0.511 Re^{-0.088} (PR)^{-0.799} (DR)^{-0.695}; \left\{ \begin{array}{l} 3200 \leq Re \leq 10500 \\ 8.42 \leq PR \leq 11.79 \\ 0.42 \leq DR \leq 0.54 \end{array} \right\} \quad (3.3)$$

$$\eta = 4.725 Re^{-0.114} (PR)^{-0.335} (DR)^{-0.282}; \left\{ \begin{array}{l} 3200 \leq Re \leq 10500 \\ 8.42 \leq PR \leq 11.79 \\ 0.42 \leq DR \leq 0.54 \end{array} \right\} \quad (3.4)$$

Various researchers have proposed correlations for Nu , f , and TPF and are summarized in Table 3.4. These studies utilize various turbulators such as circular ring turbulators [66], twisted-ring turbulators [67], V-nozzle turbulators [71], gear-ring turbulators [75], solid hollow circular disk turbulators [80], and conical-nozzle turbulators [95]. It is noticed that Re exponent for Nu correlations [66, 67, 71, 75, 80 and 95] varies between 0.6 – 0.883. The dependence of Re on Nu for the present study is expressed in Eq. 3.2. This is similar to earlier studies [66, 67, 71, 75, 80 and 95]. Correlation for f (Eq.3.3) reveals that f is a weak function of the Re . It may be noted that the dependence of Re on f may vary based on design

of turbulators. A large variation of the exponent of Re in the f correlation is reported by various researchers [66, 67, 71, 75, 80 and 95]. Turbulators are found to enhance turbulence intensity, induce flow re-circulation, disrupt boundary layers and increased surface area resulting in enhancement in the rate of heat transfer and friction factor. The deviation between present test data and the proposed correlation are shown in Figs. 3.9 – 3.11. Correlation for Nu , f and TPF (Eq. 3.2 – 3.4) predict 96%, 84% and 98% of test data, respectively within an error band of $\pm 2\%$.

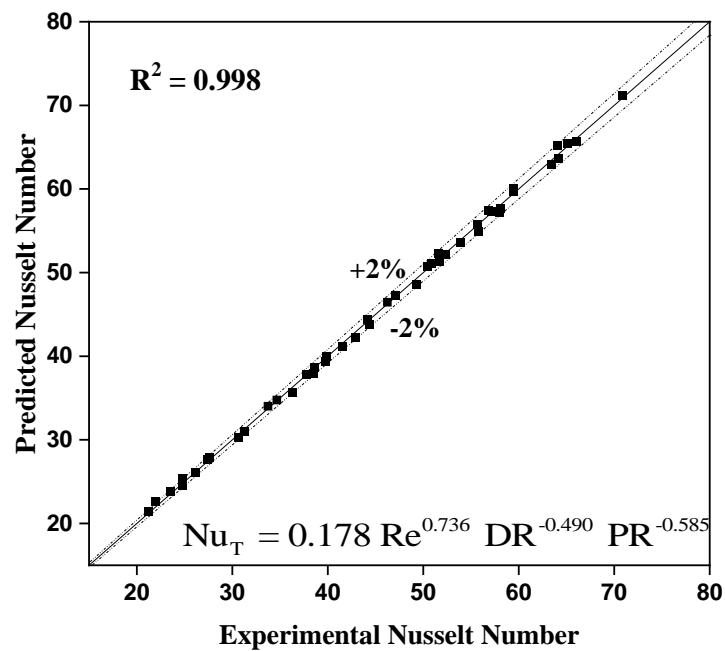


Fig. 3.9: Comparison of experimental and predicted average Nu values using PSDTs.

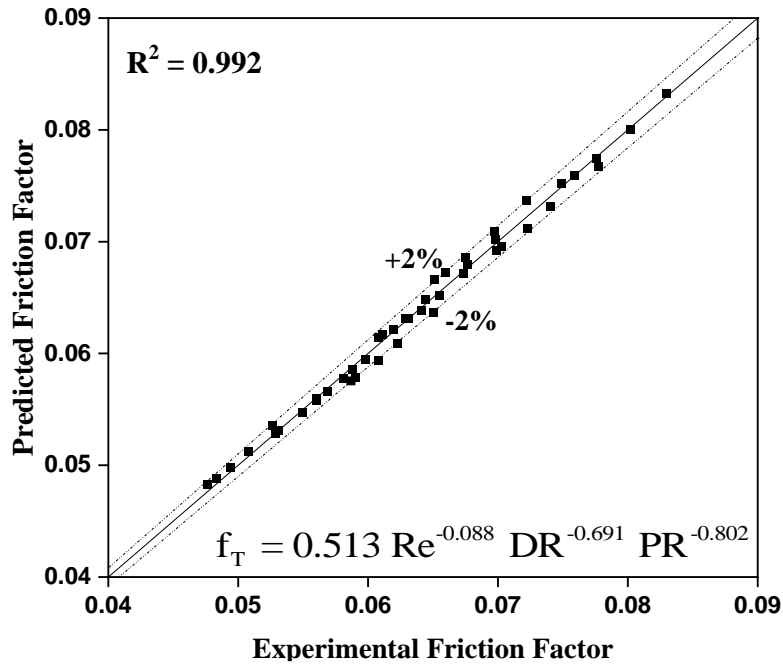


Fig. 3.10: Comparison of experimental and predicted f values using PSDTs.

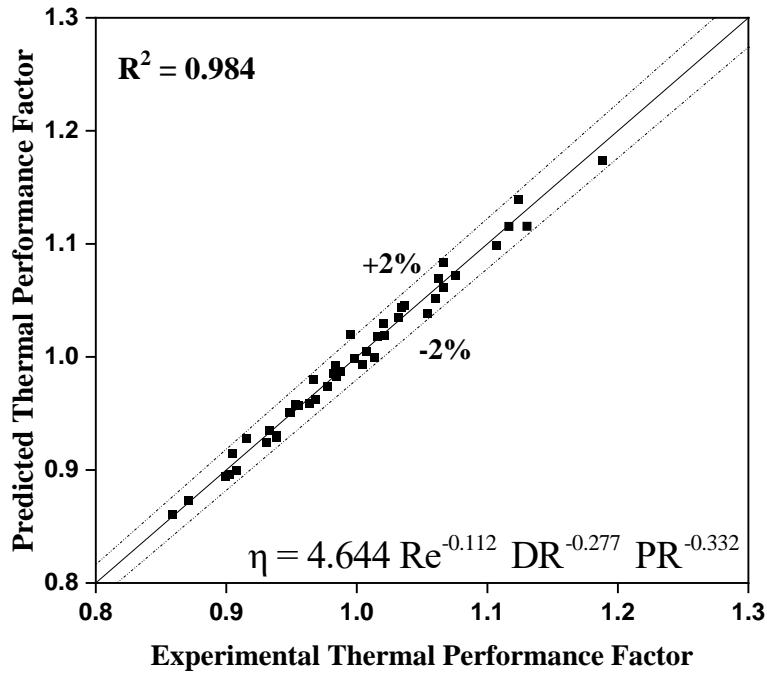


Fig. 3.11: Comparison of experimental and predicted TPF values using PSDTs.

Table 3.4: Correlations proposed by various researchers.

Source	Type/method of passive enhancement	Reynolds number	Remark/correlations
Kongkaitpaiboon [66]	Circular ring turbulators (CRT) in tube	4000 - 20000	$Nu = 0.354 Re^{0.697} Pr^{0.4} DR^{-0.555} PR^{-0.598}$ $f = 0.715 Re^{-0.081} DR^{-4.775} PR^{-0.846}$ $\eta = 5.315 Re^{-0.078} DR^{1.031} PR^{-0.317}$ <p>DR = diameter ratio PR = Pitch ratio</p>
Thianpong et al. [67]	Twisted ring turbulators in tube	6000-20000	$Nu = 0.097 Re^{0.883} Pr^{0.4} (W/D)^{0.408} (p/D)^{-0.181}$ $f = 112.795 Re^{-0.159} (W/D)^{1.665} (p/D)^{-0.736}$ <p>W/D = width ratio and p/D = Pitch ratio</p>
Eiamsa-ard and promvonge [71]	V Nozzle turbulators in tube	8000 - 18000	$Nu = 0.524 Re^{0.6} Pr^{0.4} (PR)^{-0.285}$ $f = 107 Re^{-0.42} (PR)^{-0.68}$ <p>PR (Pitch ratio) = Ratio of pitch length to tube diameter.</p>
Ruengpayungsak et al. [75]	Gear ring / circular ring turbulators in tube	6000-20000	<p>For circular ring turbulators For gear ring turbulators</p> $Nu = 0.078 Re^{0.786} Pr^{0.4} (SR)^{-0.136} \quad Nu = 0.1 Re^{0.768} Pr^{0.4} (SR)^{-0.14} (1+N)^{-0.13}$ $f = 0.788 Re^{-0.051} (SR)^{-0.486} \quad f = 2.143 Re^{-0.06} (SR)^{-0.522} (1+N)^{-0.479}$ $\eta = 5.531 Re^{-0.175} (SR)^{0.026} \quad \eta = 5.21 Re^{-0.175} (SR)^{0.034} (1+N)^{0.029}$ <p>SR = free space length ratio, N = number of tooth</p>

Table 3.4 (Continued).

Source	Type/method of passive enhancement	Reynolds number	Remark/correlations
Kumar et al. [80]	Solid hollow circular disc in tube	6000 - 24000	$\text{Nu} = 0.1248 \text{Re}^{0.7253} \text{DR}^{-0.5792} \text{PR}^{-0.088} \exp\{-0.0246(\ln \text{PR}^2)\}$ $f = 0.1284 \text{Re}^{-0.1199} \text{DR}^{-4.2233} \text{PR}^{-0.2374} \exp\{0.0033(\ln \text{PR}^2)\}$ $\eta = 5.1867 \text{Re}^{-0.1201} \text{DR}^{0.8107} \text{PR}^{0.0632} \exp\{0.0952(\ln \text{PR}^2)\} \quad ; \text{DR} =$ <p>diameter ratio and PR = Pitch ratio</p>
promvonge and Eiamsa-ard [95]	C-Nozzles turbulators in tube	8000 - 18000	$\text{Nu} = 0.143 \text{Re}^{0.736} \text{Pr}^{1/3} (\text{PR})^{-0.12}$ $f = 29 \text{Re}^{-0.197} (\text{PR})^{-0.022}$ $\eta = 2.84 \text{Re}_t^{-0.139} (\text{PR})^{-0.052} \quad ; \text{PR} = \text{Pitch ratio}$
Present Study	PSDTs in annuli	3200 - 10500	$\text{Nu}_T = 0.271 \text{Re}^{0.737} (\text{PR})^{-0.627} (\text{DR})^{-0.494}$ $f_T = 0.724 \text{Re}^{-0.088} (\text{PR})^{-0.81} (\text{DR})^{-0.67}$ $\eta = 6.285 \text{Re}^{-0.114} (\text{PR})^{-0.359} (\text{DR})^{-0.277}$

3.4 Concluding remarks

Here, tests are performed to estimate the hydrothermal behavior of DPHE with PSDTs inside annulus for varied range of pitch ratio, diameter ratio, and Reynolds number. Thermal performance is found to decrease with the increase in flow rate. This may be due to the reason that the enhancement in the pressure drop is more significant compared to the enhancement in heat transfer at higher flow rate. Also, higher value of thermal performance is obtained with lower value of diameter ratio and pitch ratio. Proposed correlation on thermal performance factor suggests that the effect of pitch ratio is more significant compared to the effect of diameter ratio and Reynolds number. Turbulators are found to increase the turbulence intensity, disrupt the boundary layer, induce flow circulation resulting in the enhancement in heat transfer.

Chapter 4

Augmentation of experimental heat transfer and pressure drop characteristics in annuli using helical surface disc turbulators

4.1 Introduction

Previous chapter (Chapter 3) reports the experimental study and the thermal-hydraulic parameters with DPHE involving plain surface disc turbulators. Based on the encouraging results, efforts have been made to propose better design of turbulators. Turbulators are found to improve turbulence intensity, enhance fluid mixing resulting in enhancement in heat transfer. Here, efforts have been made to design helical surface disc turbulators keeping in mind that helix angle can promote turbulence and improve fluid mixing. In addition to this, the pitch ratio, flow rate, and diameter ratio are varied during experiments.

In this chapter, the experimental investigation of DPHE with helical surface disc turbulators is presented. This is divided into three categories. In the first category, experiments are performed to analyze the effect of various parameters such as Reynolds number, pitch ratio, and helix angle on Nusselt number, friction factor, and thermal performance factor. Correlations are proposed for Nusselt number, friction factor, and thermal performance factor. In the second category, tests are conducted to study the influence of flow rate, diameter ratio, and pitch ratio on various parameters, namely, Nusselt number, friction factor, and thermal performance factor. Efforts have been made to propose correlations on Nusselt number, friction factor, and thermal performance factor as a function of various modeling parameters. Present experimental results are compared with the test data of other researchers. In the third category, tests are performed to study the effect of flow rate, diameter ratio, and helix angle on various thermal performance factor. Present experimental results are compared

with tests data of other researchers. Also, correlations are proposed to estimate Nusselt number, friction factor, and thermal performance factor.

4.2 Effect of pitch ratio and helix angle on thermo hydraulic performance of DPHE with helical surface disc turbulators

Here, tests are performed to examine the effect of various parameters namely, three helix angles (20° , 30° and 40°), three different pitch ratios (8.42, 9.79 and 11.79) and varied range of Reynolds number (3500 - 10500) on the thermal performance in the annuli of DPHE with helical surface disc turbulators (HSDTs). Based on the tests data thermal performance of DPHE involving helical surface disc turbulators are estimated. Also, correlations are proposed to evaluate various parameters such as Nusselt number, friction factor, and thermal performance factor.

4.2.1 Test facility, procedure and data reduction

Fig.4.1a shows schematic view of experimental apparatus used for experimental investigation. The schematic and photographic view of test specimen using helical surface disc turbulators (HSDTs) with the dimensional specification is shown in Figs. 4.1 (b–c), respectively. The experimental apparatus consists of test section, air and water flow scheme and instrumentation module. The detail of test apparatus is described in Chapter 2, and therefore, it is not elaborated here. A DPHE involving both smooth inner tube (copper tube) and outer tube (stainless steel material) is used as test specimen. The HSDTs made of stainless steel, is fitted in annuli of test section. Table 4.1 summarizes various test sections used in the present experimental study. The length of test specimen and test section was kept at 1.8 m and 1.1 m, respectively, for all the cases.

Various terminologies used in the experiments are elaborated below.

- *Pitch (P)*: The length between two succeeding turbulators, where same cross-sectional orientation coincides is termed as pitch.

- *Pitch ratio (PR)*: Ratio between turbulator pitch and outer diameter of inner tube is termed as pitch ratio.

$$PR = \frac{P}{d_o} \quad (4.1)$$

- *Diameter ratio (DR)*: Diameter ratio is defined as the ratio of outer diameter of inner tube to the inner diameter of outer tube.

$$DR = \frac{d_o}{D_i} \quad (4.2)$$

- *Helix angle (ϕ)*: Angle between helix on flank surface of HSDTs and an axial line on HSDTs is termed as helix angle (Fig. 4.1c).

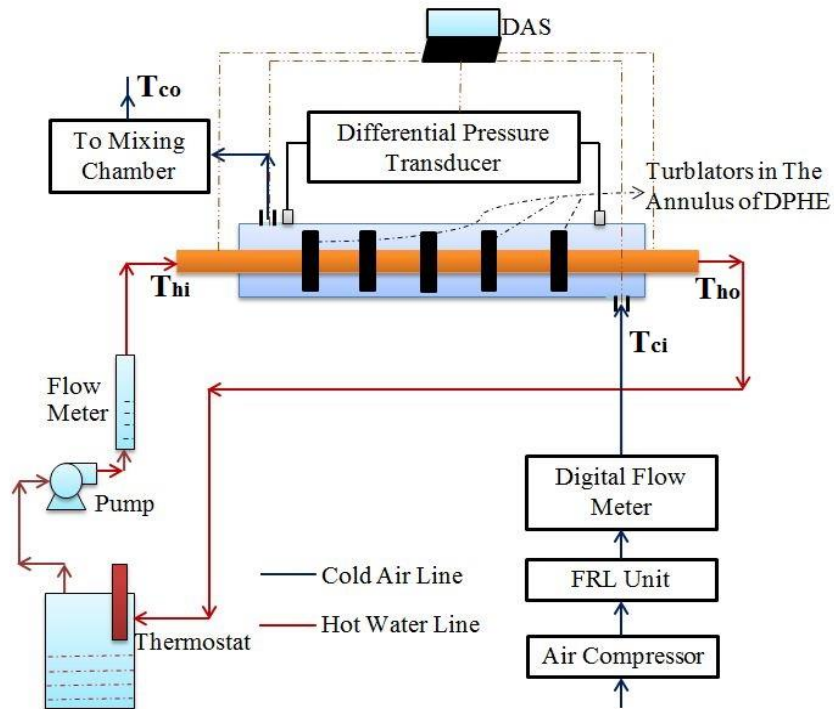


Fig. 4.1 (a): Schematic view of experimental test facility.

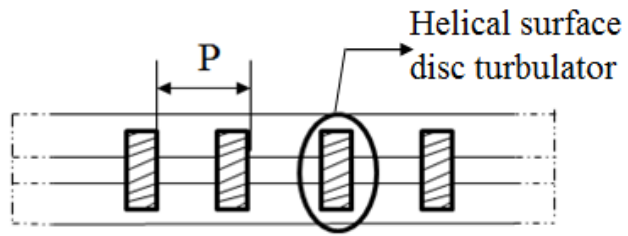


Fig. 4.1 (b): Schematic of test specimen using HSDTs.

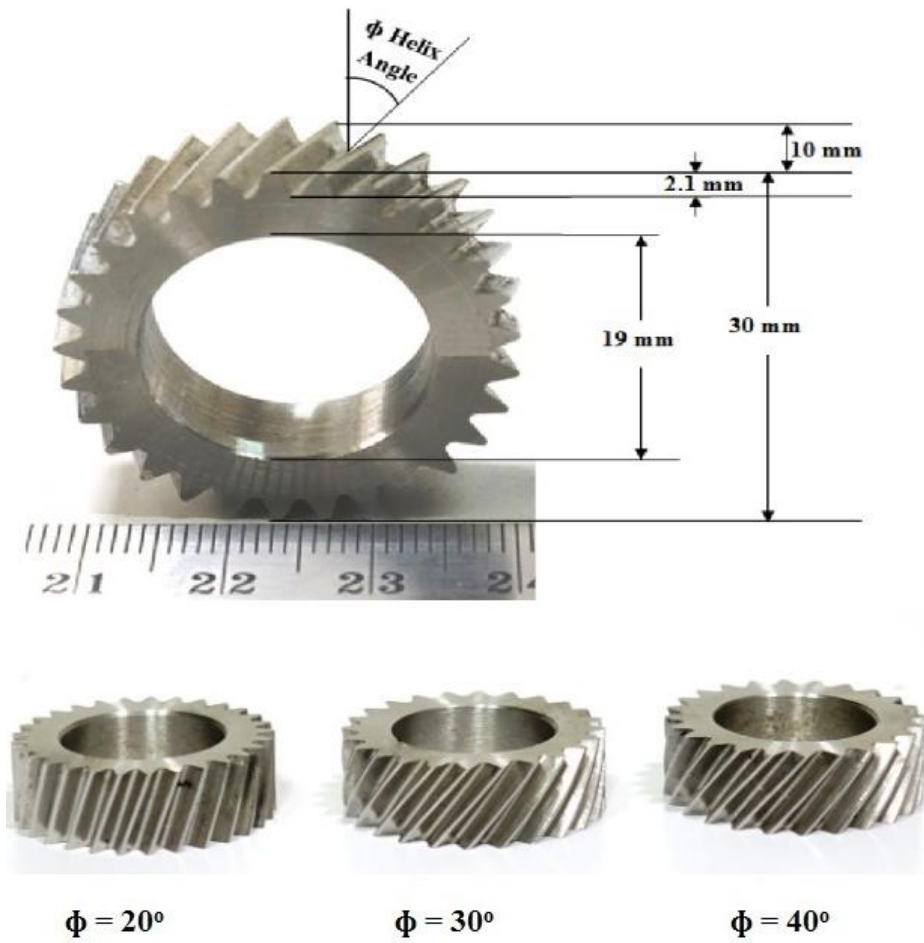
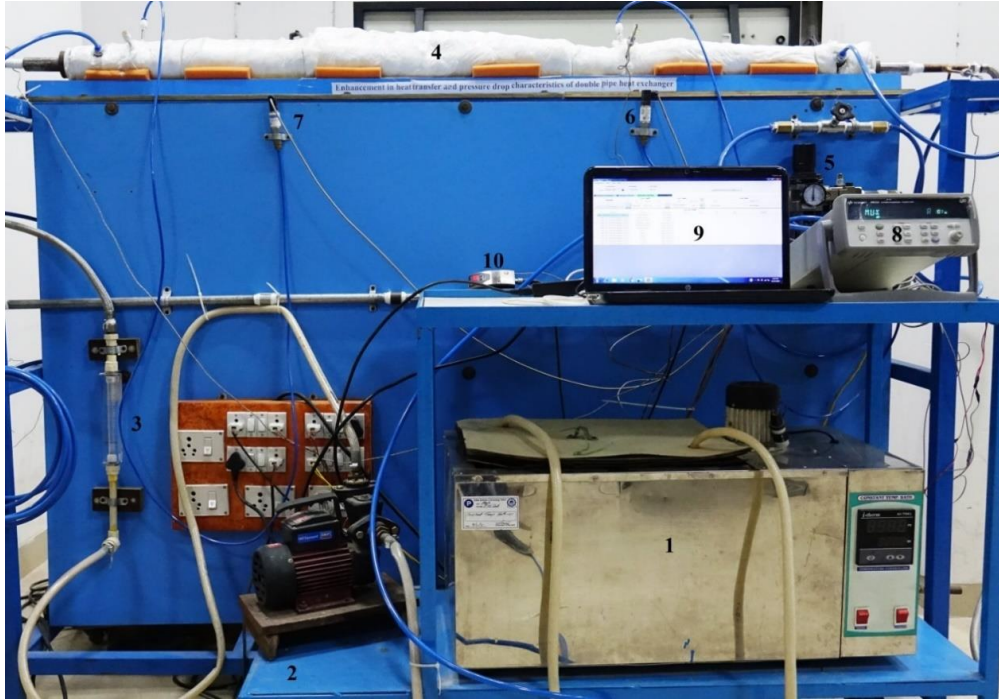


Fig 4.1 (c): Photograph of helical surface disc turbulator.

Table 4.1: Design of HSDTs involving different pitch ratios and various helix angles.

Test section	Inner tube			Outer tube			Number of HSDTs	PR	Helix Angle
	L_t (mm)	d_i (mm)	d_o (mm)	L_s (mm)	D_i (mm)	D_o (mm)			
TS-1	1800	17	19	1800	40	45	0	infinite	-
TS-2	1800	17	19	1800	40	45	6	8.42	40°
TS-3	1800	17	19	1800	40	45	5	9.79	40°
TS-4	1800	17	19	1800	40	45	4	11.79	40°
TS-5	1800	17	19	1800	40	45	6	8.42	30°
TS-6	1800	17	19	1800	40	45	5	9.79	30°
TS-7	1800	17	19	1800	40	45	4	11.79	30°
TS-8	1800	17	19	1800	40	45	6	8.42	20°
TS-9	1800	17	19	1800	40	45	5	9.79	20°
TS-10	1800	17	19	1800	40	45	4	11.79	20°



1.	Thermostat	2.	Centrifugal pump
3.	Rota meter	4.	Test section
5.	FRL unit	6.	Pressure transducer at air inlet
7.	Pressure transducer at air outlet	8.	Data Acquisition System
9.	Computer unit	10.	Airflow meter

Fig. 4.1 (d): Photographic view of test facility.

Before conducting experiments, water temperature is raised to 70- 75°C by using a constant temperature bath. Flow of compressed air is initiated along annuli of DPHE and adjusted to attain the desired Reynolds number. Subsequently, the flow of hot water is initiated along the inner tube. Fluid temperature of (air and water) at both inlet and outlet locations is recorded by using data acquisition system. Final readings are noted after the system attains thermal equilibrium. Efforts have been made to conduct number of tests run to ensure the reliability of test data. The annulus is of primary interest, and therefore experiments are performed constant water flow rate and varied range of air flow rate. Data reduction for the present investigation is same as presented in Chapter 2.

4.2.2 Results and discussion

Tests are conducted for DPHE using HSDTs with three different PR (8.42, 9.79, and 11.79) and three different helix angles (20° , 30° and 40°). In all the cases, the water (hot fluid) flows inside the inner tube, and the air (cold fluid) is issued through the annulus. The maximum difference between inlet and outlet water temperature is found to be 1°C . This may be due to the large difference in the specific heat of water and air. In such a case, outer wall of inner tube is assumed to be at constant temperature [27 -28]. Here, outer wall of outer tube is covered with the ceramic glass wool insulation and is assumed to be adiabatic. The boundary conditions (Fig. 4.2) considered in this study is of third kind [83].

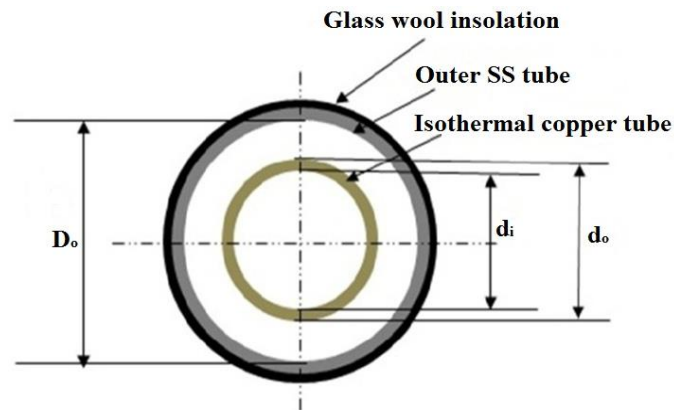


Fig. 4.2: Cross-section and boundary conditions of DPHE.

4.2.2.1 Friction factor characteristics

Fig. 4.3 depicts variation in f value of DPHE fitted with HSDTs with Re , PR, and helix angle. Here, f is observed to decrease with Re and higher f value with higher value of helix angle ($\phi = 40^\circ$). Higher value of helix angle indicates higher swirl generation inside flow regime resulting in higher value of pressure drop. Also, lowest PR value yields higher f values. It may be noted that use of HSDTs in the annulus varies path lines and streamlines that improves recirculation. This results in high turbulence intensity [65-78]. Therefore, significant drop in pressure is noticed across annuli that lead to rise in f values.

The DPHE with $PR = 8.42$ and $\phi = 40^\circ$ at $Re = 3500$ attains the highest value of friction factor ($f = 0.1037$). The maximum enhancement in friction factor with DPHE ($PR = 8.42$ and $\phi = 40^\circ$) compared to the smooth tube DPHE is found to be 11.96 at $Re = 10500$.

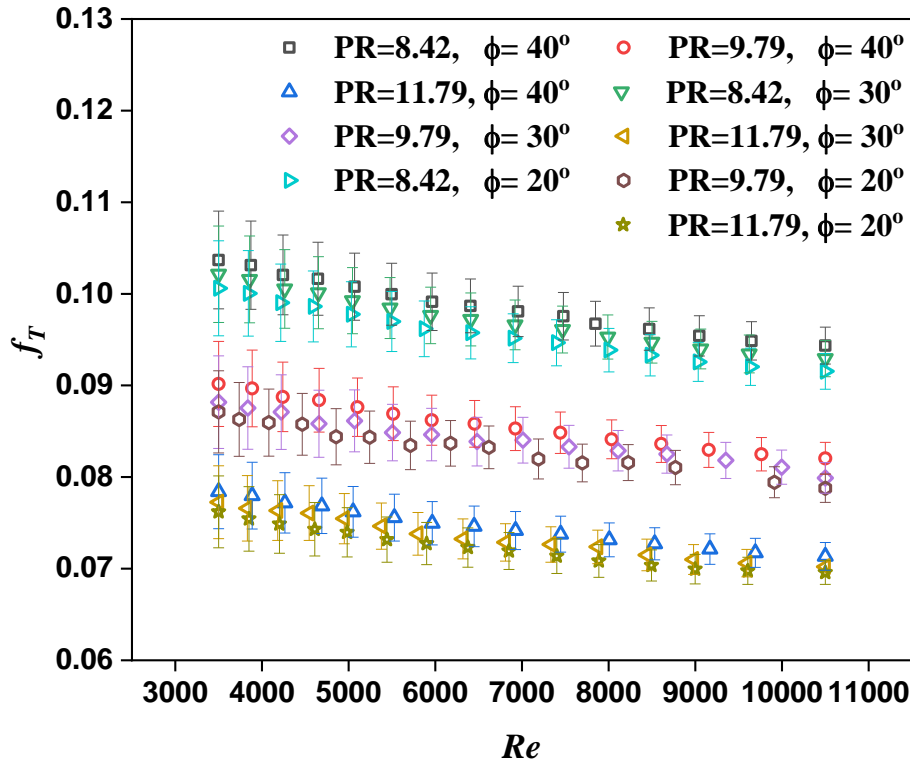


Fig. 4.3: Variation in average friction factor variation with Reynolds number.

4.2.2.2 Heat transfer enhancement

Fig. 4.4 depicts variation in Nu value of DPHE fitted with HSDTs with Re , PR , and helix angles. The DPHE fitted with HSDTs exhibits improved thermal performance compared to DPHE without HSDTs. The improvement in heat transfer is noticed with rise in Re value. The highest performance is observed for DPHE fitted with HSDTs with $\phi = 40^\circ$ and $PR = 8.42$ compared to the DPHE with HSDTs for $\phi = 20^\circ$ and $PR = 11.79$. The maximum Nu value is noticed at $Re = 10500$, $PR = 8.42$ and $\phi = 40^\circ$. The lower pitch ratio implies more number of turbulators, which results in more streamlines variation in the flow. Also, increase in helix angle results in more swirl generation and increase in the re-circulation.

Increased turbulent intensity causes better fluid mixing and improves heat transfer. Previous researchers [65-78] have also made similar observations.

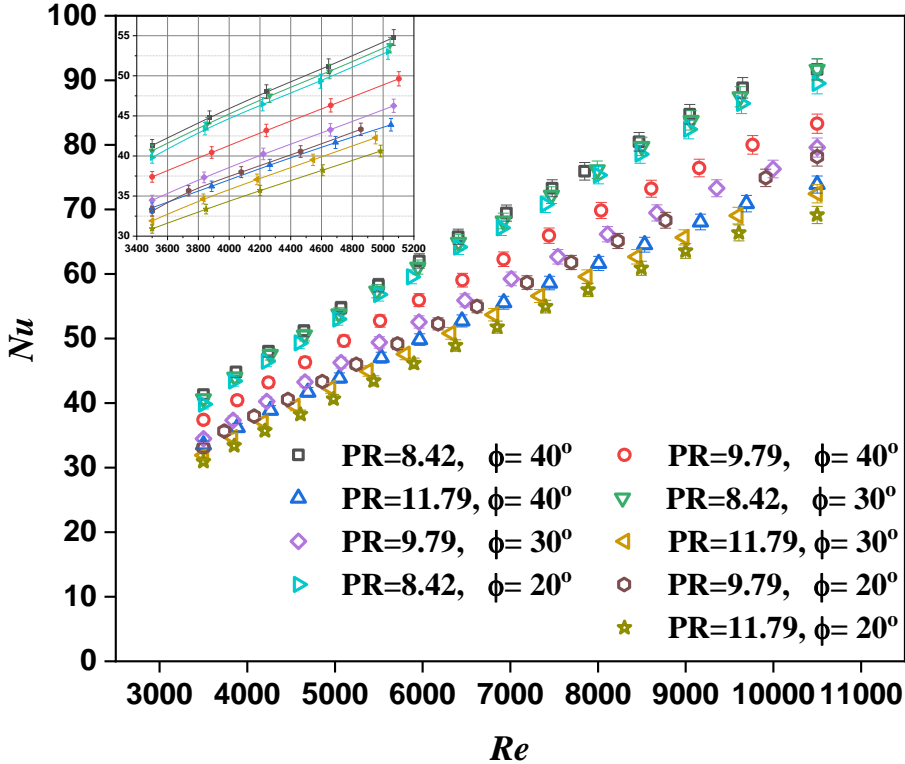


Fig. 4.4: Variation in average Nusselt number variation with Reynolds number.

4.2.2.3 Comparison of annuli with HSDTs and without HSDTs

The performance of DPHE with and without HSDTs have been compared. The Nu ratio (NR) and f ratio (FR) is estimated for analyzing the performance of the concentric DPHE with and without HSDTs. Fig. 4.5 depicts distribution of NR values (ratio of Nu values for DPHE with and without HSDTs) and FR values (ratio of f values for DPHE with and without HSDTs) for the various Re , PR, and ϕ , respectively. For each case, NR values are observed to be higher than unit value. The NR value is observed to reduce gradually with rise in Re value. The highest NR value is observed to be 3.01 for PR = 8.42 and $\phi = 40^\circ$ and $Re = 3500$. The DPHE with PR = 8.42 and $\phi = 40^\circ$ exhibits higher NR value compared to the DPHE with PR = 11.79 and $\phi = 20^\circ$. This is to be noted that increase in contact

surface area implies more number of turbulators. In such case, contact between fluid and heat transfer surface increases and results in high heat exchange. Also, turbulators increase the recirculation leads to increase in heat transfer rate. In addition, heat transfer performance increases with rise in helix angle of the HSDT. The rise in helix angle yields improved swirl generation, results in rise in turbulence intensity and mixing of the fluid [65-78] that enhances heat transfer.

The increase in FR values (Fig. 4.5) is noticed with rise in Re value, and highest FR value 11.96 is observed for DPHE fitted with HSDTs at PR = 8.42 and $\phi = 40^\circ$ at Re = 10500. The DPHE with PR = 8.42 and $\phi = 40^\circ$ exhibits higher FR value compared to the DPHE with PR = 11.79 and $\phi = 20^\circ$. The turbulators generates re-circulation and rise in helix angle causes more swirl generation, which leads high fluid mixing and turbulence intensity results in high FR value [65-78].

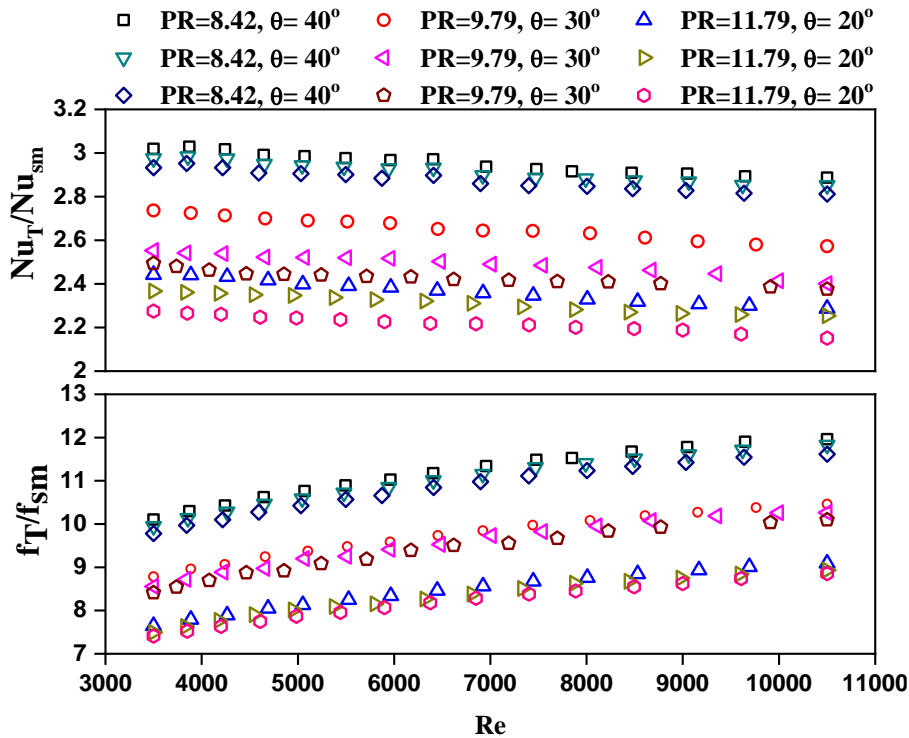


Fig. 4.5: Variation in Nusselt number ratio and friction factor ratio with Reynolds number.

4.2.2.4 Thermal performance of annuli of DPHE

The enhancement in the thermal performance reduces the size and cost of heat exchanging equipment. Therefore, thermal performance factor (TPF) is evaluated considering different parameters namely flow rate, pressure drop, and heat transfer rate [85-86] for the effective assessment of the modified DPHE. In general, TPF is employed to compare the improvement in the heat exchange rate and pressure drop. For the same pumping power, TPF is expressed as [65-78]:

$$TPF(\eta) = \frac{(Nu_T / Nu_{sm})}{(f_T / f_{sm})^{1/3}} \quad (4.3)$$

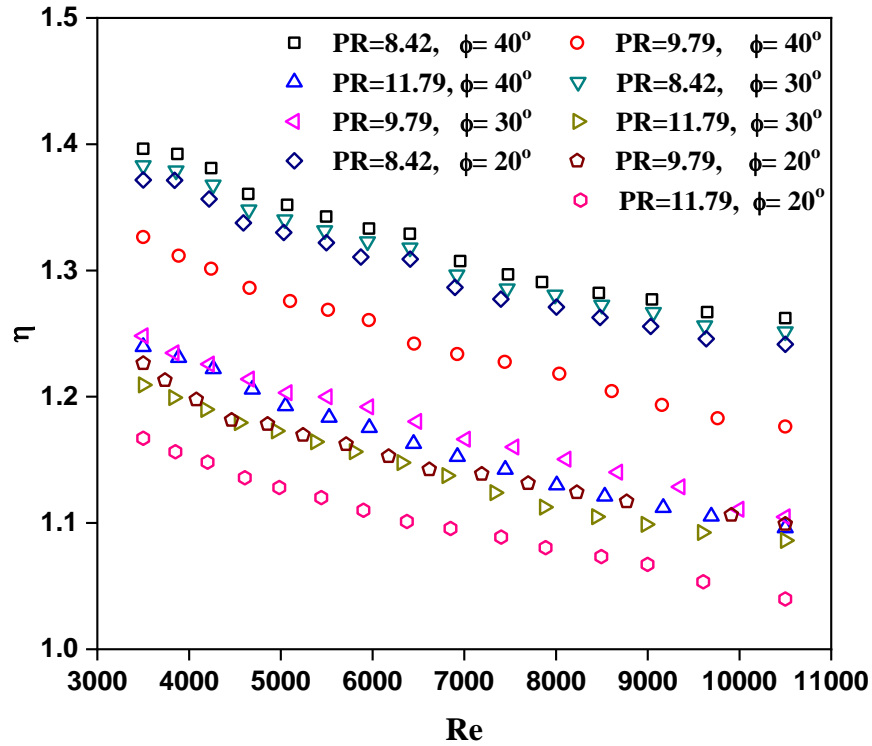


Fig. 4.6: Variation in thermal performance factor with Reynolds number.

TPF for DPHE fitted with HSDTs for various ϕ , PR, and Re are shown in Fig. 4.6. Here, TPF varies inversely with Re and PR and increases with increase in ϕ value. In each case, TPF value is observed to be higher than unit value. and

highest value of TPF is observed to be 1.39 at $Re = 3500$ for the DPHE fitted with HSDTs involving $\phi = 40^\circ$ and $PR = 8.42$.

4.2.2.5 Comparison of present thermal performance with previous studies

Fig. 4.7 shows comparison of the maximum TPF obtained by present study with the test results of Sheikholeslami and Ganji [73] that uses turbulators with perforation in annulus, experimental data of Sheikholeslami et al. [74], Kongkaitpaiboon et al. [66], and Promvonge [62] that utilize conical ring in

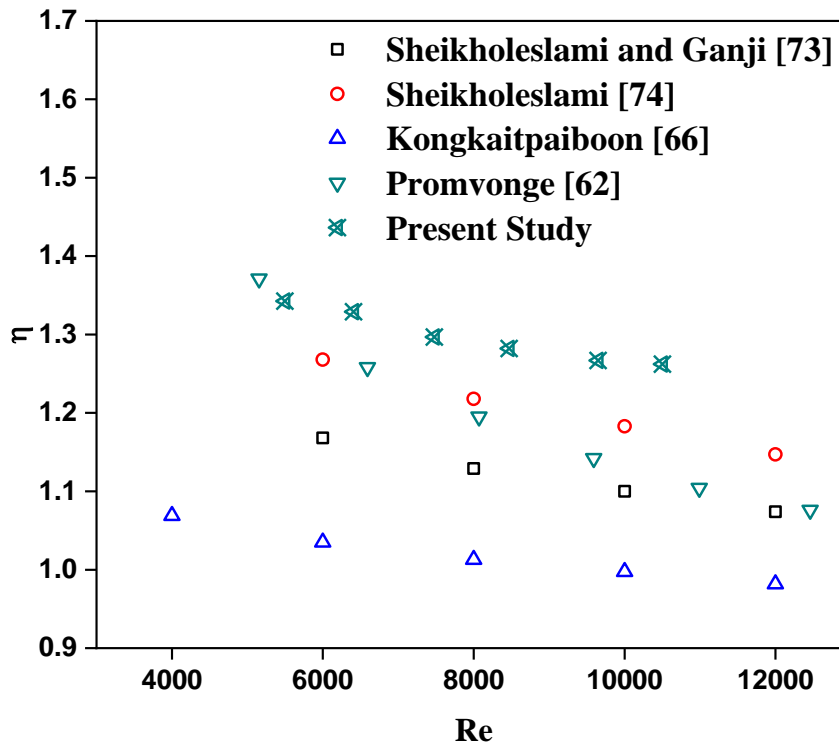


Fig. 4.7: Comparison of thermal performance factor with the previous studies.

annulus [74], circular-ring in tube [66] and wire coil turbulators involving twisted tape in tube [62]. It has been noticed from Fig. 4.7, the TPF value reduces with rise in Re value and is highest at $Re = 3500$. This has also been observed that the TPF values for the present case ($PR = 8.42$ and $\phi = 40^\circ$) are about 11 - 12%, 4 - 7%, 21 - 22% and 5 - 13% higher compared to the TPF values of Sheikholeslami

and Ganji [73], Sheikholeslami et al. [74], Kongkaietpaiboon et al. [66] and Promvonge [62], respectively. The use of HSDTs in the annulus of DPHE provides the additional recirculation due to helical surface of the disc turbulator. This may be the reason of higher thermal performance obtained in the present study with use of HSDTs in the annulus compared to the previous studies [62, 66, 73, and 74].

4.2.2.6 Correlations for various parameters

Turbulators of different shapes and designs are employed by the previous authors to improve heat transfer rate. These include experimental studies of Eiamsa-ard and Promvonge [47], Kongkaietpaiboon et al. [66], Thianpong et al. [67], Ruengpayungsak et al. [75] and Eiamsa-ard [81] that employ alternate clockwise and counterclockwise twisted tape insert, circular ring turbulators, twisted ring turbulators, gear ring turbulators, and C-nozzles turbulators, respectively. Various correlations have been proposed for Nu, f, and TPF by different researchers [47,66,67,75,81]. The authors [47,66,67,75,81] proposed correlation for various parameters and are summarized in Table 4.2.

Utilizing present experimental data, various correlations are proposed for Nu, f, and TPF and expressed in Eqs. (4.4 - 4.6). The proposed correlations are valid for varied range of PR (8.42 – 11.79), ϕ (20° – 40°) and Re (3500 -10500). The Re exponent is noticed to vary between 0.6 – 0.883 for various Nu correlation [47, 66, 67, 75, and 81]. The dependence of Re on Nu for the present study is expressed in Eq. 14 and is similar to the previous studies [47, 66, 67, 75, and 81]. Correlation for f (Eq. 15) is observed to be a weak function of Re. It may be noted that Re dependence on f, may vary based on turbulator's design. Similar observations have been made by Kongkaietpaiboon et al. [66] during their studies by using circular ring turbulators. However, The exponent of Reynolds number is found to vary significantly for various correlations proposed to estimate the friction factor [47, 61, 67, 75, and 81]. Turbulators interrupt the boundary layer thickness and enhance the intensity of turbulence resulting in better fluid mixing.

Also, these turbulators provide increased surface area for the heat, which results in the increase in heat exchange rate and pressure drop behavior. The deviation between present test data and proposed correlation is shown in Fig. 4.8. The correlations for Nu (Eq. 4.4) and TPF (Eq. 4.6) predict 91% and 97% test data, respectively within $\pm 4\%$ error band while f correlation (Eq. 4.5) predicts 98% test data within $\pm 2\%$ error band.

$$\text{Nu}_T = 0.471 \text{Re}^{0.741} \text{PR}^{-0.714} (\text{Sin}\phi)^{0.086}; \left\{ \begin{array}{l} 3500 \leq \text{Re} \leq 10500 \\ 8.42 \leq \text{PR} \leq 11.79 \\ 20^\circ \leq \phi \leq 40^\circ \end{array} \right\} \quad (4.4)$$

$$f_T = 1.275 \text{Re}^{-0.087} \text{PR}^{-0.837} (\text{Sin}\phi)^{0.050}; \left\{ \begin{array}{l} 3500 \leq \text{Re} \leq 10500 \\ 8.42 \leq \text{PR} \leq 11.79 \\ 20^\circ \leq \phi \leq 40^\circ \end{array} \right\} \quad (4.5)$$

$$\eta = 8.344 \text{Re}^{-0.102} \text{PR}^{-0.429} (\text{Sin}\phi)^{0.0751}; \left\{ \begin{array}{l} 3500 \leq \text{Re} \leq 10500 \\ 8.42 \leq \text{PR} \leq 11.79 \\ 20^\circ \leq \phi \leq 40^\circ \end{array} \right\} \quad (4.6)$$

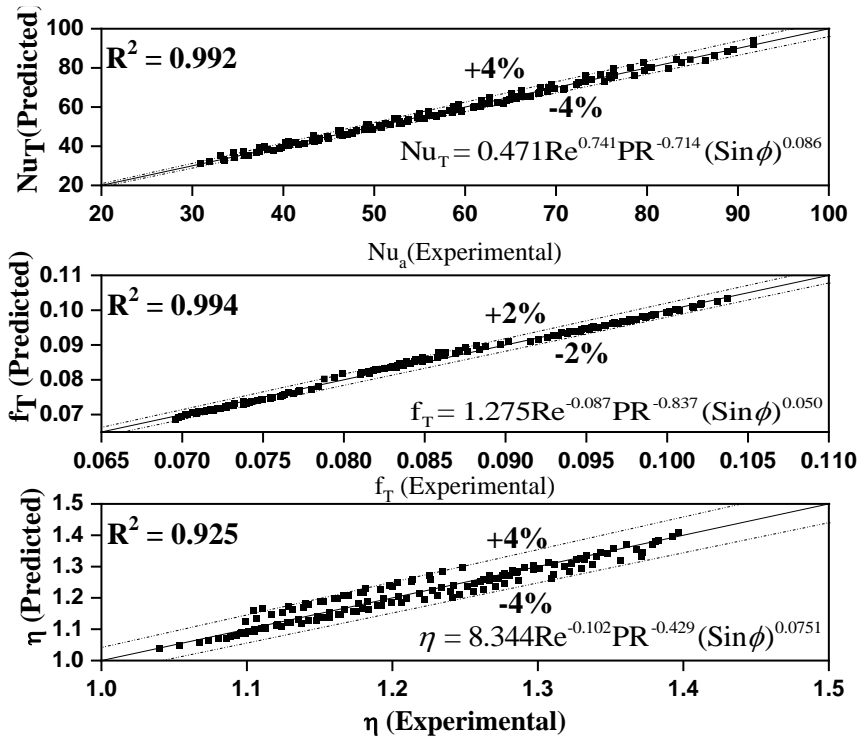


Fig. 4.8: Comparison of experimental and predicted values.

Table 4.2: Correlations proposed by various researchers.

Source	Type/augmentation method/parameters	Re	Correlations
Eiamsa-ard and promvong [47]	Alternate clockwise and counterclockwise twisted tape insert (Twist angle $\theta = 30^\circ, 60^\circ$ and 90°)	8000 - 18000	$\text{Nu} = 0.31 \text{Re}_s^{0.6} \text{Pr}^{0.4} (y/w)^{-0.36} (1 + \sin \theta)^{0.44}$ $f = 46.39 \text{Re}_s^{-0.544} (y/w)^{-0.77} (1 + \sin \theta)^{0.45}$
Roy and Saha [61]	wire coil inserts (Helix angle $\alpha = 30^\circ, 45^\circ$ and 60°)	6000 - 24000	$f = 3.55827 \text{Re}^{-0.67719} (\sin \alpha)^{0.25811} d_c^{0.33739}$
Kongkai paiboon et al. [66]	Circular ring turbulators	4000 - 20000	$f = 0.715 \text{Re}^{-0.081} DR^{-4.775} PR^{-0.846}$ $\eta = 5.315 \text{Re}^{-0.078} DR^{1.031} PR^{-0.317}$
Thianpong et al. [67]	Twisted ring turbulators	6000-20000	$\text{Nu} = 0.097 \text{Re}^{0.883} \text{Pr}^{0.4} (W/D)^{0.408} (p/D)^{-0.181}$ $f = 112.795 \text{Re}^{-0.159} (W/D)^{1.665} (p/D)^{-0.736}$

Table 4.2 (Cotinued).

Source	Type/augmentation method/parameters	Re	Correlations
Ruengpayungsak et al. [75]	Gear ring / circular ring turbulators	6000-20000	For circular ring turbulators $Nu = 0.078 Re^{0.786} Pr^{0.4} (SR)^{-0.136}$ $f = 0.788 Re^{-0.051} (SR)^{-0.486}$ $\eta = 5.531 Re^{-0.175} (SR)^{0.026}$
			For gear ring turbulators $Nu = 0.1 Re^{0.768} Pr^{0.4} (SR)^{-0.14} (1+N)^{-0.13}$ $f = 2.143 Re^{-0.06} (SR)^{-0.522} (1+N)^{-0.479}$ $\eta = 5.21 Re^{-0.175} (SR)^{0.034} (1+N)^{0.029}$
Kumar et al. [80]	hollow circular disk	6500-23000	$\eta = 5.315 Re^{-0.078} DR^{1.031} PR^{-0.317}$
promvonge and Eiamsa-ard [81]	C-Nozzles turbulators	8000 - 18000	$Nu = 0.143 Re^{0.736} Pr^{1/3} (PR)^{-0.12}$ $f = 29 Re^{-0.197} (PR)^{-0.052}$
Present Study	Helical surface disc turbulators	3500 - 10500	$Nu_T = 0.471 Re^{0.741} PR^{-0.714} (\sin \phi)^{0.086}$ $f_T = 1.275 Re^{-0.087} PR^{-0.837} (\sin \phi)^{0.050}$ $\eta = 8.344 Re^{-0.102} PR^{-0.429} (\sin \phi)^{0.0751}$

4.3 Effect of diameter ratio and pitch ratio on thermo hydraulic performance of DPHE with helical surface disc turbulators

Here, tests are performed to examine the effect of various parameters namely, different diameter ratios (0.42, 0.475 and 0.54) various pitch ratios (8.42, 9.79 and 11.79) and various Reynolds numbers (3500 - 10500) on the thermal performance in the annuli of DPHE with helical surface disc turbulators (HSDTs). Based on the tests data thermal performance of DPHE involving helical surface disc turbulators are estimated. Also, correlations are proposed to evaluate various parameters such as Nusselt number, friction factor, and thermal performance factor.

4.3.1 Test facility, procedure and data reduction

Test facility and procedure are discussed in the earlier section (section 4.2.1). However, test sections used for this study are different. Table 4.3 summarizes test sections used in the present experimental study. The length of test specimen and test section was kept 1.8 m and 1.1 m, respectively, for all the cases. Data reduction for the present investigation is same as presented in Chapter 2.

4.3.2 Results and discussion

Tests are conducted for DPHE using HSDTs with different diameter ratio (0.42, 0.475 and 0.54) various pitch ratio (8.42, 9.79, and 11.79) and Reynolds number (3500 - 10500).

4.3.2.1 Friction factor characteristics

Fig. 4.9 depicts the variation in characteristics of f values of DPHE using HSDTs with Re, PR, and DR. The f values are found to be decreased gradually with increase in Re. Higher value of the f value is obtained for the lower value of DR.

Table 4.3: Design of HSDTs involving different diameter ratios and various pitch ratios.

Test section	DR	Tube			shell			Pitch ratio	Number of HSDTs
		L _t (mm)	d _i (mm)	d _o (mm)	L _s (mm)	D _i (mm)	D _o (mm)		
TS1	0.54	1800	17	19	1800	35	40	Infinite	0
TS2	0.54	1800	17	19	1800	35	40	11.79	4
TS3	0.54	1800	17	19	1800	35	40	9.79	5
TS4	0.54	1800	17	19	1800	35	40	8.42	6
TS5	0.475	1800	17	19	1800	40	45	Infinite	0
TS6	0.475	1800	17	19	1800	40	45	11.79	4
TS7	0.475	1800	17	19	1800	40	45	9.79	5
TS8	0.475	1800	17	19	1800	40	45	8.42	6
TS9	0.420	1800	17	19	1800	45	50	Infinite	0
TS10	0.420	1800	17	19	1800	45	50	11.79	4
TS11	0.420	1800	17	19	1800	45	50	9.79	5
TS12	0.420	1800	17	19	1800	45	50	8.42	6

Lower value of DR indicates higher annulus diameter resulting higher value of friction in the fluid layers. Similar results for the friction factor have been reported by Dirker et al. [84]. It is observed that for the same DR, lower value of PR exhibits higher f value. The use of turbulators in the annulus causes the variation in streamlines and the path lines resulting in generation of higher re-circulation, leads to increase turbulence intensity [65-78] which causes more pressure drops, resulting in increase in f values. The f values for the different configurations (DR= 0.42, Re = 3500), (DR = 0.475, Re = 3500) and (DR = 0.53, Re = 3500) are found to be 0.111, 0.103 and 0.0954, respectively. The maximum enhancement factor in f value was found to be 13.06 for DR= 0.42, and PR = 8.42 at Re = 10500 compared to the smooth tube DPHE.

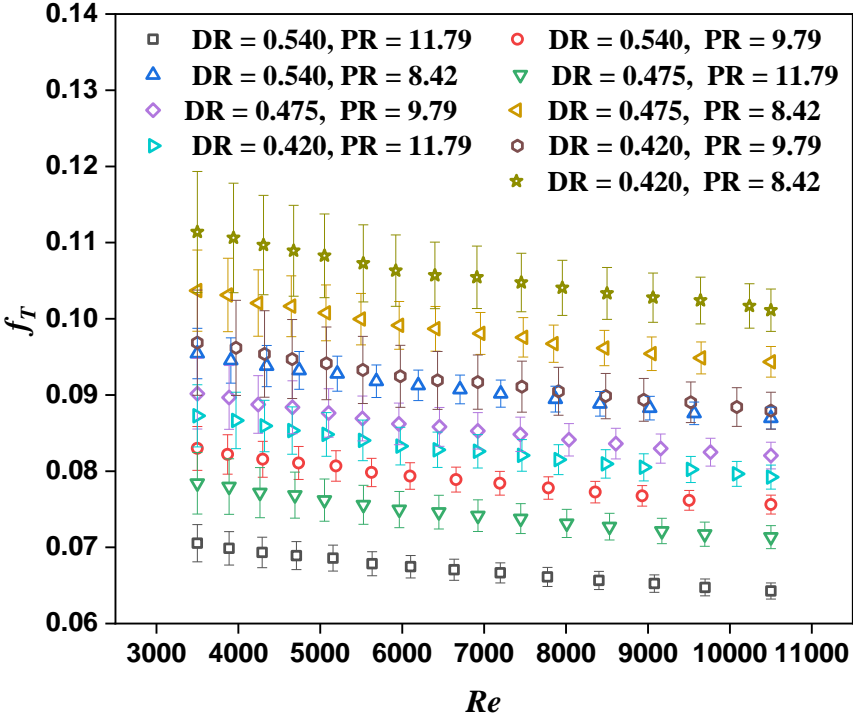


Fig. 4.9: Variation of average friction factor with Reynolds number in the annulus using HSDTs.

4.3.2.2 Heat transfer enhancement

Fig. 4.10 depicts the variation Nu variations with Re for various values of PR and DR . It has been noted that the use of HSDTs exhibits better heat transfer performance compared to smooth tubes DPHE without HSDTs. Also, the enhancement in heat transfer is found to increase with the increase in the Re value. The DPHE using HSDTs with $PR = 8.42$ and $DR = 0.42$ exhibits better heat transfer performance. While DPHE using HSDTs with $PR = 11.79$ and $DR = 0.54$ exhibits lowest heat transfer performance. At $Re = 10500$, $DR = 0.42$ and $PR = 8.42$, the DPHE with HSDTs exhibits the highest Nu value. This may be due to the fact that lower DR and PR results in higher turbulators effect. This leads to higher re-circulation, resulting in better mixing of the fluid [65-78]. This enhances the heat transfer performance of the DPHE. Similar observations have been made by previous researchers [65-78].

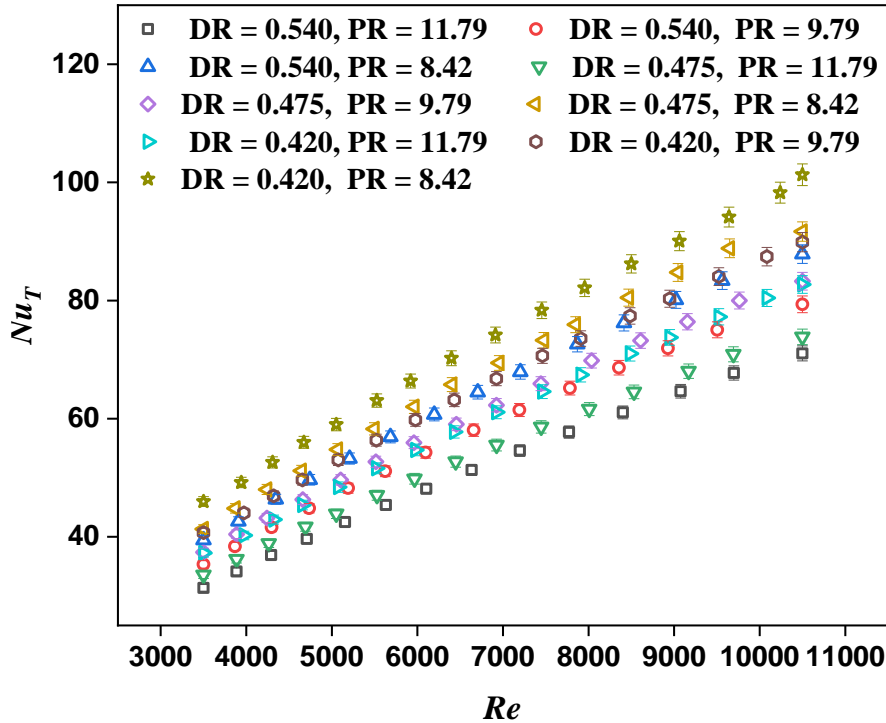


Fig. 4.10: Variation in average Nusselt number with Reynolds number.

4.3.2.3 Comparison of annuli with HSDTs and without HSDTs

Here, efforts have been made to compare the performance of DPHE using HSDTs to the DPHE without HSDTs. The variation of Nu ratio (ratio of Nu for the DPHE with HSDTs to that of DPHE without HSDTs) with varied range of Re, PR, and DR (Fig. 4.11). For all the cases, the Nu ratio is found to be greater than unity value and is found to decrease gradually with the increase in Re. The maximum Nu ratio is found to be 3.28 for PR = 8.42.

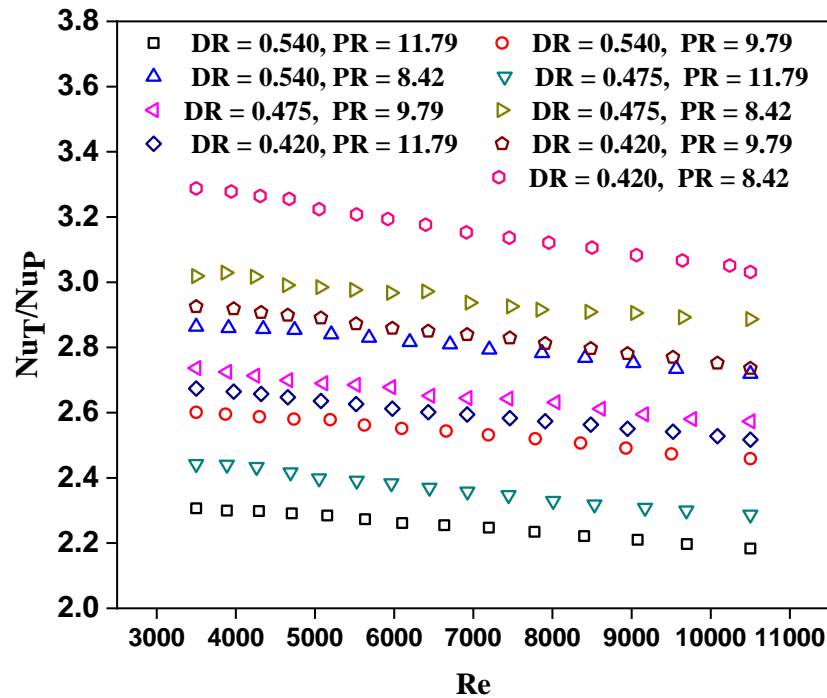


Fig. 4.11: Variation in Nusselt number ratio with Reynolds number.

The variation of f ratio (ratio of f value for DPHE with HSDTs to the DPHE without HSDTs) with Re for various values of PR and DR (Fig. 4.12). The f ratio increases with an increase in the Re value and attains the maximum value of 13.06 for PR = 8.42 and DR = 0.42 at Re = 10500. The DPHE with pitch ratio = 8.42 and DR=0.42 exhibits higher f ratio compared to the DPHE with, pitch ratio = 11.79 and DR= 0.54.

It may be noted that turbulators provide the higher heat transfer surface area to the flow inside annulus [65-78] and increase the turbulence intensity inside flow regime which promotes fluid mixing at different fluid layers and the higher heat transfer rate is achieved.

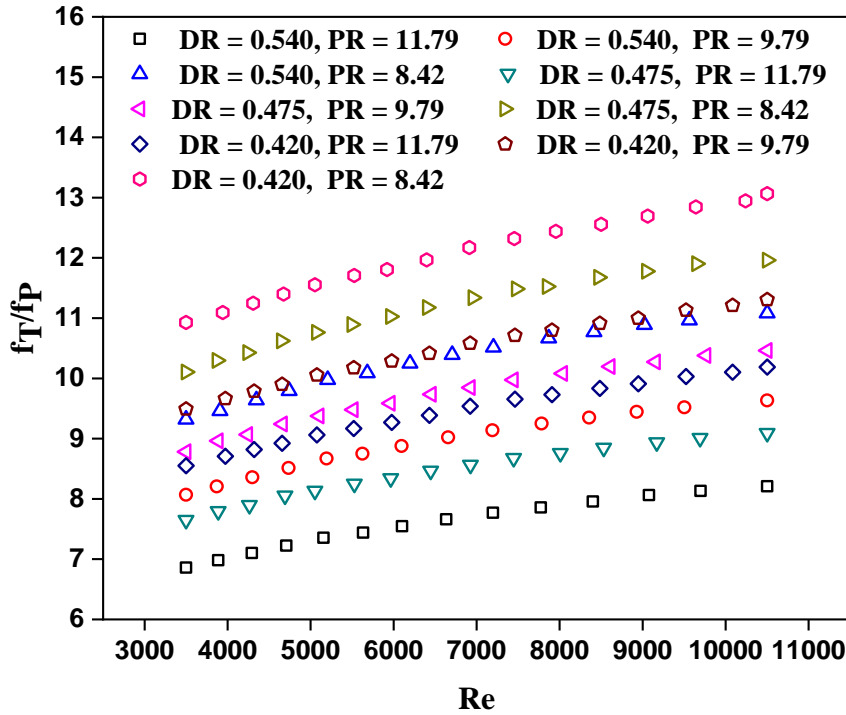


Fig. 4.12: Variation in friction factor ratio with Reynolds number.

4.3.2.4 Thermal performance of annuli of DPHE with HSDTs

The effective assessment of the modified surfaces directly relates to the cost of operation in heat exchangers. The performance evaluation criteria have been selected based on various parameters such as pressure drop, heat transfer rate, and flow rate [85-86].

Thermal performance factor is usually used to evaluate the effect of enhancement in heat transfer rate compared to the increase in the pressure drop. For the same pumping power condition, the TPF is similar to Eq. 4.3. The TPF for various PR of DPHE equipped with HSDTs at different DR and Re is shown in Fig. 4.13. For all the cases tested in this study, TPF is found to be greater than

unity. The maximum value of TPF for DPHE using HSDTs with pitch ratio = 8.42 and DR = 0.42, is found to be 1.48 at Re = 3500.

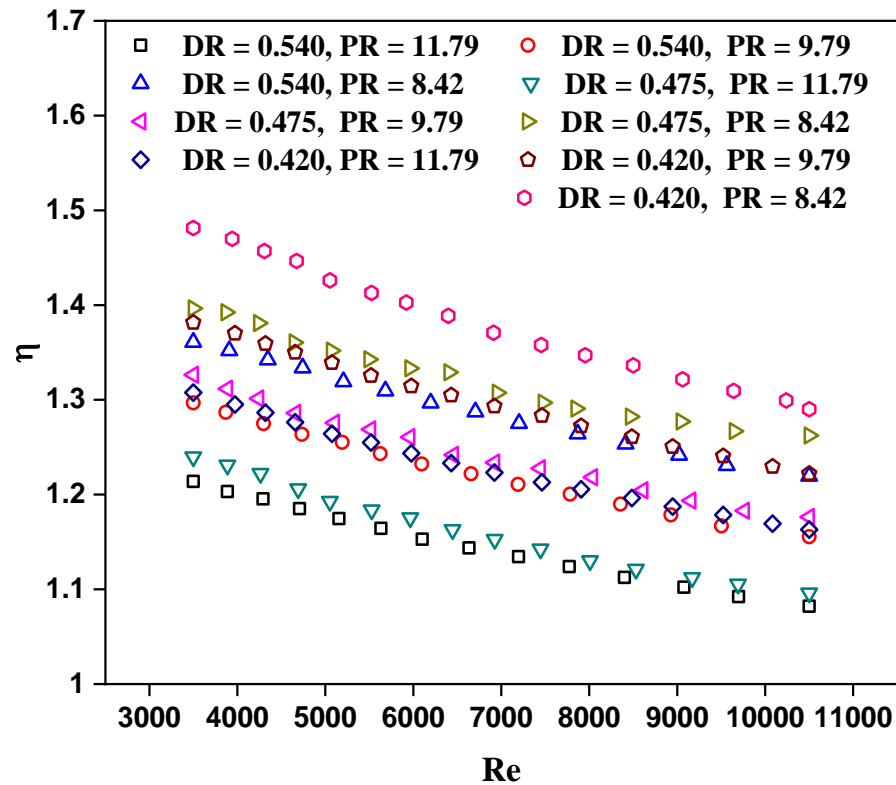


Fig. 4.13: Variation in thermal performance factor with Reynolds number in the annulus.

4.3.2.5 Correlations for various parameters

Present test data are used to derive the correlation for Nu, f , and TPF as a function of various parameters such as Reynolds number, pitch ratio, and diameter ratio by using the least square method of regression analysis and is expressed in Eqs. 4.7-4.9. The proposed correlations are valid for wide range of Reynolds number (Re = 3500 – 10500), pitch ratio (PR = 8.42 -11.79), and diameter ratio (DR = 0.42 - 0.54)

$$Nu_T = 0.271 Re^{0.737} (PR)^{-0.627} (DR)^{-0.494}, \left\{ \begin{array}{l} 3500 \leq Re \leq 10500 \\ 8.42 \leq PR \leq 11.79 \\ 0.42 \leq DR \leq 0.54 \end{array} \right\} \quad (4.7)$$

$$f_T = 0.724 Re^{-0.088} (PR)^{-0.81} (DR)^{-0.67}, \left\{ \begin{array}{l} 3500 \leq Re \leq 10500 \\ 8.42 \leq PR \leq 11.79 \\ 0.42 \leq DR \leq 0.54 \end{array} \right\} \quad (4.8)$$

$$\eta = 6.285 Re^{-0.114} (PR)^{-0.359} (DR)^{-0.277}, \left\{ \begin{array}{l} 3500 \leq Re \leq 10500 \\ 8.42 \leq PR \leq 11.79 \\ 0.42 \leq DR \leq 0.54 \end{array} \right\} \quad (4.9)$$

Wide variety of studies has been reported that consider numerous turbulent promoters of different shapes, types with various working fluid in order to enhance the heat transfer rate. Various researchers have proposed correlations for the Nu , f , and TPF. Some of their correlations for Nu , f , and TPF have been summarized in Table 4.4. It is observed that the exponent of Re for Nu correlations varies significantly based on turbulators designs. These turbulators disrupt the boundary layer by generating re-circulation inside flow regime resulting in increase in the turbulent intensity. Also, these turbulent promoters provide higher heat transfer surface area and hence affect the heat transfer rate significantly. In view of this, the exponent of the Re is higher in the present proposed correlations (Eq. 4.7). Earlier, different authors have conducted experiments with twisted tape and wire coil turbulators in tube [62], circular ring turbulators in tube [66], V nozzle turbulators in tube [71], gear ring turbulators in tube [75], solid hollow circular disc in tube [80], and C-nozzles turbulators in tube [95]. These authors have proposed correlation for Nusselt number and friction factor as a function of different operating parameters including Reynolds number. Similar value of exponent for Reynolds number have been reported by previous researchers [62,66,71,75,80,95]. It has been noted that f is a weak function of Re in turbulent regime similar to the other existing correlations [66, 75]. The exact dependence of f values with Re is not clear. Some studies [66, 75 and 80] report f is a weak function of Re based on their investigation. On the contrary, some

authors [62 and 71] observed the f strongly depends on Re . This may be the reason that f is the weak function of Re for the present proposed correlation.

Also, attempts have been made to compare the present test data with the proposed correlations and are shown in Figs. 4.14 – 4.15. In the case of Nu and f , proposed correlations (Eq. 4.7 – 4.8) are able to predict 80%, 92% of experimental test data, respectively within an error band of $\pm 2\%$ (Fig. 8-9). Also, the proposed correlation of TPF (Eq. 4.9) is able to predict 68% of test data within an error band of $\pm 1\%$ (Fig.16).

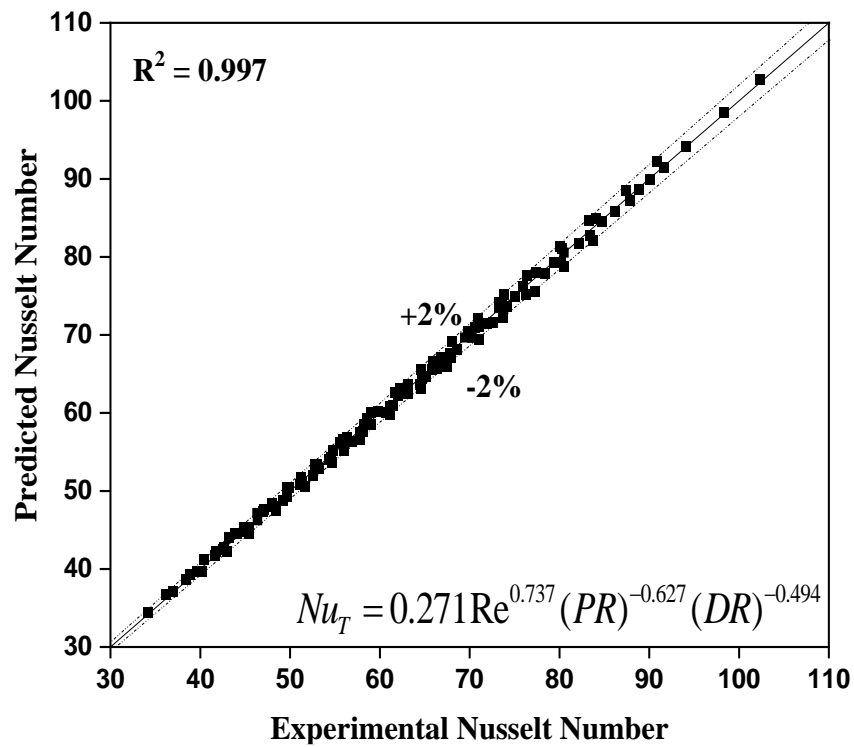


Fig. 4.14: Comparison of experimental and predicted values of average Nusselt number.

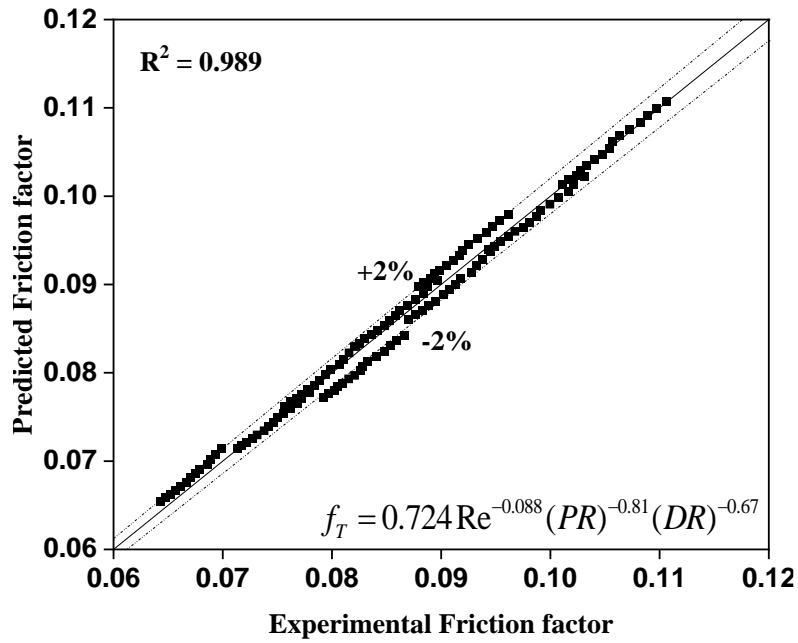


Fig. 4.15: Comparison of experimental and predicted values of average friction factor.

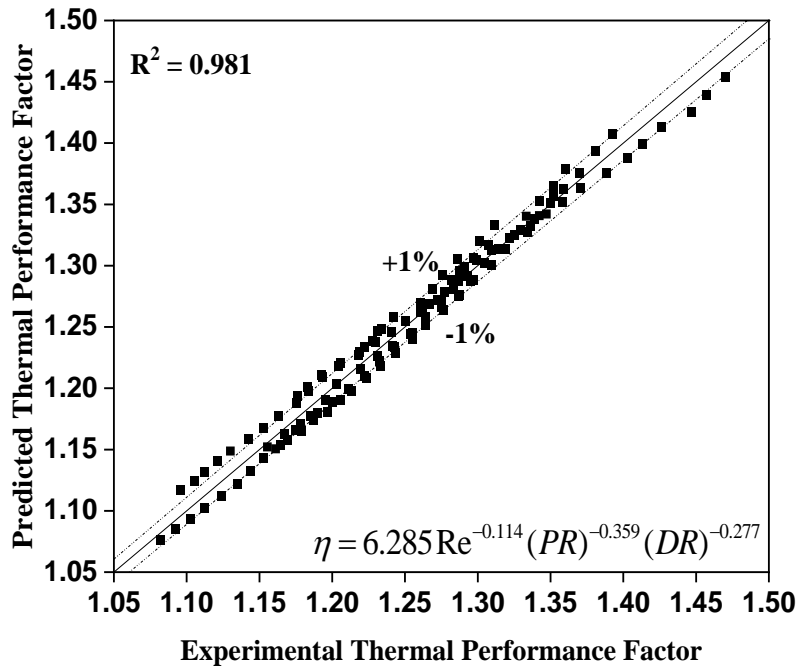


Fig. 4.16: Comparison of experimental and predicted values of thermal performance factor.

Table 4.4: Correlations proposed by various researchers.

Source	Type/method of passive enhancement	Reynolds number	Remark/correlations
Promvonge [62]	Twisted tape and wire coil turbulators in tube	3000 - 18000	$Nu = 4.47 Re^{0.5} Pr^{0.4} (CR)^{-0.382} Y^{-0.38}$ $f = 338.37 Re^{-0.367} (CR)^{-0.887} Y^{-0.455}$ <p>CR (coil spring pitch ratio) = H/D, Y = Twist ratio of tape insert</p>
Kongkaitpaiboon [66]	Circular ring turbulators (CRT) in tube	4000 - 20000	$Nu = 0.354 Re^{0.697} Pr^{0.4} DR^{-0.555} PR^{-0.598}$ $f = 0.715 Re^{-0.081} DR^{-4.775} PR^{-0.846}$ $\eta = 5.315 Re^{-0.078} DR^{1.031} PR^{-0.317}$
Thianpong et al. [67]	Twisted ring turbulators in tube	6000-20000	$Nu = 0.097 Re^{0.883} Pr^{0.4} (W/D)^{0.408} (p/D)^{-0.181}$ $f = 112.795 Re^{-0.159} (W/D)^{1.665} (p/D)^{-0.736}$
Eiamsa-ard and promvonge [71]	V Nozzle turbulators in tube	8000 - 18000	$Nu = 0.524 Re^{0.6} Pr^{0.4} (PR)^{-0.285}$ $f = 107 Re^{-0.42} (PR)^{-0.68}$ <p>PR (Pitch ratio) = Ratio of pitch length to tube diameter.</p>

Table 4.4 (Continued).

Source	Type/method of passive enhancement	Reynolds number	Remark/correlations
Ruengpayungsak et al. [75]	Gear ring / circular ring turbulators in tube	6000-20000	For circular ring turbulators $Nu = 0.078 Re^{0.786} Pr^{0.4} (SR)^{-0.136}$ $f = 0.788 Re^{-0.051} (SR)^{-0.486}$ $\eta = 5.531 Re^{-0.175} (SR)^{0.026}$ For gear ring turbulators $Nu = 0.1 Re^{0.768} Pr^{0.4} (SR)^{-0.14} (1+N)^{-0.13}$ $f = 2.143 Re^{-0.06} (SR)^{-0.522} (1+N)^{-0.479}$ $\eta = 5.21 Re^{-0.175} (SR)^{0.034} (1+N)^{0.029}$
Kumar et al. [80]	Solid hollow circular disc in tube	6000 - 24000	$Nu = 0.1248 Re^{0.7253} DR^{-0.5792} PR^{-0.088} \exp\{-0.0246(\ln PR^2)\}$ $f = 0.1284 Re^{-0.1199} DR^{-4.2233} PR^{-0.2374} \exp\{0.0033(\ln PR^2)\}$ $\eta = 5.1867 Re^{-0.1201} DR^{0.8107} PR^{0.0632} \exp\{0.0952(\ln PR^2)\}$
promvonge and Eiamsa-ard [95]	C-Nozzles turbulators in tube	8000 - 18000	$Nu = 0.143 Re^{0.736} Pr^{1/3} (PR)^{-0.12}$ $f = 29 Re^{-0.197} (PR)^{-0.022}$ $\eta = 2.84 Re^{-0.139} (PR)^{-0.052}$
Present Study	HSDTs	3500 - 10500	$Nu_T = 0.271 Re^{0.737} (PR)^{-0.627} (DR)^{-0.494}$ $f_T = 0.724 Re^{-0.088} (PR)^{-0.81} (DR)^{-0.67}$ $\eta = 6.285 Re^{-0.114} (PR)^{-0.359} (DR)^{-0.277}$

4.3.2.6 Comparison of present thermal performance with previous studies

Here, present correlation for TPF (Eq. 4.9) is used to correlate the test data of previous study made in the annulus of DPHE by using discontinuous helical turbulators [72], perforated turbulators [73] and conical ring turbulators [74] and is shown in Fig. 4.17.

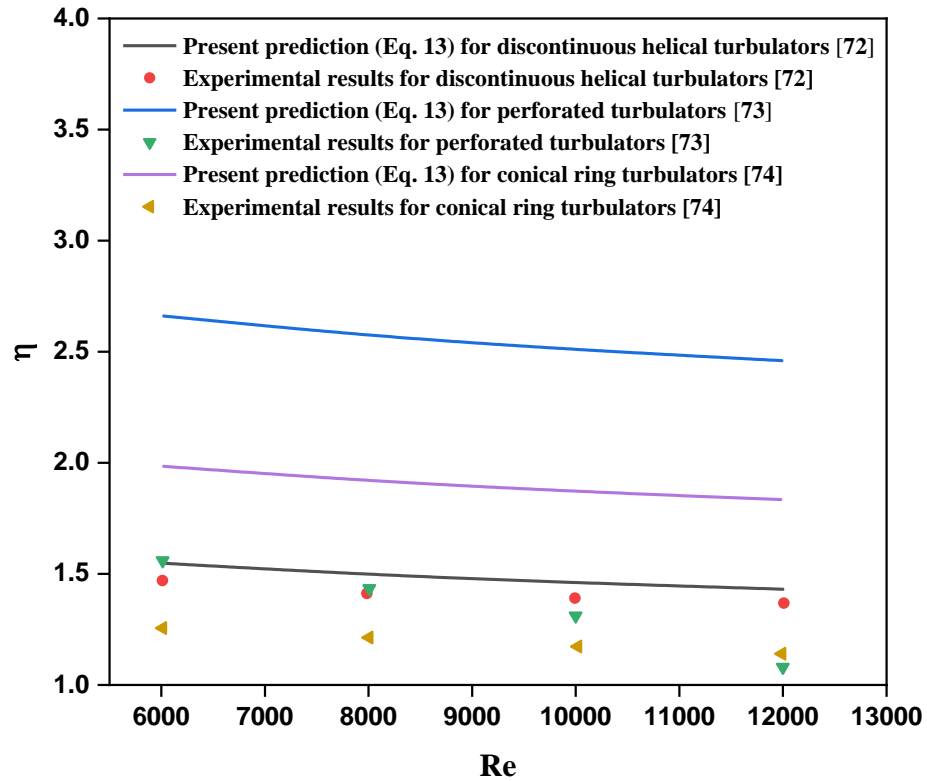


Fig. 4.17: Comparison of present prediction for thermal performance factor with previous work.

The TPF obtained by the present prediction (Eq. 4.9) exhibit good agreement with the test data obtained by using discontinuous helical turbulators for DR = 0.6 and PR = 5.83. While, maximum deviation of present prediction (Eq. 4.9) with the test data obtained by using perforated turbulator [73] with DR = 0.6 and PR = 1.29 and conical ring turbulators [74] with DR = 0.6 and PR = 2.92 is found to be 55% and 35%, respectively.

4.4 Effect of diameter ratio and helix angle on thermo hydraulic performance of DPHE with helical surface disc turbulators

Here, tests are performed to examine the effect of various parameters namely, different diameter ratio (0.42, 0.475 and 0.54) various helix angles (20°, 30° and 40°) and Reynolds number (3500 - 10500) on the thermal performance in the annuli of DPHE with plain surface disc turbulators (PSDTs). Based on the tests data thermal performance of DPHE involving helical surface disc turbulators are estimated. Also, correlations are proposed to evaluate various parameters such as Nusselt number, friction factor, and thermal performance factor.

4.4.1 Test facility, procedure and data reduction

Test facility and procedure are discussed in the earlier section (section 4.2.1). However, test sections used for this study are different. Table 4.5 summarizes test sections used in the present experimental study. The length of test specimen and test section was kept 1.8 m and 1.1 m, respectively, for all the cases. Data reduction for the present investigation is the same as presented in chapter 2.

4.4.2 Results and discussion

Tests are conducted for DPHE using HSDTs with different diameter ratio (0.42, 0.475 and 0.54) various helix angles (20°, 30° and 40°) and Reynolds number (3500 - 10500).

4.4.2.1 Friction factor characteristics

The variation of friction factor characteristics of the annulus of DPHE using helical surface disc turbulators with various values of Reynolds number, helix angle, and diameter ratio is shown in Fig. 4.18. It has been found that the friction

Table 4.5: Design of HSDTs involving different diameter ratio and various helix angle.

Test section	DR	Tube			shell			Number of Turbulators	Helix Angle
		L _t (mm)	d _i (mm)	d _o (mm)	L _s (mm)	D _i (mm)	D _o (mm)		
TS1	0.54	1800	17	19	1800	35	40	0	-
TS2	0.54	1800	17	19	1800	35	40	6	40°
TS3	0.54	1800	17	19	1800	35	40	6	30°
TS4	0.54	1800	17	19	1800	35	40	6	20°
TS5	0.475	1800	17	19	1800	40	45	0	-
TS6	0.475	1800	17	19	1800	40	45	6	40°
TS7	0.475	1800	17	19	1800	40	45	6	30°
TS8	0.475	1800	17	19	1800	40	45	6	20°
TS9	0.420	1800	17	19	1800	45	50	0	-
TS10	0.420	1800	17	19	1800	45	50	6	40°
TS11	0.420	1800	17	19	1800	45	50	6	30°
TS12	0.420	1800	17	19	1800	45	50	6	20°

factor decreases gradually with the increase in Reynolds number. Also, higher value of the friction factor is obtained for the lower value of the diameter ratio. Lower value of DR indicates higher annulus diameter, leading to higher value of friction in the fluid layers. Similar results for the friction factor have been reported by earlier researchers [84-94].

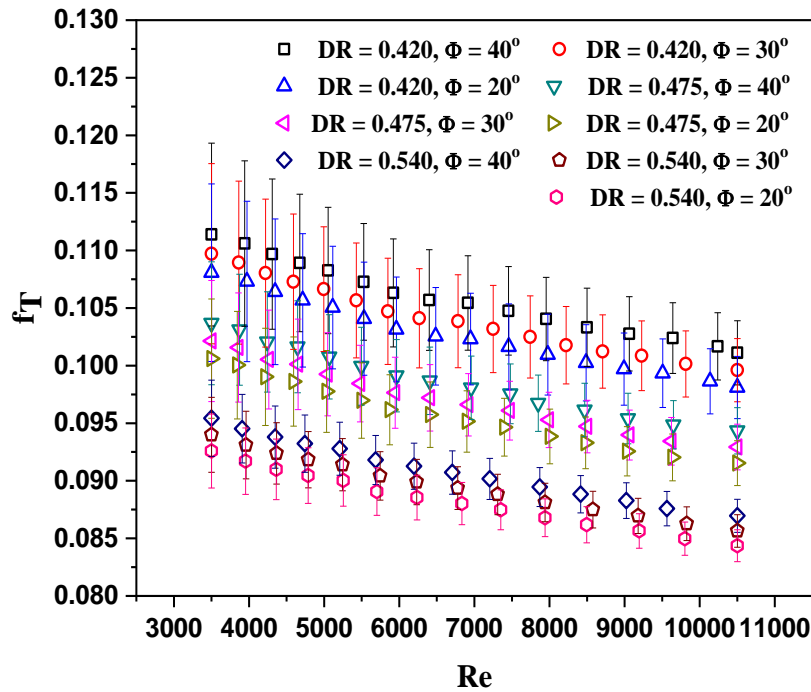


Fig. 4.18: Variation of average friction factor with Reynolds number in the annulus using HSDTs.

It is observed that higher helix angle exhibits higher friction factor coefficient for the same diameter ratio. Helical surface promotes the swirl inside flow regime. Higher helix angle promotes higher swirl effect resulting in higher friction value. Similar results have been observed in case of twisted tapes [47] and helical screw tape/wire coil inserts [61]. It may be noted that the variation in streamline and path line due to turbulators results in higher re-circulation. This generates higher turbulence intensity [65-78], resulting in the higher pressure drop inside flow passage. The maximum value of friction factor is obtained at higher helix angle, lower value of diameter ratio, and Reynolds Number. For a $\phi = 40^\circ$,

Re = 3500 the friction factor values for diameter ratios DR = 0.42, 0.475 and 0.53 are found to be 0.1113, 0.1036 and 0.0954 respectively.

4.4.2.2 Heat transfer enhancement

The variation of average Nusselt number with Reynolds number for the different helix angle and different diameter ratios is shown in Fig. 4.19.

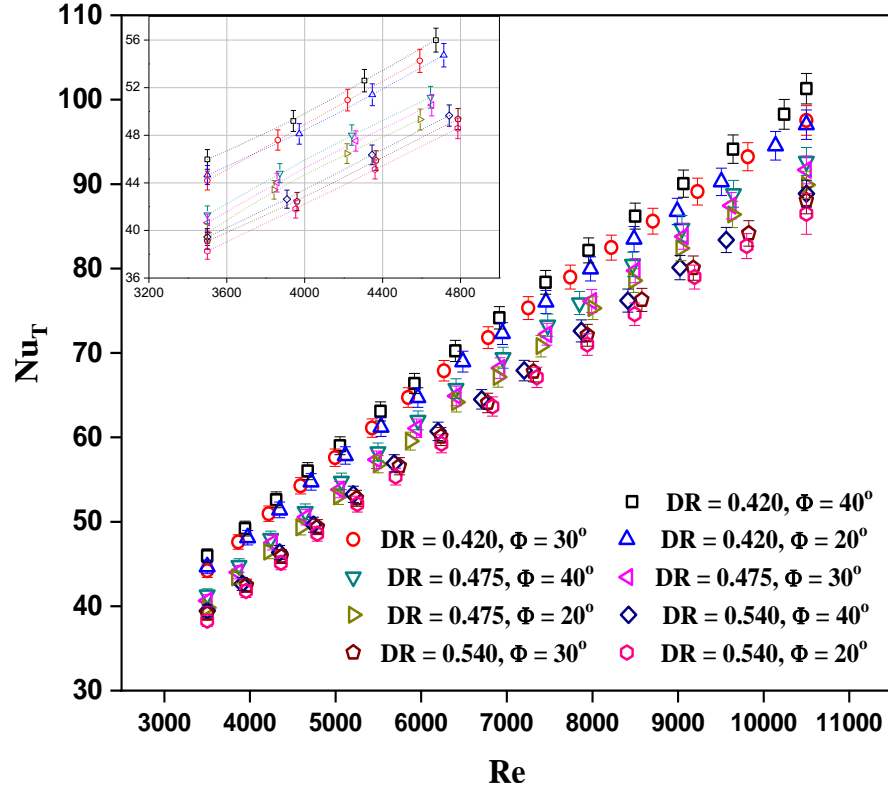


Fig. 4.19: Variation of average Nusselt number with Reynolds number in the annulus using HSDTs.

The use of helical surface disc turbulators inside the annulus of DPHE exhibits better heat transfer performance compared to annulus of smooth tubes DPHE without turbulators. It is observed that the enhancement in heat transfer increases with the increase in the Reynolds number. DPHE with helical surface disc turbulators for $\phi = 40^\circ$ and DR = 0.42 exhibits better heat transfer performance compared to the DPHE with helical surface disc turbulators for $\phi =$

20° and DR = 0.5. The highest Nusselt number is obtained at Re = 10500, DR = 0.42 and $\phi = 40^\circ$. This may be due to the fact that lower diameter ratio poses higher annulus space resulting in more variation in streamlines and higher helix angle result in higher swirl generation. Hence higher re-circulation is achieved, resulting in better turbulence and mixing of the fluid. This enhances the heat transfer performance of the DPHE. Similar observations have been made by previous researchers [47-62 and 65-78].

4.4.2.3 Comparison of annuli with HSDTs and without HSDTs

Present study introduces the Nusselt number ratio in order to compare the performance of DPHE with HSDTs to the smooth tube DPHE without HSDTs. Here, Nusselt number ratio is defined as the ratio of Nusselt number for DPHE with HSDTs to the Nusselt number for DPHE without HSDTs. This is also termed as enhancement factor in Nusselt number.

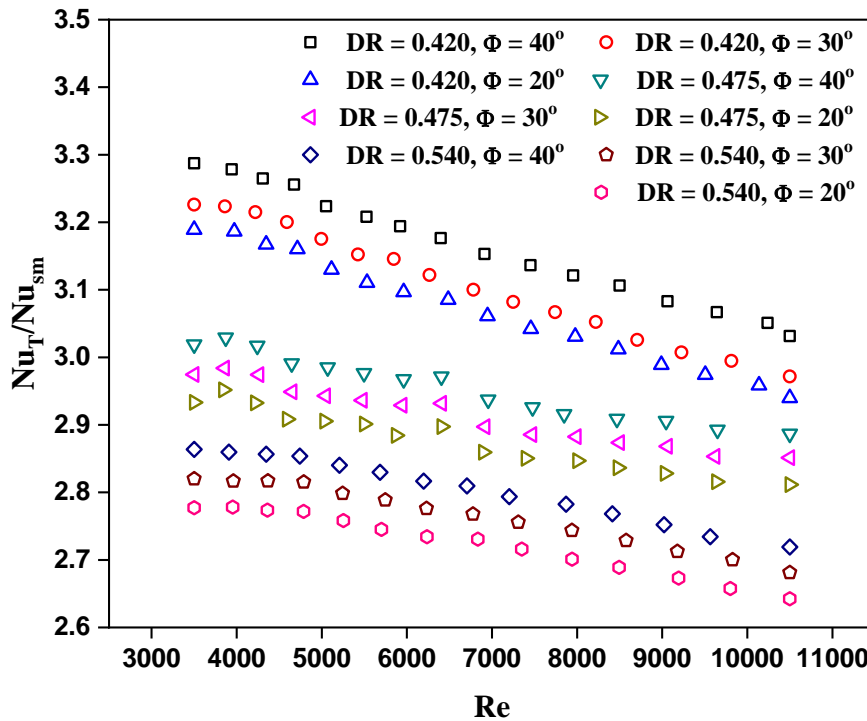


Fig. 4.20: Variation in Nusselt number ratio with Reynolds number in the annulus.

Fig. 4.20 depicts the variation in Nusselt number ratio for various values of Reynolds number, different helix angles, and different diameter ratios. The Nusselt number ratio is found to be greater than unity for all the cases. Nusselt number ratio decreases gradually with the increase in the Reynolds number and increases with decrease in diameter ratio and increase in the helix angle (fig. 4.20). The DPHE with HSDTs for $\phi = 40^\circ$ and DR = 0.42 exhibits the highest enhancement factor in Nusselt number compared to the DPHE using HSDTs for $\phi = 20^\circ$ and DR = 0.53 at Re = 3500. It may be noted that the wetted perimeter increases with the increasing helix angle of the helical surface disc turbulators and the fluid licks a larger surface area resulting in a better heat transfer compared to the DPHE without turbulators. Also, higher helix angle generates higher recirculation inside flow region, leading to enhancement in heat transfer rate. It is observed that with the increase in the diameter ratio, the turbulator effect decreases. This may be due to the fact that higher diameter ratio poses lower annular space and hence path line (travel path) is reduced resulting in the reduction of mixing of the fluid [47-62 and 65 - 78].

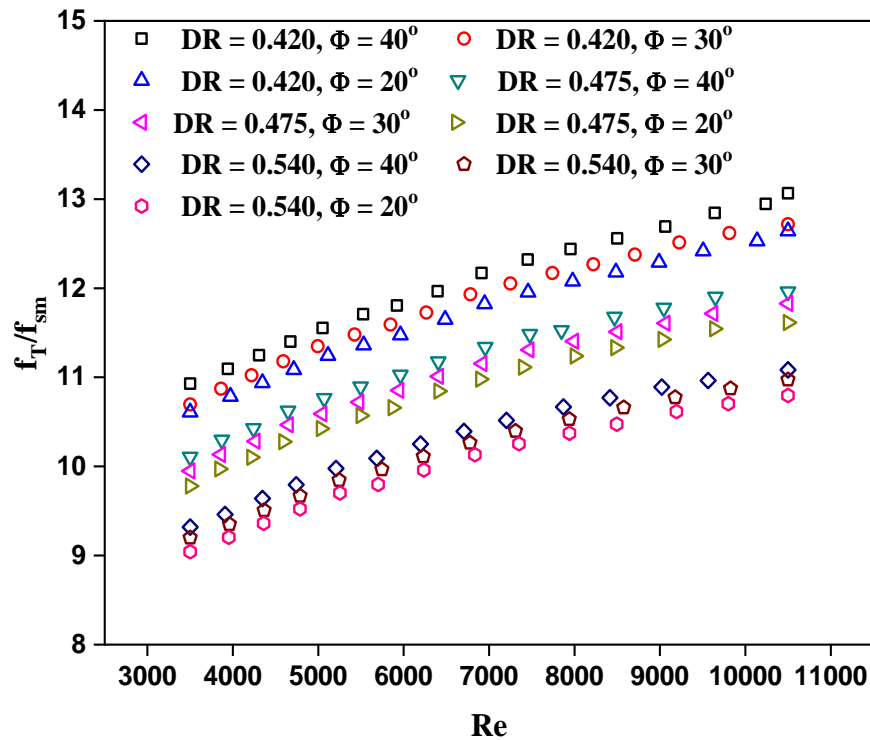


Fig. 4.21: Variation in friction factor ratio with Reynolds number in the annulus.

The variation of friction factor ratio (ratio of friction factor for DPHE with HSDTs to the friction factor for DPHE without HSDTs and also termed as enhancement factor in friction factor) with Reynolds number for different helix angle and different diameter ratios is shown in Fig. 4.21. The friction factor ratio increases gradually with the increase in Reynolds number. The highest enhancement factor in friction factor is obtained for the DPHE using HSDTs at $\phi = 40^\circ$ and DR=0.42 compared to the DPHE using HSDTs at $\phi = 20^\circ$ and DR = 0.53 at Re= 10500.

It may be noted that turbulators promote re-circulation and subsequently increase the heat transfer area inside the flow regime [65-78]. Also, higher recirculation is achieved as the helix angle increases for the helical surface disc turbulators [47 and 62]. These turbulence promoters (turbulators) create or increase the turbulence intensity inside flow regime which reduces the thermal boundary layer and increase the fluid mixing at different fluid layers resulting in higher heat transfer rate [65-78].

4.4.2.4 Comparison of present Nusselt number with previous studies

Fig. 4.22 depicts the comparison of Nusselt number obtained from the present experimental investigation with the test data of Sheikholeslami and Ganji [73], Kongkaitpaiboon et al. [66], Ruengpayungsak et al. [75], Sheikholeslami et al. [76] and Kumar et al. [78, 80]. Studies have been made to estimate heat transfer characteristics in the double pipe heat exchanger by using perforated turbulator [73] and perforated circular ring turbulators [76]. While tests have been carried out in the round tube fitted with circular ring turbulators [66], gear ring as turbulator [75], solid hollow circular disk as turbulator [78, 80] to evaluate the heat transfer characteristics.

Present test results exhibit higher value of Nusselt number compared to the other studies such as Sheikholeslami and Ganji [73], Ruengpayungsak et al. [75] and Sheikholeslami et al. [76]. This may be due to the fact that helical

surface provides the additional circulation inside the flow regime. While test results obtained by solid perforated hollow circular disk [78] and solid hollow circular disk [80] shows the higher value of the Nusselt number compared to the present results. While present test results agree with the test results obtained for the round tube fitted with the circular ring turbulator [66].

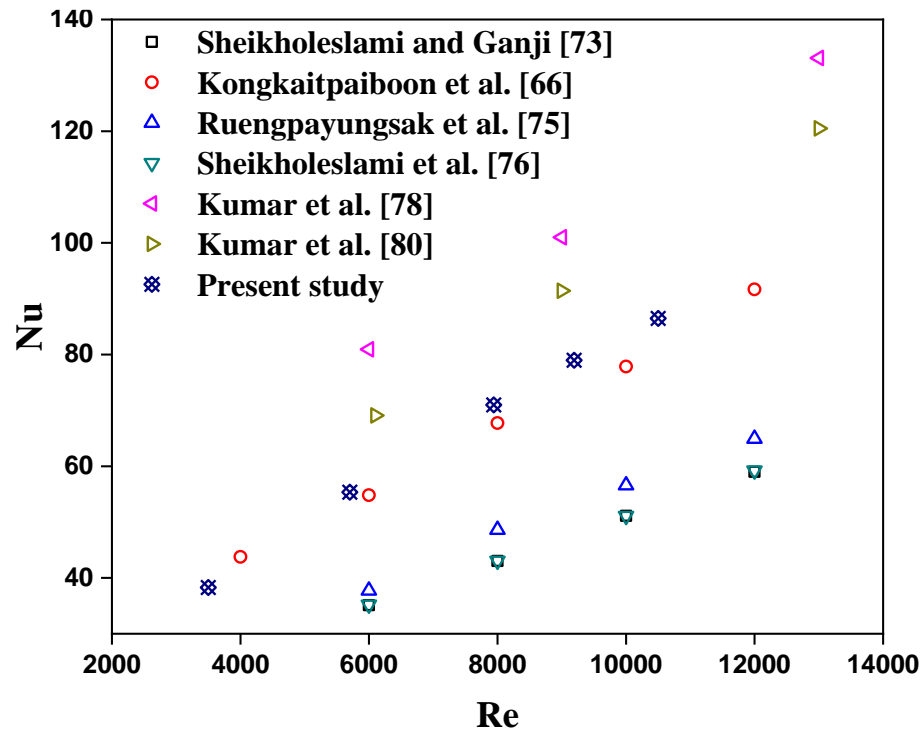


Fig. 4.22: Comparison of experimental Nusselt number.

4.4.2.5 Comparison of present friction factor with previous studies

Fig. 4.23 depicts the comparison of friction factor obtained from the present experimental investigation with the test data Sheikholeslami and Ganji [70], Kongkaitpaiboon et al. [66], Ruengpayungsak et al. [75], Sheikholeslami et al. [76] and Kumar et al. [78, 80].

Present test results exhibit higher value of friction factor compared to the friction factor values obtained by Sheikholeslami and Ganji [73] and Sheikholeslami et al. [76] in their experimental study. Helical surface provides the additional circulation inside the flow regime, and therefore, higher friction factor

values are obtained in the present investigation. While test results obtained by circular ring turbulator [66], solid perforated hollow circular disk [78] and solid hollow circular disk [80] shows the higher value of the friction compared to the present results while present tests result agree with the tests result obtained for the round tube fitted with the gear ring turbulator [75].

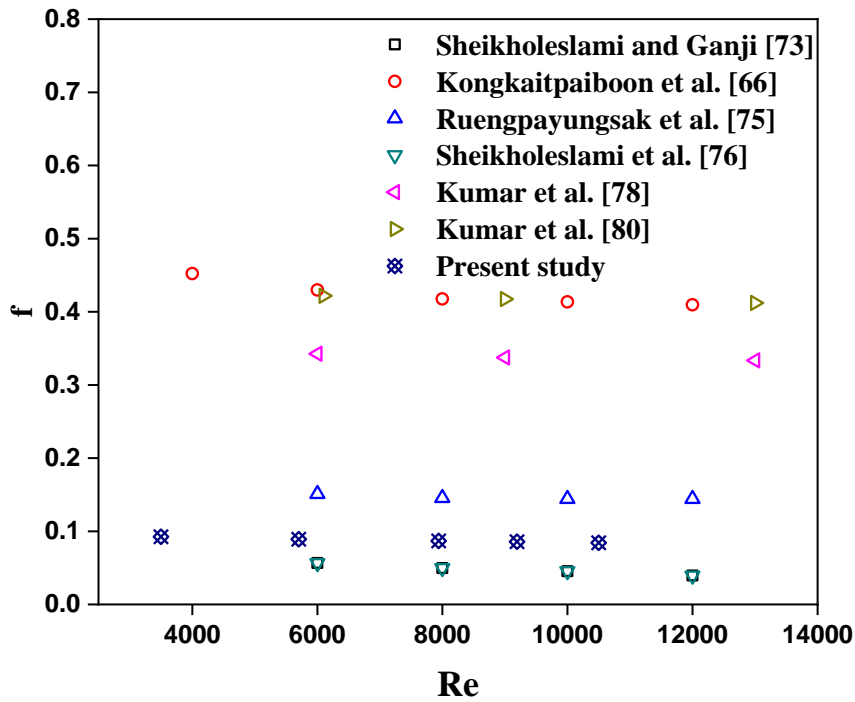


Fig. 4.23: Comparison of experimental friction factor.

4.4.2.6 Thermal performance of annuli of DPHE with HSDTs

The effective assessment of the modified heat exchangers directly relates to the operating cost of the heat exchangers. The thermal performance factor is calculated based on the various parameters such as pressure drop, heat transfer rate, and flow rate and is defined as the ratio of heat transfer rate for the modified tube heat exchanger to the smooth tube heat exchanger.

It is argued that the temperature difference between the heat transfer surface and bulk fluid for both the modified tube and smooth tube can be

considered same. For constant pumping power, thermal performance factor can be expressed as in Eq. 4.3.

The TPF for various PR of DPHE equipped with HSSTs at different DR and Re is shown in Fig. 4.24. For all the cases tested in this study, TPF is found to be greater than unity. The maximum value of TPF for DPHE using HSSTs with pitch ratio = 8.42 and DR = 0.42, is found to be 1.48 at Re = 3500.

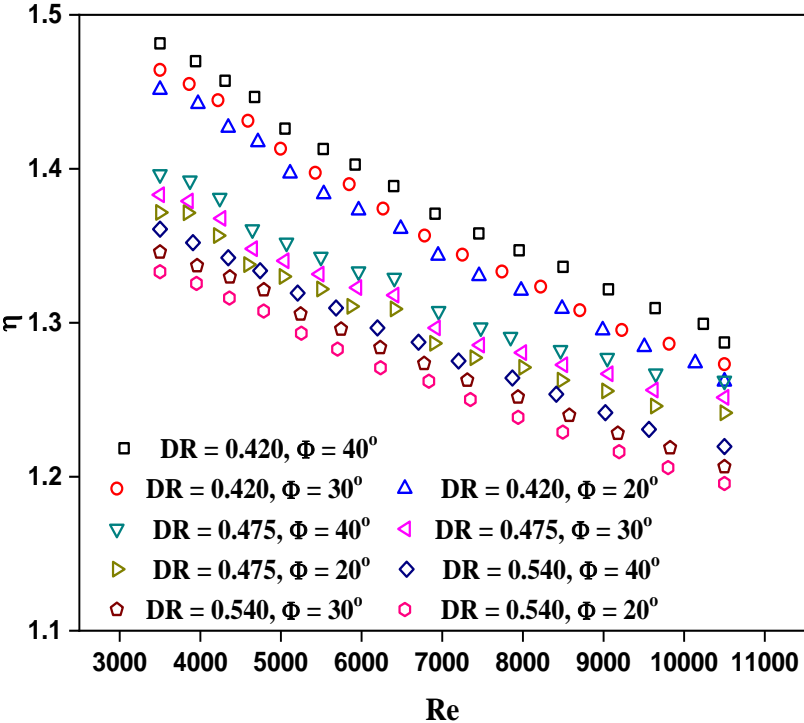


Fig. 4.24: Variation in thermal performance factor with Reynolds number in the annulus.

4.4.2.7 Correlations for various parameters

Here, efforts have been made to propose correlations for various parameters such as Nusselt number friction factor and thermal performance factor using the present test data. By utilizing the least square method of regression analysis, the correlations for Nusselt number friction factor and thermal performance factor have been expressed as a function of Reynolds number,

diameter ratio, and helix angle and is expressed in Eqs. 4.10 – 4.12. The correlations are valid for the varied range of Reynolds number, helix angle (20°, 30° and 40°) and diameter ratio (0.42, 0.475 and 0.54).

Numerous studies have been reported that consider various turbulent promoters of different shapes and types in order to enhance the heat transfer rate. Several correlations have been proposed to evaluate the Nusselt number, friction factor, and thermal performance factor. Some of these correlations for predicting Nusselt number, friction factor, and thermal performance factor have been summarized in Table 4.6, respectively. The exponent of Reynolds number in the proposed correlation (Eq. 4.10) is found to vary significantly based on the design of the turbulence promoters. Turbulent promoters were found to disrupt the boundary layer by generating re-circulation inside flow regime and increase the turbulent intensity. It is interesting to note that higher heat transfer surface area provided by the various turbulence promoters significantly affect the heat transfer rate in a heat exchanging equipment. This may be reason of higher Reynolds number exponent in the present proposed correlation for Nusselt number (Eq. 4.10). The higher Re exponent similarly were observed in the previous experimental investigations [66, 67, 75, 95] while utilizing different turbulators such as circular ring turbulators [66], twisted ring turbulators [67], gear ring turbulators [75] and C-nozzles turbulators [95] in their heat exchanging tube.

$$Nu_T = 0.0737 Re^{0.74} DR^{-0.464} (\sin \phi)^{0.0443}; \left\{ \begin{array}{l} 3500 \leq Re \leq 10500 \\ 20^\circ \leq \phi \leq 40^\circ \\ 0.42 \leq DR \leq 0.54 \end{array} \right\} \quad (4.10)$$

$$f_T = 0.14 Re^{-0.089} DR^{-0.61} (\sin \phi)^{0.047}; \left\{ \begin{array}{l} 3500 \leq Re \leq 10500 \\ 20^\circ \leq \phi \leq 40^\circ \\ 0.42 \leq DR \leq 0.54 \end{array} \right\} \quad (4.11)$$

$$\eta = 3.04 Re^{-0.110} DR^{-0.222} (\sin \phi)^{0.055}; \left\{ \begin{array}{l} 3500 \leq Re \leq 10500 \\ 20^\circ \leq \phi \leq 40^\circ \\ 0.42 \leq DR \leq 0.54 \end{array} \right\} \quad (4.12)$$

Table 4.6: Correlations proposed by various researchers.

Source	Type/method of passive enhancement	Re	Remark/correlations
Eiamsa-ard and promvonge [47]	Clockwise and counterclockwise twisted tape inserts (Twist angle $\theta = 30^\circ, 60^\circ$ and 90°)	8000 - 18000	$Nu = 0.31 Re_s^{0.6} Pr^{0.4} (y/w)^{-0.36} (1 + \sin \theta)^{0.44}$ $f = 46.39 Re_s^{-0.544} (y/w)^{-0.77} (1 + \sin \theta)^{0.45}$
Roy and Saha [61]	Helical screw-tape with oblique teeth inserts (Tooth angle θ) wire coil inserts (Helix angle $\alpha = 30^\circ, 45^\circ$ and 60°)	6000 - 24000	$Nu_m = 5.172 Gz^{0.27481} Re^{0.25883} Pr^{0.29649} Gr^{0.25381} P^{0.24716} t_{hl}^{0.29982}$ $\times (\sin \theta)^{0.26538} (\sin \alpha)^{0.24715} d_c^{0.25931} \left(\frac{\mu_b}{\mu_w} \right)^{0.14}$ $f = 3.55827 Re^{-0.67719} (\sin \alpha)^{0.25811} d_c^{0.33739}$
Promvonge [62]	Twisted tape and wire coil turbulators	3000 - 18000	$Nu = 4.47 Re^{0.5} Pr^{0.4} (CR)^{-0.382} Y^{-0.38}$ $f = 338.37 Re^{-0.367} (CR)^{-0.887} Y^{-0.455}$
Kongkai paiboon [66]	Circular ring turbulators	4000 - 20000	$Nu = 0.354 Re^{0.697} Pr^{0.4} DR^{-0.555} PR^{-0.598}$ $f = 0.715 Re^{-0.081} DR^{-4.775} PR^{-0.846}$ $\eta = 5.315 Re^{-0.078} DR^{1.031} PR^{-0.317}$

Table 4.6 (Continued).

Source	Type/method of passive enhancement	Re	Remark/correlations		
Thianpong et al. [67]	Twisted ring turbulators	6000-20000	$Nu = 0.097 Re^{0.883} Pr^{0.4} (W/D)^{0.408} (p/D)^{-0.181}$ $f = 112.795 Re^{-0.159} (W/D)^{1.665} (p/D)^{-0.736}$		
Ruengpayungsak et al. [75]	Gear ring / circular ring turbulators	6000-20000	<table style="width: 100%; border: none;"> <tr> <td style="width: 50%; border: none;"> For circular ring turbulators $Nu = 0.078 Re^{0.786} Pr^{0.4} (SR)^{-0.136}$ $f = 0.788 Re^{-0.051} (SR)^{-0.486}$ $\eta = 5.531 Re^{-0.175} (SR)^{0.026}$ </td> <td style="width: 50%; border: none;"> For gear ring turbulators $Nu = 0.1 Re^{0.768} Pr^{0.4} (SR)^{-0.14} (1+N)^{-0.13}$ $f = 2.143 Re^{-0.06} (SR)^{-0.522} (1+N)^{-0.479}$ $\eta = 5.21 Re^{-0.175} (SR)^{0.034} (1+N)^{0.029}$ </td> </tr> </table>	For circular ring turbulators $Nu = 0.078 Re^{0.786} Pr^{0.4} (SR)^{-0.136}$ $f = 0.788 Re^{-0.051} (SR)^{-0.486}$ $\eta = 5.531 Re^{-0.175} (SR)^{0.026}$	For gear ring turbulators $Nu = 0.1 Re^{0.768} Pr^{0.4} (SR)^{-0.14} (1+N)^{-0.13}$ $f = 2.143 Re^{-0.06} (SR)^{-0.522} (1+N)^{-0.479}$ $\eta = 5.21 Re^{-0.175} (SR)^{0.034} (1+N)^{0.029}$
For circular ring turbulators $Nu = 0.078 Re^{0.786} Pr^{0.4} (SR)^{-0.136}$ $f = 0.788 Re^{-0.051} (SR)^{-0.486}$ $\eta = 5.531 Re^{-0.175} (SR)^{0.026}$	For gear ring turbulators $Nu = 0.1 Re^{0.768} Pr^{0.4} (SR)^{-0.14} (1+N)^{-0.13}$ $f = 2.143 Re^{-0.06} (SR)^{-0.522} (1+N)^{-0.479}$ $\eta = 5.21 Re^{-0.175} (SR)^{0.034} (1+N)^{0.029}$				
Kumar et al. [80]	hollow circular disk	6500-23000	$\eta = 5.315 Re^{-0.078} DR^{1.031} PR^{-0.317}$		
promvonge and Eiamsa-ard [95]	C-Nozzles turbulators	8000 - 18000	$Nu = 0.143 Re^{0.736} Pr^{1/3} (PR)^{-0.12}$ $f = 29 Re^{-0.197} (PR)^{-0.052}$		
Present Study	Discontinuous type helical surface disc turbulators	3500 - 10500	$Nu_T = 0.0737 Re^{0.74} DR^{-0.464} (\sin \phi)^{0.0443}$ $f_T = 0.14 Re^{-0.089} DR^{-0.61} (\sin \phi)^{0.047}$ $\eta = 3.04 Re^{-0.110} DR^{-0.222} (\sin \phi)^{0.055}$		

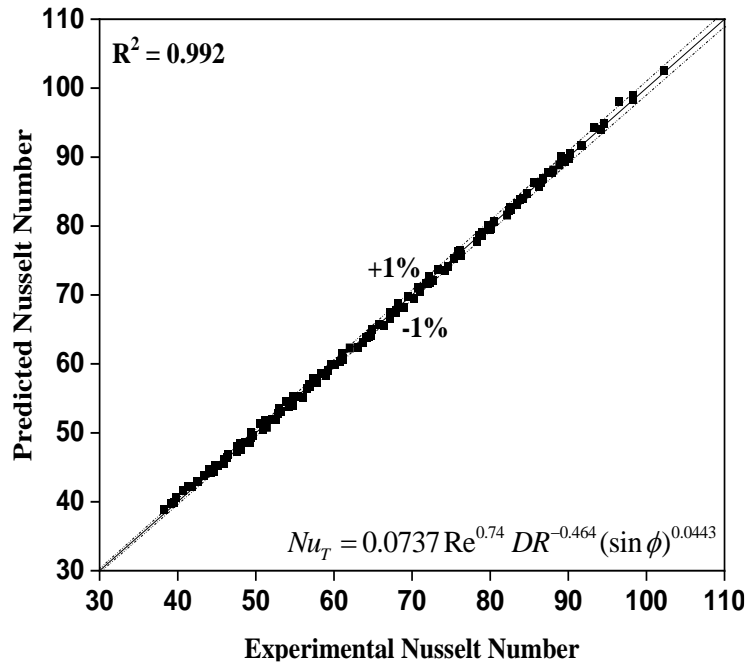


Fig. 4.25: Comparison of experimental and predicted values of average Nusselt number.

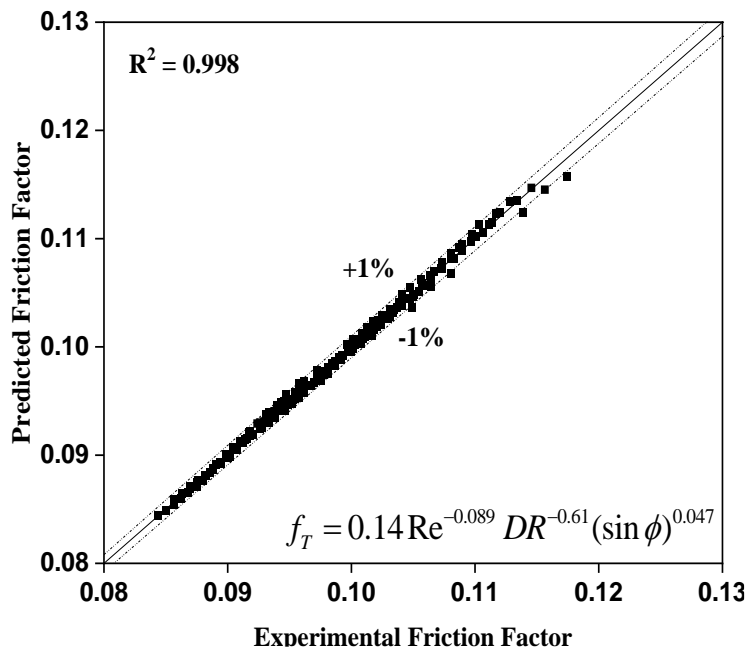


Fig. 4.26: Comparison of experimental and predicted values of average friction factor.

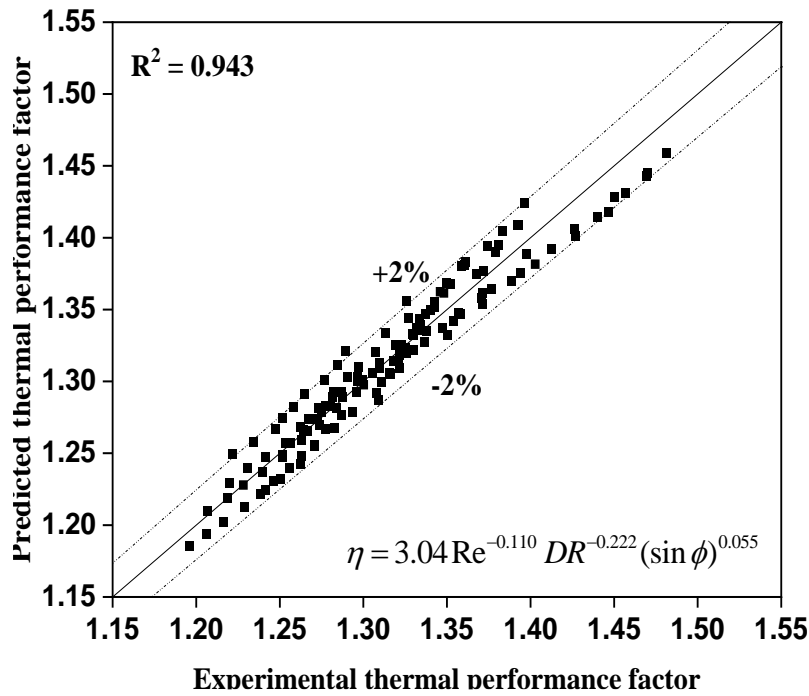


Fig. 4.27: Comparison of experimental and predicted values of thermal performance factor.

The friction factor correlation (Eq. 4.11) is found to be the weak function of the Reynolds number. The exponent of Reynolds number for the present correlation is similar to the previous correlations [66, 67, 75 and 95] for the turbulators. While using the tape insert and wire coil insert [47-62] in the tube, the friction factor strongly depends on the Reynolds number. This may be the reason that friction factor is weak function for the present proposed correlation for the DPHE with HSDTs.

Here, an effort has been made to compare the present test data with the proposed correlations (Figs. 4.25 – 4.27). The proposed correlation for the Nusselt number (Eq. 4.10) is able to predict 79% of test data within an error band of $\pm 1\%$ and is shown in Fig. 4.25. While the proposed correlation for the friction factor (Eq. 4.11) is able to predict 97% of test data within an error band of $\pm 1\%$ (Fig. 4.26). While in case of thermal performance factor, the proposed correlation (Eq. 4.12) is able to predict the 96% of test data within an error band of $\pm 2\%$ (Fig. 4.27).

4.5 Concluding remarks

In this chapter, the thermo-hydraulic behavior of DPHE with helical surface disc turbulators is studied through experimental investigation. This chapter includes three different studies. This is detailed below.

The first study considers the effect of Reynolds number, pitch ratio, and helix angle of helical surface disc turbulator on the thermo-hydraulic performance of DPHE. The study reports the variation of various parameters such as Nusselt number, friction factor, and thermal performance factor with Reynolds number, pitch ratio, and helix angle. It is observed that the pitch ratio significantly affects the thermal performance compared to the helix angle and Reynolds number. The thermal performance is found to increase with the increase in helix angle.

The second study considers the effect of Reynolds number, diameter ratio, and pitch ratio of helical surface disc turbulator on heat transfer and pressure drop characteristics of DPHE. The study reports the variation of various parameters such as Nusselt number, friction factor, and thermal performance factor with Reynolds number, pitch ratio, and diameter ratio. The helix angle ($\phi = 40^\circ$) is kept constant in this study. The thermal performance of DPHE is found to vary significantly by using helical surface disc turbulators. The thermal performance was found to increase with the decrease in the pitch ratio and diameter ratio.

The third study considers the effect of Reynolds number, diameter ratio, and helix angle of helical surface disc turbulator on thermal and fluid flow characteristics of DPHE. The study reports the variation of various parameters such as Nusselt number, friction factor, and thermal performance factor with Reynolds number, helix angle, and diameter ratio. The pitch ratio (PR = 8.42) is kept constant in this study. The thermal performance was found to increase with the decrease in the diameter ratio and with increase in helix angle.

Chapter 5

Conclusions and scope of future work

5.1 Introduction

Present dissertation reports the experimental investigation on heat transfer and pressure drop characteristics in the annuli of double pipe heat exchanger by employing various passive augmentation techniques. The DPHE utilizes water as hot fluid and air is considered as cold fluid. Initially, the DPHEs made of smooth inner tube and corrugated outer tube is used to study the improvement in the thermal performance. Later on, turbulators of various configuration (plain surface disc turbulator and helical surface disc turbulators) are used to evaluate the enhancement in the thermal performance. During tests, temperature of both hot fluid and cold fluid at inlet and exit are measured. In addition to this, the pressure drop along the test section is measured. Based on the measured test data, various parameter such as Nusselt number, friction factor and thermal performance factor are estimated. The effect of various parameters such as flow rate, helix angle, diameter ratio and pitch ratio on Nusselt number, friction factor and thermal performance factor are discussed. Present experimental investigation is classified into two categories based on the passive augmentation techniques. First category involves the experimental study with corrugated tube while, the second category involves the use of turbulators to enhance the thermal performance. Significant outcomes obtained from the present experimental investigations are discussed, and the conclusions are enlisted in this chapter.

5.2 Experimental study with corrugated outer tube in the DPHE

Efforts have been made to carry out the experimental investigation to evaluate the heat transfer and pressure drop characteristics of DPHE with corrugated outer tube and smooth inner tube. Water (hot fluid) flows in the inner tube and air (cold fluid) flows through the annulus. Tests are conducted for air with uniform wall temperature condition. The effect of corrugated outer

tube is analyzed with three corrugation pitches ($P = 10, 20$ and 30 mm), three diameter ratios ($DR = 0.53, 0.44$ and 0.40) and $Re = 3500 - 10,500$. The significant findings from the investigation are summarized below.

- The maximum enhancement in f value is found to be 81 % at $P = 10$ mm, $DR = 0.40$ and $Re = 3500$, while maximum enhancement in Nu is found to be 71% at $P = 10$ mm, $DR = 0.40$ and $Re = 10500$ compared to the smooth tube DPHE.
- Nu is found to increase with the decrease in the values of P and DR . Lower value of P and DR exhibit better mixing of the fluid and increase in turbulence in the flow. For the cases studied here, the maximum Nu is found to be 99.79 for $P = 10$ mm and $DR = 0.40$ at $Re = 10500$.
- The f value is found to increase with the decrease in the values of P and DR . The maximum f value is found to be 0.047 for $P = 10$ mm, $DR = 0.40$ and $Re = 3500$.
- In case of corrugated outer tube in DPHE, TPF is found to be greater than unity for all the cases considered here. Maximum value of TPF is obtained at $Re = 3500$, $P = 10$ mm and $DR = 0.40$.
- Based on test data correlations have been proposed for Nu , f and TPF. These correlations are valid for the varied range of Reynolds number ($3500 - 10500$), pitch ($10 - 30$ mm), and diameter ratio ($0.40 - 0.53$). The proposed correlation for Nu is able to predict 96% of the test data within an error band of $\pm 9\%$. While in case of f , proposed correlations are able to predict 92% of experimental test data within an error band of $\pm 5\%$. Also, the proposed correlation for the TPF is able to predict 94% of experimental test data within an error band of $\pm 5\%$. These correlations show good agreement with the test data.

5.3 Experimental investigation involving various configuration of surface disc turbulators in DPHE

Efforts have been made to evaluate the thermal and flow characteristics using surface disc turbulators in the annuli of DPHE through experimental

investigation. This study has been divided into two categories. This includes plain surface disc turbulators and helical surface disc turbulators.

Plain surface disc turbulators

Here, tests are carried for varied range of Reynolds number (3200 - 10500), diameter ratios (0.420 - 0.540), and pitch ratios (8.42 - 11.79). Water (hot fluid) flows in the inner tube and air (cold fluid) flows through the annulus. The tests are conducted for air with uniform wall temperature condition. The effects of PSDTs in annulus have been analyzed and following conclusions are made from the analysis.

- The highest value of enhancement factor for Nu and f are found to be 2.37 and 9.58, respectively for DPHE with PSDTs at DR = 0.42 and PR = 8.42.
- The Nu and f values varies inversely with DR and PR.
- The TPF is found to be higher than unity value for DPHE with PSDTs at DR = 0.42, PR = 8.42. While, for other configurations, the thermal performance is less than unity after certain Re value.
- Present study describes correlations for Nu, f and TPF. The correlations for Nu, f and TPF predict 96%, 84% and 98% of test data, respectively within an error band of $\pm 2\%$. These correlations are valid for the varied range of Reynolds number (3200 – 10500), pitch ratio (8.42 – 11.79).

Helical surface disc turbulators

Efforts have also been made to evaluate the heat transfer and pressure drop characteristics using helical surface disc turbulators in the annuli of DPHE through experimental investigation with three different pitch ratios (8.42, 9.79 and 11.79), three different diameter ratios (0.420, 0.475 and 0.540), three helix angle (20°, 30° and 40°) and varied range of Re (3500 – 10500). Hot water is issued in the inner tube, while air as cold working fluid flows through the annulus. The study is divided into three categories. In the first category, experiments are performed to analyze the effect of various

parameters such as Reynolds number, pitch ratio, and helix angle on Nusselt number, friction factor, and thermal performance factor. In the second category, tests are conducted to study the influence of flow rate, diameter ratio, and pitch ratio on various parameters, namely, Nusselt number, friction factor, and thermal performance factor. In the third category, tests are performed to study the effect of flow rate, diameter ratio, and helix angle on various thermal performance factor.

HSDTs in the annuli with three helix angles (20°, 30° and 40°), three different pitch ratios (8.42, 9.79 and 11.79) and varied range of Reynolds number (3500 - 10500).

- For $\phi = 40^\circ$ and PR = 8.42, the maximum value of Nusselt number ratio (at Re = 3500) and friction factor ratio (at Re = 10500) are found to be 3.01 and 11.96, respectively.
- Nu and f values were found to increase for low PR value and high ϕ value.
- The TPF of the DPHE fitted with HSDTs is found to be greater than unity. The maximum value of thermal performance factor (TPF) is found to be 1.39 at $\phi = 40^\circ$, PR = 8.42 and Re = 3500.
- Correlations are proposed for Nu, f and TPF and are valid for the varied range of Reynolds number (3500 – 10500), helix angle (20o-40o) and pitch ratio (8.42 – 11.79). The correlations for Nu and TPF predict 91% and 97% test data, respectively within $\pm 4\%$ error band while f correlation predicts 98% test data within $\pm 2\%$ error band.

HSDTs in the annuli with three diameter ratios (0.54, 0.475 and 0.42), three different pitch ratios (8.42, 9.79 and 11.79) and varied range of Reynolds number (3500 - 10500).

- For DR = 0.42 and PR = 8.42, the DPHE with HSDTs exhibit maximum value of Nusselt number and friction factor at Re = 10500.
- The Nu and f values were found to increase with the decrease in PR and DR. The TPF is found to be greater than unity for all the cases considered here. The maximum TPF is obtained for the DPHE using

turbulators for PR = 8.42 and DR = 0.42 at lowest value of Re (Re = 3500).

- Based on test data correlations have been proposed for Nusselt number and friction factor. These correlations are valid for the varied range of Reynolds number (3500 - 10500), pitch ratio (8.42 – 11.79) and diameter ratio (0.42 - 0.54). The proposed correlation for Nusselt number is able to predict 80% test data within error band of $\pm 2\%$ within error band of $\pm 2\%$. While correlation of friction factor is able to predict 92% of test data within an error band of $\pm 2\%$. Also, the proposed correlation of thermal performance factor is able to predict 68% of test data within an error band of $\pm 1\%$.

HSDTs in the annuli with three diameter ratios (0.54, 0.475 and 0.42), three different helix angles (20°, 30° and 40°) and varied range of Reynolds number (3500 - 10500).

- The Nusselt number was found to increase with the increase in Reynolds number, and increase in helix angle. While, Nusselt number was found to decrease with increase in diameter ratio. The friction factor increases with increase in helix angle and decreases with the increase in diameter ratio and Reynolds number.
- The maximum enhancement factor in Nusselt number is found to be 3.28 for DPHE with HSDTs compared with DPHE without turbulators at DR = 0.42, $\phi = 40^\circ$ and Re = 3500. While, the maximum value of enhancement factor in friction factor is found to be 13.6 at Re = 10500 with DPHE with HSDTs compared to the DPHE without turbulators at DR = 0.42 and $\phi = 40^\circ$.
- The thermal performance factor is found to be greater than unity for all the cases considered here. The maximum thermal performance factor is obtained using HSDTs for DR = 0.42, $\phi = 40^\circ$ at Re = 3500.
- Based on test data correlations have been proposed for Nusselt number, friction factor and thermal performance factor. These correlations are valid for the varied range of Reynolds number (3500 - 10500), helix angle (20o- 40o) and diameter ratio (0.42 - 0.54). The

proposed correlations for Nusselt number and friction factor are able to predict 79% and 97 % test data within error band of $\pm 1\%$, respectively. While the proposed correlation for the thermal performance factor is able to predict 96% of test data within an error band of $\pm 2\%$.

In the present experimental investigations, tests are performed using different passive technique in DPHE. These include corrugated tubes and helical surface disc tabulators (HSDT). Here, DPHE made of smooth inner tube and outer corrugated tube is found to exhibit highest thermal performance factor of 1.99 with $P = 10$ mm and $DR = 0.40$ at $Re = 3500$. While, HSDTs are found to exhibit highest thermal performance factor of 1.48 with $DR = 0.42$, $PR = 8.42$, helix angle = 40° at $Re = 3500$ amongst all turbulators. In view of this, it is recommend to use corrugated DPHE in a heat exchanging equipment in order to obtain higher thermal performance. Many a times, considering the constraints in manufacturing process involved in the development of corrugated tube heat exchangers, one can use helical surface disc turbulators (HSDTs) in heat exchanging equipment for reasonable enhancement in thermal performance.

5.4 Scope of future work

The heat transfer and pressure drop characteristic for the double pipe heat exchanger is of great interest due to its wide applications such as in pasteurizing, reheating, preheating, digester heating, solar air heater and effluent heating processes, space heating, processing of papers, drying of vegetable products. DPHEs are also being used in various small industries due to their low cost in design and maintenance. Therefore, it is more important to study various augmentation techniques to enhance thermal performance of DPHEs. Suitable design of heat exchanger with passive techniques not only reduce the size and cost of the equipment but also improve the efficiency of the system. Present experimental study carried out in this dissertation may provide useful information for the further investigation in this area. In view of this, certain future direction of the present work is discussed below.

- Corrugated geometries of different design should be investigated in order to find the best corrugated geometry with higher thermal performance.
- Various turbulator geometries involving double helical surface need to be investigated in order to evaluate thermal performance of DPHE.
- Numerical investigation needs to be performed to find out optimum design of DPHE.
- Heat exchangers with varied range of fluid combination need to be studied to find the thermal performance.
- Heat exchangers with varied range of fluid temperature need to be studied.
- Three fluid heat exchangers also need to be studied considering its possible application for the waste heat recovery systems.

References

- [1] M. U. Sajid, H. M. Ali, Recent advances in application of nanofluids in heat transfer devices: A critical review, *Renewable and Sustainable Energy Reviews* 103 (2019) 556–592.
- [2] M. Awais, A. Arafat, A. Bhuiyan, Heat and mass transfer for compact heat exchanger (CHXs) design: A state-of-the-art review, *International Journal of Heat and Mass Transfer* 127 (2018) 359–380.
- [3] B. Kumar, G. P. Srivastava, M. Kumar, A. K. Patil, A review of heat transfer and fluid flow mechanism in heat exchanger tube with inserts, 123 (2018) 126-137.
- [4] S. Liu, M. Sakr, A comprehensive review on passive heat transfer enhancements in pipe exchangers, *Renewable and Sustainable Energy Reviews* 19 (2013) 64 – 81.
- [5] T. Alam, M. Kim, A comprehensive review on single phase heat transfer enhancement techniques in heat exchanger applications, *Renewable and Sustainable Energy Reviews* 81 (2018) 813–839.
- [6] M. Omid, M. Farhadi, M. Jafari, A comprehensive review on double pipe heat exchangers, *Applied Thermal Engineering* 110 (2017) 1075–1090.
- [7] M. Sheikholeslami, M. Gorji-Bandpy, D. D. Ganji, Review of heat transfer enhancement methods: Focus on passive methods using swirl flow devices, *Renewable and Sustainable Energy Reviews* 49 (2015) 444–469.

- [8] A. M. Fsadni, J. P. M. Whitty, A review on the two-phase heat transfer characteristics in helically coiled tube heat exchangers, *International Journal of Heat and Mass Transfer* 95 (2016) 551–565.
- [9] Z. S. Kareem, M. N. M. Jaafar, T. M. Lazim, S. Abdullah, A. F. Abdulwahid, Passive heat transfer enhancement review in corrugation, *Experimental Thermal and Fluid Science* 68 (2015) 22–38.
- [10] S. Bhattacharyya, A. C. Benim, H. Chattopadhyay, A. Banerjee, Experimental investigation of heat transfer performance of corrugated tube with spring tape inserts, *Experimental Heat Transfer*, (2018) DOI: 10.1080/08916152.2018.1531955.
- [11] S. Rainieri, G. Pagliarini, Convective heat transfer to temperature dependent property fluids in the entry region of corrugated tubes, *Int. J. Heat Mass Transfer* 45 (2002) 4525-4536.
- [12] S. W. Ahn. Experimental Studies on Heat Transfer in the Annuli with Corrugated Inner Tubes. *KSME International Journal* 17 (8) (2003) 1226- 1233.
- [13] P.G. Vicente, A. Garcia, A. Viedma, Mixed convection heat transfer and isothermal pressure drop in corrugated tubes for laminar and transition flow, *Int. Comm. Heat Mass Transfer* 31 (2004) 651-662.
- [14] K. Aroonrat, A. S. Dalkilic, S. Wongwises. Experimental Study on Evaporative Heat Transfer and Pressure Drop of R-134a Flowing Downward Through Vertical Corrugated Tubes with Different Corrugation Pitches. *Experimental heat transfer*, 26 (2013) 41-63.
- [15] S. Pethkool, S. Eiamsa-ard, S. Kwankaomeng, P. Promvonge, Turbulent heat transfer enhancement in a heat exchanger using helically

- corrugated tube, *International Communication in Heat and Mass Transfer*, 38 (2011) 340-347.
- [16] K. Wongcharee, S. Eiamsaard, Heat transfer enhancement by using CuO/ water nanofluid in corrugated tube equipped with twisted tape, *International Communication in Heat and Mass Transfer*, 39 (2012) 251-257.
- [17] H. Han, B. Xi Li, H. Wu, W. Shao, Multi-objective shape optimization of double pipe heat exchanger with inner corrugated tube using RSM method. *International Journal of Thermal Sciences* 90 (2015) 173-186.
- [18] H. S. Dizaji, S. Jafarmadar, F. Mobadersani, Experimental studies on heat transfer and pressure drop characteristics for new arrangements of corrugated tubes in a double pipe heat exchanger, *International Journal of Thermal Sciences* 96 (2015) 211-220.
- [19] H. S. Dizaji, S. Jafarmadar, Experiments on new arrangements of convex and concave corrugated tubes through a double pipe heat exchanger, *Experimental Heat Transfer*, 29 (2016) 1-16.
- [20] A. R. Darzi, M. Farhadi, K. Sedighi, Experimental investigation of convective heat transfer and friction factor of Al₂O₃/water nanofluid in helically corrugated tube, *Experimental Thermal and Fluid Science* 57 (2014) 188–199.
- [21] V. Srinivasan, R. N. Christensen, Experimental investigation of heat transfer and pressure drop characteristics of flow through spirally fluted tubes, *Experimental Thermal and Fluid Science* 1992; 5:820-827.

- [22] A. Barba, S. Rainieri, M. Spiga, Heat transfer enhancement in corrugated tube, *International Communication in Heat and Mass Transfer* 29 (3) (2002) 313–322.
- [23] A. Herless, E Franz, M Breuer, Experimental investigation of heat transfer and friction factor characteristic of fully developed gas flow in single-start and three-start corrugated tubes, *International Journal of Heat and Mass Transfer* 103 (2016) 538-547.
- [24] R. Bhadouriya, A. Agrawal, S.V. Prabhu, Laminar flow heat transfer studies in a twisted square duct for constant wall heat flux boundary condition, in: *Sadhana Academy Proceedings in Engineering Science*, 40 (2) (2015) 467-485.
- [25] M. Farnam, M. K. Aliabadi, M.J. Asadollahzadeh, Heat transfer intensification of agitated U-tube heat exchanger using twisted-tube and twisted-tape as passive techniques, 133 (2018) 137 -147.
- [26] X. Li, D. Zhu, Y. Yin, A. Tu, S. Liu, Parametric study on heat transfer and pressure drop of twisted oval tube bundle within line layout. *International Journal of Heat and Mass Transfer* 135 (2019) 860–872.
- [27] R. Bhadouriya, A. Agrawal, S.V. Prabhu, Experimental and numerical study of fluid flow and heat transfer, *International Journal of Heat and Mass Transfer* 82 (2015) 143-158.
- [28] R. Bhadouriya, A. Agrawal, S. V. Prabhu, Experimental and numerical study of fluid flow and heat transfer in an annulus of inner twisted square duct and outer circular pipe, *International Journal of Thermal Sciences* 94 (2015) 96-109.

- [29] X. H. Tan, D. S. Zhu, G. Y. Zhou, L. D. Zeng, Experimental and numerical study of convective heat transfer and fluid flow in twisted oval tubes, *International Journal of Heat and Mass Transfer* 55 (2012) 4701–4710.
- [30] X. Tang, X. Dai, D. Zhu, Experimental and numerical investigation of convective heat transfer and fluid flow in twisted spiral tube, *International Journal of Heat and Mass Transfer* 90 (2015) 523–541.
- [31] S. Yang, L. Zhang, H. Xu, Experimental study on convective heat transfer and flow resistance characteristics of water flow in twisted elliptical tubes, *Applied Thermal Engineering* 31 (2011) 2981–2991.
- [32] L. B. Wang, W. Q. Tao, Q. W. Wang, Y. L. He, Experimental and Numerical Study of Turbulent Heat Transfer in Twisted Square Ducts, *J. Heat Transfer* 123(5) (2001) 868–877.
- [33] S. Xie, Z. Liang, J. Zhang, L. Zhang, Y. Wang, H. Ding, Numerical investigation on flow and heat transfer in dimpled tube with teardrop dimples, *International Journal of Heat and Mass Transfer* 131 (2019) 713–723.
- [34] P. Kumar, A. Kumar, S. Chamoli, M. Kumar, Experimental investigation of heat transfer enhancement and fluid flow characteristics in a protruded surface heat exchanger tube, *Experimental Thermal and Fluid Science* 71 (2016) 42–51.
- [35] S. Xie, Z. Liang, L. Zhang, Y. Wang, H. Ding, J. Zhang, Numerical investigation on heat transfer performance and flow characteristics in enhanced tube with dimples and protrusions, *International Journal of Heat and Mass Transfer* 122 (2018) 602–613.

- [36] L. Jianfeng, S. Xiangyang, D. Jing, Y. Jianping, Transition and turbulent convective heat transfer of molten salt in spirally grooved tube, *Experimental Thermal and fluid science* 47 (2013) 180-185.
- [37] A. Kumar, B. N. Prasad, Investigation of twisted tape inserted solar water heaters-heat transfer, friction factor and thermal performance results, *Renewable Energy* 19 (2000) 379–398.
- [38] E. Esmaeilzadeh, H. Almohammadi, A. Nokhosteen, A. Motezaker, A. N. Omrani, Study on heat transfer and friction factor characteristics of γ -Al₂O₃/water through circular tube with twisted tape inserts with different thicknesses, *International Journal of Thermal Sciences* 85 (2014) 72–83.
- [39] C. Thianpong, P. Eiamsa-ard, K. Wongcharee, S. Eiamsa-ard, Compound heat transfer enhancement of a dimpled tube with a twisted tape swirl generator, *International Communication in Heat and Mass Transfer* 36 (2009) 698–704.
- [40] S. Eiamsa-ard, K. Yongsiri, K. Nanana, C. Thianpong, Heat transfer augmentation by helically twisted tapes as swirl and turbulence promoters, *Chemical Engineering and Processing: process intensification* 60 (2012) 42–48.
- [41] S. Jaisankar, T. K. Radhakrishnan, K. N. Sheeba, Experimental studies on heat transfer and thermal performance characteristics of thermosyphon solar water heating system with helical and Left–Right twisted tapes, *Energy Conversion and Management* 52 (2011) 2048–2055.

- [42] S. Chougule, S. K. Sahu, Comparative study on heat transfer enhancement of low volume concentration of Al₂O₃/Water and CNT/Water nano fluids in transition regime using helical screw tape inserts, *Chemical Engineering and Processing: Process Intensification* 88 (2015) 78–88.
- [43] S. N. Sarada, A. N. S. R. Raju, K. K. Radha, L. S. Sunder, Enhancement of heat transfer using varying width twisted tape inserts, *International Journal of Engineering, Science and Technology* 2 (2010) 107–118.
- [44] K. Wongcharee, S. Eiamsa-ard, Friction and heat transfer characteristics of laminar swirl flow through the round tubes inserted with alternate clock- wise and counter-clockwise twisted-tapes, *International communication in heat and mass transfer* 38 (2011) 348–352.
- [45] S. Eiamsa-ard, C. Thianpong, P. Eiamsa-ard, P. Promvonge, Convective heat transfer in a circular tube with short-length twisted tape insert, *International communication in heat and mass transfer* 36 (2009) 365–371.
- [46] K. Wongcharee, S. Eiamsa-ard, Heat transfer enhancement by twisted tapes with alternate-axes and triangular, rectangular and trapezoidal wings, *Chemical Engineering and Processing: Process Intensification*, 50 (2011) 211–219.
- [47] S. Eiamsa-ard, P. Promvonge. Performance assessment in a heat exchanger tube with alternate clockwise and counter-clockwise twisted-

- tape inserts, *International Journal of Heat and Mass Transfer* 53 (2010) 1364–1372.
- [48] P. Seemawute, S. Eiamsa-ard, Thermohydraulics of turbulent flow through a round tube by a peripherally-cut twisted tape with an alternate axis, *International Communication in Heat and Mass Transfer* 37 (2010) 652–659.
- [49] M. M. K. Bhuiya, ASM Sayem, M. Islam, M. S. U. Chowdhury, M. Shahabuddin, Performance assessment in a heat exchanger tube fitted with double counter twisted tape inserts, *International communication in heat and mass transfer* 50 (2014) 25–33.
- [50] P. Promvong, S. Pethkool, M. Pimsarn, C. Thianpong, Heat transfer augmentation in a helical-ribbed tube with double twisted tape inserts, *International communication in heat and mass transfer* 39 (2012) 953–959.
- [51] M. K. Bhuiya, MSU. Chowdhury, M. Shahabuddin, M. Saha, L. A. Memon, Thermal characteristics in a heat exchanger tube fitted with triple twisted tape inserts, *International communication in heat and mass transfer*, 48 (2013) 124–132.
- [52] C. Vashistha, A. K. Patil, M. Kumar, Experimental investigation of heat transfer and pressure drop in a circular tube with multiple inserts, *Applied Thermal Engineering* 96 (2016) 117–129.
- [53] M. K. Bhuiya, A. K. Azad, M. S. U. Chowdhury, M. Saha. Heat transfer augmentation in a circular tube with perforated double counter twisted tape inserts, *International Communications in Heat and Mass Transfer* 74 (2016) 18–26.

- [54] S. W. Chang, W. L. Cai, R. S. Syu, Heat transfer and pressure drop measurements for tubes fitted with twin and four twisted fins on rod, *Experimental Thermal and Fluid Science* 74 (2016) 220–234.
- [55] C. Thianpong, P. Eiamsa-ard, P. Promvonge, S. Eiamsa-ard, Effect of perforated twisted-tapes with parallel wings on heat transfer enhancement in a heat exchanger tube, *Energy Procedia* 14 (2012) 1117–1123.
- [56] P. Murugesan, K. Mayilsamy, S. Suresh, P. S. S. Srinivasan, Heat transfer and pressure drop characteristics in a circular tube fitted with and without V-cut twisted tape insert, *International Communication in Heat and Mass Transfer* 38 (2011) 329–334.
- [57] S. Eiamsa-ard, P. Seemawute, K. Wongcharee. Influences of peripherally-cut twisted tape insert on heat transfer and thermal performance characteristics in laminar and turbulent tube flows, *Experimental Thermal and Fluid Science* 34 (2010) 711–719.
- [58] S. Eiamsa-ard, P. Promvonge, Thermal characteristics in round tube fitted with serrated twisted tape, *Applied Thermal Engineering* 30 (2010) 1673–1682.
- [59] S. Eiamsa-ard, K. Wongcharee, P. Eiamsa-ard, C. Thianpong, Heat transfer enhancement in a tube using delta-winglet twisted tape inserts, *Applied Thermal Engineering*, 30 (2010) 310–318.
- [60] S. R. Shabaniyan, M. Rahimi, M. Shahhosseini, A. A. Alsairafi, CFD and experimental studies on heat transfer enhancement in an air cooler equipped with different tube insert, *International Communication in Heat and Mass Transfer*, 38 (2011) 383–390.

- [61] S Roy, S K Saha, Thermal and friction characteristics of laminar flow through a circular duct having helical screw-tape with oblique teeth inserts and wire coil, *Experimental Thermal and Fluid Science* 68 (2015) 733–743.
- [62] P. Promvonge, Thermal augmentation in circular tube with twisted tape and wire coil turbulators, *Energy Conversion and Management* 49 (2008) 2949–2955.
- [63] K. A. Hamid, W. H. Azmi, R. Mamat, K. V. Sharma, Heat transfer performance of TiO₂–SiO₂ nanofluids in a tube with wire coil inserts, *Applied Thermal Engineering* 152 (2019) 275–286.
- [64] O. Keklikcioglu, V. Ozceyhan, Experimental investigation on heat transfer enhancement of a tube with coiled-wire inserts installed with a separation from the tube wall, *International Communications in Heat and Mass Transfer* 78 (2016) 88–94.
- [65] P. Promvonge, N Koolnapadol, M. Pimsarn, C. Thianpong, Thermal performance enhancement in a heat exchanger tube fitted with inclined vortex rings, *Applied Thermal Engineering* 62 (2014) 285–292.
- [66] V. Kongkaitpaiboon, K. Nanan, S. Eiamsa-ard, Experimental investigation of convective heat transfer and pressure loss in a round tube fitted with circular ring turbulators, *International Communication in Heat and Mass Transfer* 37 (2010) 568–574.
- [67] C. Thianpong, K. Yongsiri, K. Nanan, S. Eiamsa-ard, Thermal performance evaluation of heat exchangers fitted with twisted-ring turbulators, *International Communication in Heat and Mass Transfer* 39 (2012) 861–868.

- [68] S. Eiamsa-ard, V. Kongkaitpaiboon, K. Nanan, Thermohydraulics of turbulent flow through heat exchanger tubes fitted with circular-rings and twisted tapes, *Chinese Journal of Chemical Engineering* 21 (6) (2013) 585–593.
- [69] S. Akansu, Heat transfers and pressure drops for porous-ring turbulators in a circular pipe, *Applied Energy* 83 (2006) 280–298.
- [70] H. Karakaya, A. Durmus, Heat transfer and exergy loss in conical spring turbulators, *International Journal of Heat and Mass Transfer* 60 (2013) 756–762.
- [71] S. Eiamsa-ard, P. Promvong, Experimental investigation of heat transfer and friction characteristics in a circular tube fitted with V-nozzle turbulators, *International Communications in Heat and Mass Transfer* 33 (2006) 591–600.
- [72] M. Sheikholeslami, M. G. Bandy, D. D. Ganji, Effect of discontinuous helical turbulators on heat transfer characteristics of double pipe water to air heat exchanger, *Energy Conversion and Management* 118 (2016) 75–87.
- [73] M. Sheikholeslami, D. D. Ganji, Heat transfer improvement in a double pipe heat exchanger by means of perforated turbulators, *Energy Conversion and Management* 127 (2016) 112–123.
- [74] M. Sheikholeslami, D. D. Ganji, M. Gorji-Bandy, Experimental and numerical analysis for effects of using conical ring on turbulent flow and heat transfer in a double pipe air to water heat exchanger, *Applied Thermal Engineering* 100 (2016) 805–819.

- [75] K. Ruengpayungsak, K. Wongcharee, C. Thianpong, M. Pimsarn, V. Chuwattanakul, S. Eiamsa-ard, Heat transfer evaluation of turbulent flows through gear-ring elements, *Applied Thermal Engineering* 123 (2017) 991–1005.
- [76] M. Sheikholeslami, M. Gorji-Bandpy, D.D. Ganji, Experimental study on turbulent flow and heat transfer in an air to water heat exchanger using perforated circular-ring, *Experimental Thermal and Fluid Science* 70 (2016) 185–195.
- [77] M. Sheikholeslami, D.D. Ganji, Heat transfer enhancement in an air to water heat exchanger with discontinuous helical turbulators; experimental and numerical studies, *Energy*, 116 (1) (2016) 341-352.
- [78] A. Kumar, S. Singh, S. Chamoli, M. Kumar, Experimental investigation on thermo-hydraulic performance of heat exchanger tube with solid and perforated circular disk along with twisted tape insert, *Heat Transfer Engineering* (2018).
<https://doi.org/10.1080/01457632.2018.1436618>
- [79] S. Skullong, P. Promvonge, C. Thianpong, N. Jayranaiwachira, M. Pimsarn, Thermal performance of heat exchanger tube inserted with curved winglet tapes, *Applied Thermal Engineering* 129 (2018) 1197–1211.
- [80] A. Kumar, S. Chamoli, M. Kumar, Experimental investigation on thermal performance and fluid flow characteristics in heat exchanger tube with solid hollow circular disk inserts, *Applied Thermal Engineering* 100 (2016) 227–236.

- [81] P. Promvonge, S. Eiamsa-ard, Heat transfer and turbulent flow friction in a circular tube fitted with conical-nozzle turbulators, *International Communications in Heat and Mass Transfer* 34 (2007) 72–82.
- [82] H. K. Dawood, H. A. Mohammed, N. A. C. Sidik, K. M. Munisamy, M. A. Wahid, Forced natural and mixed- convection heat transfer and fluid flow in annulus: a review, *International Communications in Heat and Mass Transfer* 62 (2015) 45–47.
- [83] F. P. Incropera, D. P. Dewitt, *Fundamentals of heat and mass transfer*, fourth edition, John Wiley and Sons, (1996) 419-481.
- [84] J. Dirker, J. P. Meyer, Convection heat transfer in concentric annuli. *Experimental heat transfer* 17 (1), (2004) 19-29.
- [85] R. L. Webb, E. R. G. Eckert, Application of rough surfaces to heat exchanger design, *Journal of Heat and Mass Transfer*, 15 (1972) 1647-1658.
- [86] R. L. Webb, M. J. Scott, A parametric analysis of the performance of internally finned tubes for heat exchanger application, *Journal of Heat Transfer* 102 (1980) 38-43.
- [87] Y. Hong, J. Dua, S. Wang, S. Huang, Heat transfer and flow behaviors of a wavy corrugated tube, *Applied Thermal Engineering* 126 (2017) 151–166.
- [88] W. Wang, Y. Zhang, B. Li, Y. Li, Numerical investigation of tube-side fully developed turbulent flow and heat transfer in outward corrugated tubes, *International Journal of Heat and Mass Transfer* 116 (2018) 115–126.

- [89] V. Srinivasan, R. N. Christensen, Experimental investigation of heat transfer and pressure drop characteristics of flow through spirally fluted tubes, *Experimental Thermal and Fluid Science* 5 (1992) 820-827.
- [90] M. Sun, M. Zeng, Investigation on turbulent flow and heat transfer characteristics and technical economy of corrugated tube, *Applied Thermal Engineering* 129 (2018) 1–11.
- [91] P. Naphon, M. Nuchjapo, J. Kurujareon, Tube side heat transfer coefficient and friction factor characteristics of horizontal tubes with helical rib, *Energy Conversion and Management*, 47 (2006), 3031-3044.
- [92] P. Bharadwaj, A. D. Khondge, A. W. Date, Heat transfer and pressure drop in a spirally grooved tube with twisted tape insert, *International Journal of Heat and Mass Transfer* 52 (2009) 1938–1944.
- [93] J. Meng, X. Liang, Z. Chen, Z. Li, Experimental study on convective heat transfer in alternating elliptical axis tubes, *Experimental Thermal and Fluid Science* 29 (2005) 457–465.
- [94] W. R. Vanzyl, J. Dirker, J. P. Meyer, Single-Phase Convective Heat Transfer and Pressure Drop Coefficients in Concentric Annuli, *Heat Transfer Engineering*, 34(13), (2013) 1112–1123.
- [95] P. Promvonge, S. Eiamsa-ard, Heat transfer in a circular tube fitted with free-spacing snail entry and conical-nozzle turbulators, *International Communications in Heat and Mass Transfer* 34 (2007) 838–848.

Appendix I

Experimental uncertainty

The thermodynamic performance of double pipe heat exchanger with passive enhancement techniques have been studied through experimental investigation.

The present study involves measurement of various parameters such as length, diameter of test section, temperatures and flow rate of air and water, and pressure drop of air along the length of test section. It is to be noticed that error in the test results initiates because of deviation of primary measured quantities. In view this, attempts have been made to use pre-calibrated instruments to minimize the error in the measurement. Here, an error analysis is made to estimate the errors associated in the various parameters following the procedure suggested by Coleman and Steele [1] as:

If R is the dependent variable and is function of n independent variable then,

$$R = f (v_1, v_2, v_3, \dots, v_n) \quad \text{Eq. (I.1)}$$

Let the uncertainties associated with independent variable be $e_1, e_2, e_3, \dots, e_n$ and resulting uncertainty of R be e and expressed as:

$$e = \left[\left(\frac{\partial R}{\partial v_1} e_1 \right)^2 + \left(\frac{\partial R}{\partial v_2} e_2 \right)^2 + \left(\frac{\partial R}{\partial v_3} e_3 \right)^2 + \dots + \left(\frac{\partial R}{\partial v_n} e_n \right)^2 \right]^{1/2} \quad \text{Eq. (I.2)}$$

In this study, several test facilities have been developed to evaluate the thermal performance of double pipe heat exchanger with various passive enhancement techniques. Here, steel rule and Vernier caliper are used to measure the dimensions of the test specimen. Various instruments such as rotameter and digital air counter is used to measure water flow rate and air flow rate, respectively. The temperatures of the hot fluid (water) and cold fluid (air) are measured by using RTD during experiments. Here, differential pressure transmitter is used to measure the pressure drop between two

different locations of the pipe. The error associated with various parameters namely water and air flow rates, air and water temperatures (inlet and outlet), pressure drop, diameter and length of the test section are listed in Table I.1. These parameters were used to estimate the combined uncertainty in Reynolds number, Nusselt number and friction factors. The errors associated in the parameters are detailed below.

Table I.1: Uncertainties in instruments

Instrument	Range	Variable measured	Error
RTD	-200°C to +850 °C	Fluid temperature	0.1°C
Measuring Tape	0-5m	Length measurement	1 mm
Vernier calipers	0-150mm	Diameter (D)	0.01 mm
Air flow meter	0.25 – 75 m ³ /h	Air volume flow rate	3%
Differential pressure transducer	0-250 mbar	Pressure drop across test section	0.25%
Rotameter	0 -15 lpm	Water flow rate	0.1 lpm
Stopwatch	-	Time (t)	0.01 second

(a) Density of air (ρ)

$$\rho_{air} = \frac{P_{in,air}}{RT_{ci}}$$

Uncertainty in air density

$$e_{\rho} = \left[\left\{ \frac{\partial \rho}{\partial T_{ci}} (e_{T_{ci}}) \right\}^2 + \left\{ \frac{\partial \rho}{\partial P_{in,air}} (e_{P_{in,air}}) \right\}^2 \right]^{1/2}$$

$$= \sqrt{(5.2 \times 10^{-5})^2 + (3.89 \times 10^{-3})^2} = 3.89 \times 10^{-3}$$

$$\% e_{\rho} = \frac{100 \times e_{\rho}}{\rho} = \frac{100 \times 3.89 \times 10^{-3}}{1.56} = 0.25\%$$

(b) Air velocity (V)

$$V_{air} = \frac{Q_v}{A_c}$$

Uncertainty in Air Velocity

$$e_{V_{air}} = \left[\left\{ \frac{\partial V_{air}}{\partial Q_v} (e_{Q_v}) \right\}^2 + \left\{ \frac{\partial V_{air}}{\partial A_c} (e_{A_c}) \right\}^2 \right]^{1/2}$$

$$= \sqrt{(0.08)^2 + (0.02)^2} = 0.08$$

$$\% e_{V_{air}} = \frac{100 \times e_{V_{air}}}{V_{air}} = \frac{100 \times 0.08}{2.66} = 3\%$$

(c) Annulus area of cross section (A_c)

$$A_c = \frac{\pi}{4} (D_i^2 - d_o^2)$$

Uncertainty in A_c

$$e_{A_c} = \left[\left\{ \frac{\partial A_c}{\partial D_i} (e_{D_i}) \right\}^2 + \left\{ \frac{\partial A_c}{\partial d_o} (e_{d_o}) \right\}^2 \right]^{1/2}$$

$$= \sqrt{(0.55)^2 + (0.3)^2} = 0.63$$

$$\% e_{A_c} = \frac{100 \times e_{A_c}}{A_c} = \frac{100 \times 0.63}{678.6} = 0.093\%$$

Here, $D_i = 35\text{mm}$ and $d_o = 19\text{ mm}$.

(d) Reynolds number for air (Re)

$$Re = \frac{\rho v D_h}{\mu}$$

Uncertainty in Re is given by

$$e_{Re} = \left[\left\{ \frac{\partial Re}{\partial \rho} (e_\rho) \right\}^2 + \left\{ \frac{\partial Re}{\partial V} (e_V) \right\}^2 + \left\{ \frac{\partial Re}{\partial D_h} (e_{D_h}) \right\}^2 \right]^{1/2}$$

$$e_{Re} = [8.85^2 + 106.33^2 + 2.21^2]^{1/2}$$

$$e_{Re} = 106.72$$

$$\% e_{Re} = \frac{100 \times e_{Re}}{Re} = \frac{100 \times 106.72}{3542} = 3.01\%$$

(e) Friction factor for air (f)

$$f = \frac{\Delta p}{2 \left(\frac{L}{D_h} \right) \rho V^2}$$

Uncertainty in f is given by

$$e_f = \left[\left\{ \frac{\partial f}{\partial \Delta p} (e_{\Delta p}) \right\}^2 + \left\{ \frac{\partial f}{\partial D_h} (e_{D_h}) \right\}^2 + \left\{ \frac{\partial f}{\partial L} (e_L) \right\}^2 + \left\{ \frac{\partial f}{\partial \rho} (e_\rho) \right\}^2 + \left\{ \frac{\partial f}{\partial V} (e_V) \right\}^2 \right]^{1/2}$$

$$e_f = \left[(2.31 \times 10^{-4})^2 + (5.79 \times 10^{-5})^2 + (8.27 \times 10^{-5})^2 + (2.31 \times 10^{-4})^2 + (5.56 \times 10^{-3})^2 \right]^{1/2}$$

$$e_f = 5.57 \times 10^{-3}$$

$$\% e_f = \frac{100 \times e_f}{f} = \frac{100 \times 5.57 \times 10^{-3}}{0.09259} = 6.02\%$$

(f) Heat flux of hot fluid (Q_h)

$$Q_h = \dot{m}_h C p_h (T_{hi} - T_{ho})$$

Uncertainty in Q_h is given by

$$e_{Q_h} = \left[\left\{ \frac{\partial Q_h}{\partial m_h} (e_{m_h}) \right\}^2 + \left\{ \frac{\partial Q_h}{\partial T_{hi}} (e_{T_{hi}}) \right\}^2 + \left\{ \frac{\partial Q_h}{\partial T_{ho}} (e_{T_{ho}}) \right\}^2 \right]^{1/2}$$

$$e_{Q_h} = [2.38^2 + 7.23^2 + 7.23^2]^{1/2}$$

$$e_{Q_h} = 10.5$$

$$\% e_{Q_h} = \frac{100 \times e_{Q_h}}{Q_h} = \frac{100 \times 10.5}{246.59} = 4.26\%$$

(g) Heat flux of cold fluid (Q_c)

$$Q_c = \dot{m}_c C p_c (T_{co} - T_{ci})$$

Uncertainty in Q_c is given by

$$e_{Q_c} = \left[\left\{ \frac{\partial Q_c}{\partial m_c} (e_{m_c}) \right\}^2 + \left\{ \frac{\partial Q_c}{\partial T_{co}} (e_{T_{co}}) \right\}^2 + \left\{ \frac{\partial Q_c}{\partial T_{ci}} (e_{T_{ci}}) \right\}^2 \right]^{1/2}$$

$$e_{Q_c} = \left[(2.2 \times 10^{-5})^2 + 0.028^2 + 0.028^2 \right]^{1/2}$$

$$e_{Q_c} = 0.038$$

$$\% e_{Q_c} = \frac{100 \times e_{Q_c}}{Q_c} = \frac{100 \times 0.038}{25.98} = 0.15\%$$

(h) Average heat flux (Q_{avg})

$$Q_{avg} = \frac{Q_h + Q_c}{2}$$

Uncertainty in Q_{avg} is given by

$$e_{Q_{avg}} = \left[\left\{ \frac{\partial Q_{avg}}{\partial Q_h} (e_{Q_h}) \right\}^2 + \left\{ \frac{\partial Q_{avg}}{\partial Q_c} (e_{Q_c}) \right\}^2 \right]^{1/2}$$

$$e_{Q_{avg}} = [5.25^2 + 0.022^2]^{1/2}$$

$$e_{Q_{avg}} = 5.25$$

$$\% e_{Q_{avg}} = \frac{100 \times e_{Q_{avg}}}{Q_{avg}} = \frac{100 \times 5.25}{136.28} = 3.85\%$$

(i) logarithmic mean temperature difference (ΔT_{LMTD})

$$\Delta T_{LMTD} = \frac{(T_{hi} - T_{co}) - (T_{ho} - T_{ci})}{\ln \left(\frac{T_{hi} - T_{co}}{T_{ho} - T_{ci}} \right)}$$

Uncertainty in ΔT_{LMTD} is given by

$$e_{\Delta T_{LMTD}} = \left[\left\{ \frac{\partial \Delta T_{LMTD}}{\partial T_{hi}} (e_{T_{hi}}) \right\}^2 + \left\{ \frac{\partial \Delta T_{LMTD}}{\partial T_{co}} (e_{T_{co}}) \right\}^2 + \left\{ \frac{\partial \Delta T_{LMTD}}{\partial T_{ho}} (e_{T_{ho}}) \right\}^2 + \left\{ \frac{\partial \Delta T_{LMTD}}{\partial T_{ci}} (e_{T_{ci}}) \right\}^2 \right]^{1/2}$$

$$e_{\Delta T_{LMTD}} = \left[(5.4 \times 10^{-3})^2 + (1.08 \times 10^{-1})^2 + (9.92 \times 10^{-2})^2 + (4.64 \times 10^{-3})^2 \right]^{1/2}$$

$$e_{\Delta T_{LMTD}} = 0.147$$

$$\% e_{\Delta T_{LMTD}} = \frac{100 \times e_{\Delta T_{LMTD}}}{\Delta T_{LMTD}} = \frac{100 \times 0.147}{39.39} = 0.37\%$$

(j) Heat transfer coefficient of air (h)

$$h = \frac{Q_{avg}}{A_s \Delta T_{LMTD}}$$

Here, heat transfer coefficient of air is assumed to be overall heat transfer coefficient. Because, thermal resistance due to hot fluid is negligible as explained in the section 2.3.

Uncertainty in h is given by

$$e_h = e_U = \left[\left\{ \frac{\partial U}{\partial Q_{avg}} (e_{Q_{avg}}) \right\}^2 + \left\{ \frac{\partial U}{\partial A_s} (e_{A_s}) \right\}^2 + \left\{ \frac{\partial U}{\partial (\Delta T)_{LMTD}} (e_{(\Delta T)_{LMTD}}) \right\}^2 \right]^{1/2}$$

$$e_h = [2^2 + 0.06^2 + 0.22^2]^{1/2}$$

$$e_h = 2.02$$

$$\% e_h = \frac{100 \times e_h}{h} = \frac{100 \times 2.02}{57.94} = 3.5\%$$

(k) Nusselt number for air (Nu)

$$Nu = \frac{h D_h}{k}$$

Uncertainty in Nu is given by

$$e_{Nu} = \left[\left\{ \frac{\partial Nu}{\partial h} (e_h) \right\}^2 + \left\{ \frac{\partial Nu}{\partial D_h} (e_{D_h}) \right\}^2 \right]^{1/2}$$

$$e_{Nu} = [1.22^2 + 0.022^2]^{1/2}$$
$$e_{Nu} = 1.22$$

$$\%e_{Nu} = \frac{100 \times e_{Nu}}{Nu} = \frac{100 \times 1.22}{35.08} = 3.5\%$$

Additional Reference

[I.1] H. W. Coleman and W. G. Steele, "Experimental and uncertainty analysis for engineers", Wiley, New York, 1989.

List of Publications

(A) Publications from PhD thesis work:

A1. In Refereed Journals

1. S. Yadav, S. K. Sahu, Effect of helical surface disc turbulators on heat transfer and friction factor characteristics in the annuli of double pipe heat exchanger: An experimental study, *Chemical Engineering & Technology* 46 (2019) 1205 – 1213. **(IF: 2.418)**.
<https://doi.org/10.1002/ceat.201800251>
2. S. Yadav, S. K. Sahu, Heat transfer and friction factor characteristics of annuli formed by smooth inner tube and corrugated outer tube – An Experimental study, *Experimental Heat Transfer* 30(1) (2020) 18-39. **(IF: 2.0)**
<https://doi.org/10.1080/08916152.2019.1569179>
3. S. Yadav, S. K. Sahu, Heat transfer augmentation in double pipe water to air counter flow heat exchanger with helical surface disc turbulators, *Chemical Engineering and Processing - Process Intensification*, 135 (2019) 120 – 132. **(IF: 3.031)**
<https://doi.org/10.1016/j.cep.2018.11.018>
4. S. Yadav, M. P. Paulraj, S. K. Sahu, Thermal performance of air to water heat exchanger with plain surface disc turbulators: Experimental and numerical study, *Heat and Mass Transfer*, 56 (2020) 1777 – 1791. **(IF: 1.551)**.
<https://doi.org/10.1007/s00231-020-02824-x>
5. S. Yadav, S. K. Sahu, Effect of helical surface disc turbulator on thermal and friction characteristics of double pipe water to air heat exchanger, *Experimental Heat Transfer* (2020). **(Article in press, IF: 2.0)**.
<https://doi.org/10.1080/08916152.2020.1714819>

A2. In Referred Conferences

1. S. Yadav, A. K. Sharma, S. K. Sahu, Thermal performance in annuli of double pipe heat exchanger using helical surface disc turbulators. Proceedings of 7th International and 45th National Conference on Fluid Mechanics and Fluid Power Dec 10-12, 2018. IIT Bombay, Mumbai, India (Paper ID: FMFP2018–578).
2. S. Yadav, M. P. Paulraj, S. K. Sahu, Experimental investigation of heat transfer and friction factor characteristics using helical surface ring turbulators in an annuli of double pipe heat exchanger, In Proceedings of ASME 2018 Power Conference collocated with the 12th International Conference on Energy Sustainability and the ASME 2018 Nuclear Forum, Florida, USA 24-28 June, 2018, pp. V002T12A006. **(Qualified student award)**

<https://doi.org/10.1115%2Fpower2018-7231>

3. S. Yadav, N. Anand, S. K. Sahu, Thermal performance in an annuli formed by smooth inner tube and outer corrugated tube for turbulent flow regime in the counter flow condition, In Proceedings of the 24th National and 2nd International ISHMT-ASTFE Heat and Mass Transfer Conference (IHMTTC-2017) , Hyderabad India, PP 1651-1656, (Paper ID: IHMTTC2017-09-0902).

<http://dx.doi.org/10.1615/IHMTTC-2017.2290>

4. S. Yadav, A. K. Sharma, S. K. Sahu, Experimental investigation of heat transfer and friction factor characteristics of annuli formed by smooth inner tube and corrugated outer tube in turbulent flow, Proceedings of 6th International and 43rd National Conference on Fluid Mechanics and Fluid Power Dec 15-17, 2016, MNIT, Allahabad, India (Paper ID: FMFP2016–147).

(B) Other publications during PhD:

B1. In Refereed Journals

1. S. Yadav, K. Sudhakar, Different domestic designs of solar stills: A review, Renewable and Sustainable Energy Reviews 47 (2015) 718–731. **(IF: 10.556)**

<https://doi.org/10.1016/j.rser.2015.03.064>

B2. In Refereed Conferences

1. A. K. Sharma, U. K. Lodhi, G. Kumar, S. Yadav, S. K. Sahu, Rewetting analysis of downward facing hot surfaces using mist jet. Proceedings of 7th International and 45th National Conference on Fluid Mechanics and Fluid Power Dec 10-12, 2018, IIT Bombay, Mumbai, India (Paper ID: FMFP2018–752).
2. A. K. Sharma, S. K. Mishra, M. Modak, S. Yadav, A. K. Jain, S. K. Sahu, Experimental investigation of rewetting during quenching of hot surface by round jet impingement using aqueous surfactants. Proceedings of 6th International and 43rd National Conference on Fluid Mechanics and Fluid Power Dec 15-17, 2016, MNIT, Allahabad, India (Paper ID: FMFP2016–352).

Curriculum vitae

Saurabh Yadav

Doctoral Research Scholar
Indian Institute of Technology Indore
Mobile +91-7987213705
Email: saurabhyadav1124@gmail.com
phd1401203007@iiti.ac.in



Research and Teaching Interests

Renewable Energy, Waste heat recovery system, solar desalination, Heat exchangers, Fluid and thermal engineering.

Education

Indian Institute of Technology Indore	Indore, MP, India
Ph.D. – Mechanical Engineering	2014 - Present
Maulana Azad National Institute of Technology, Bhopal	Bhopal, MP, India
MTech. – Renewable Energy	2012 - 2014
Madhav Institute of Technology and Science, Gwalior	Gwalior, MP, India
B. E. – Mechanical Engineering	2007 - 2011

Research and Teaching Experience

Teaching Assistant	12/2014 - Present
Indian Institute of Technology Indore	
Teaching Assistant	07/2012 – 06/2014
Maulana Azad National Institute of Technology, Bhopal	

Honour, Award, Membership and key accomplishments

- ✓ Complimentary registration, lodging, ticket to award banquet in the international conference ASME 2018 power and energy conference and exhibition held at Lake Buena Vista, Florida, USA 2018.
- ✓ Qualified student award in the international conference ASME 2018 power and energy conference and exhibition held at Lake Buena Vista, Florida, USA 2018.
- ✓ Best oral presentation award in the international conference on Sustainable Approaches for Green Computing, Economy and

Environment 2013 held at V. M. K. V. Engineering College, Salem TN-India.

- ✓ ASME Student member (Membership number: 102231812) during 2018-19.
 - ✓ Lifetime member of Indian Association of Hydrogen Energy and Advance Material Student chapter, Energy Center, MANIT, Bhopal.
 - ✓ Teaching Assistant Fellowship from MHRD Govt. of India during July 2012 to June 2014 and Dec. 2014 to present.
-

Publications

Paper in Refereed Journals	Papers in Refereed Conference Proceedings		Patent - Published	Total
Published/accepted	International	National		
6	7	0	1	14

Google Scholar:

<https://scholar.google.co.in/citations?user=bn0JmK0AAAAJ&hl=en>

Research Gate: https://www.researchgate.net/profile/Saurabh_Yadav15

Google Scholar Citations: 84; h-index: 4, i-10 index: 1, as on May 29, 2020

Review Services

- Heat Transfer – Asian Research - Wiley
 - Renewables: Wind Water Solar - Springer
 - Renewable and Sustainable energy reviews – Elsevier
 - Experimental Heat Transfer - Taylor & Francis
 - Journal of Testing and Evaluation - ASTM International
 - Smart Grid and Renewable Energy
 - Mechanical Engineering Research Day Seminar (Int. Conference)
-

Personal Profile

Name: Saurabh Yadav

Father's Name: Mr. Gopal Krishna Yadav

Date of Birth: November 24, 1988

Languages Known: English and Hindi

Permanent Address:

44- Digrra Gali Katra Bazzar, Sabalgarh, District-Morena,

MP - 476229

India.
